# CHAPTER 1

# INTRODUCTION TO BIOMEDICAL SIGNALS



## 1.1 The Nature of Biomedical Signals

Living organisms are made up of many component *systems* — the human body, for example, includes the nervous system, the cardiovascular system, and the musculoskeletal system, among others. Each system is made up of several subsystems that carry on many *physiological processes.* For example, the cardiac system performs the important task of rhythmic pumping of blood throughout the body to facilitate the delivery of nutrients, as well as pumping blood through the pulmonary system for oxygenation of the blood itself.

Physiological processes are complex phenomena, including nervous or hormonal stimulation and control; inputs and outputs that could be in the form of physical material, neurotransmitters, or information; and action that could be mechanical, electrical, or biochemical. Figure 1.1 shows a schematic representation of a generic physiological system to support the present discussion. Most physiological processes are accompanied by or manifest themselves as *signals* that reflect their nature and activities. Such signals could be of many types, including biochemical in the form of hormones and neurotransmitters, electrical in the form of potential or current, and physical in the form of pressure or temperature.

Diseases or defects in a biological system cause alterations in its normal physiological processes, leading to *pathological processes* that affect the performance, health, and general well-being of the system. A pathological process is typically associated with signals that are different in some aspects from the corresponding normal signals. If we possess a good understanding of a system of interest, it becomes possible to observe the corresponding signals and assess the state of the system. The task is not difficult when the signal is simple and appears at the outer surface of the body. For example, most infections cause a rise in the temperature of the body, which may be sensed easily, albeit in a

*Biomedical Signal Analysis,* Third Edition. Rangaraj M. Rangayyan and Sridhar Krishnan.

Companion Website: www.wiley.com/go/rangayyan3e

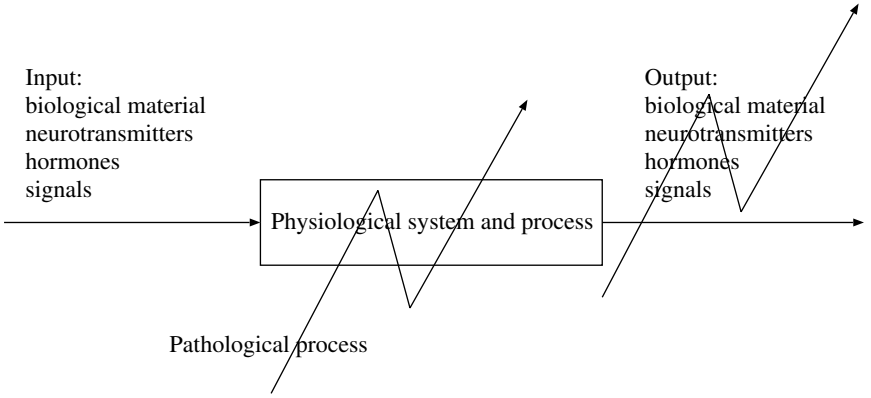


**Figure 1.1** Schematic representation of a generic physiological system with various types of possible inputs and outputs. The effect of a pathological process is depicted by the zigzag line across the system and the list of possible outputs. When both the input and output are signals, the physiological system shown may be viewed as a typical signal processing system in electrical engineering.

relative and *qualitative* manner, via the palm of one's hand. Objective or *quantitative* measurement of temperature requires an instrument, such as a thermometer.

A single measurement $x$ of temperature is a *scalar* and represents the thermal state of the body at a *particular or single instant of time* $t$ and at a particular position. If we record the temperature continuously in some form, such as a magnetic tape, we obtain a *signal as a function of time*; such a signal may be expressed in *continuous-time* or *analog* form as $x(t)$. When the temperature is measured at *discrete* instants of time, it may be expressed in *discrete-time* form as $x(nT)$ or $x(n)$, where $n$ is the index or measurement sample number of the array of values, and $T$ represents the uniform interval between the time instants of measurement. A discrete-time signal that can take amplitude values only from a limited list of *quantized* levels is called a *digital* signal.

(*Note:* The sampling of an analog signal has important implications on the accuracy of its representation and analysis as a discrete-time signal [1–3]. Quantization of an analog signal introduces errors in its digital representation; the use of optimal quantizers minimizes such errors [2, 4, 5]. The use of digital filters and computers with short word lengths also introduces limitations and errors in digital signal processing (DSP) [2, 3]. The distinction between discrete-time and digital signals [3,6] and their processing may not be important in most practical applications with currently available computers.)

In intensive-care monitoring, the tympanic (eardrum) temperature may sometimes be measured using an infrared sensor. Occasionally, when catheters are being used for other purposes, a temperature sensor may also be introduced into an artery or the heart to measure the *core* temperature of the body. It then becomes possible to obtain a continuous measurement of temperature, although only a few samples taken at intervals of a few minutes may be stored for subsequent analysis. Figure 1.2 illustrates representations of temperature measurements as a scalar, an array, and a signal plotted as a function of time. It is obvious that the graphical representation facilitates easier and faster comprehension of trends in the temperature than the numerical format. Long-term recordings of temperature can facilitate the analysis of temperature-regulation mechanisms [7, 8].

Let us now consider another basic measurement in healthcare and monitoring: blood pressure (BP). Each measurement consists of two values — the systolic pressure and the diastolic pressure. BP is measured in millimeters of mercury (*mm of Hg*) in clinical practice, although the international standard unit for pressure is the *Pascal*, with $1\ Pa = 0.0075$ *mm of Hg*. A single BP measurement could thus be viewed as a *vector* $\mathbf{x} = [x_1, x_2]^T$ with two components: $x_1$ indicating the systolic pressure and $x_2$ indicating the diastolic pressure. When BP is measured at a few instants of time,

$$x = 33.5\ ^\circ C$$

(a)

| Time ($h$) | 08:00 | 10:00 | 12:00 | 14:00 | 16:00 | 18:00 | 20:00 | 22:00 | 24:00 |
|---|---|---|---|---|---|---|---|---|---|
| $x(n)$ ($^\circ C$) | 33.5 | 33.3 | 34.5 | 36.2 | 37.3 | 37.5 | 38.0 | 37.8 | 38.0 |

(b)

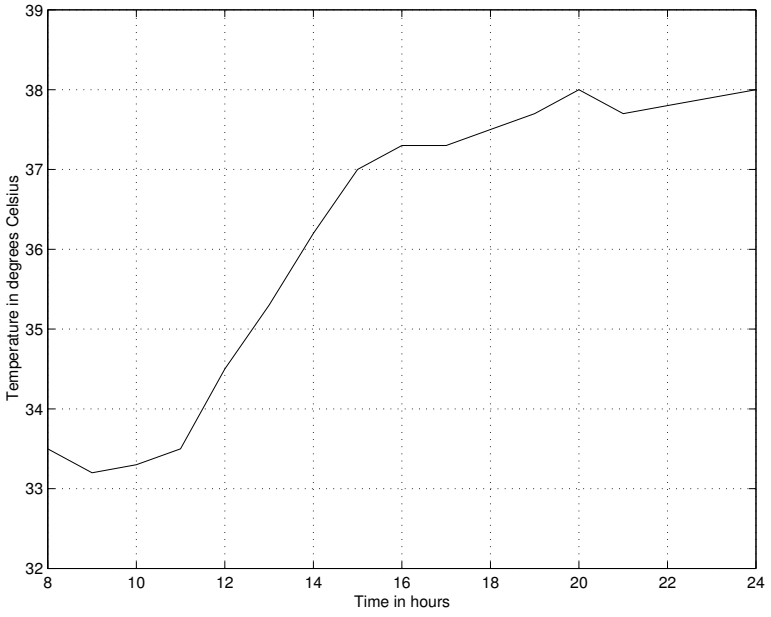


(c)

**Figure 1.2** Measurements of the temperature of a patient presented as (a) a scalar with one temperature measurement $x$ at an unspecified instant of time, (b) an array $x(n)$ made up of several measurements at different instants of time, and (c) a plot of the signal $x(n)$ or $x(t)$. The horizontal axis of the plot represents time in *hours*; the vertical axis gives temperature in *degrees Celsius*. Data courtesy of Foothills Hospital, Calgary.

we obtain an array of vectors $\mathbf{x}(n)$. In intensive-care monitoring and surgical procedures, a pressure transducer may sometimes be inserted into a blood vessel along with other devices. It then becomes possible to obtain the arterial systolic and diastolic BP as a continuous-time recording, although the values may be transferred to a computer and stored only at sampled instants of time that are several seconds or minutes apart. (Note that, although the systolic and diastolic pressure values are quoted together for the same nominal time instant, they do not occur together and are separated by at least a part of a cardiac cycle corresponding to systole; in practice, their measurement may be separated by several cardiac cycles or a few seconds.) The signal may then be expressed as a function of time $\mathbf{x}(t)$. Figure 1.3 shows BP measurements as a single two-component vector, as an array of vectors, and as a plot as a function of time. It is clear that the plot as a function of time facilitates rapid observation of trends in the pressure.

$$\mathbf{x} = \begin{bmatrix} x_1 \\ x_2 \end{bmatrix} = \begin{bmatrix} \text{Systolic} \\ \text{Diastolic} \end{bmatrix} = \begin{bmatrix} 122 \\ 66 \end{bmatrix}$$

(a)

| Time ($h$) | 08:00 | 10:00 | 12:00 | 14:00 | 16:00 | 18:00 | 20:00 | 22:00 | 24:00 |
|---|---|---|---|---|---|---|---|---|---|
| Systolic | 122 | 102 | 108 | 94 | 104 | 118 | 86 | 95 | 88 |
| Diastolic | 66 | 59 | 60 | 50 | 55 | 62 | 41 | 52 | 48 |

(b)

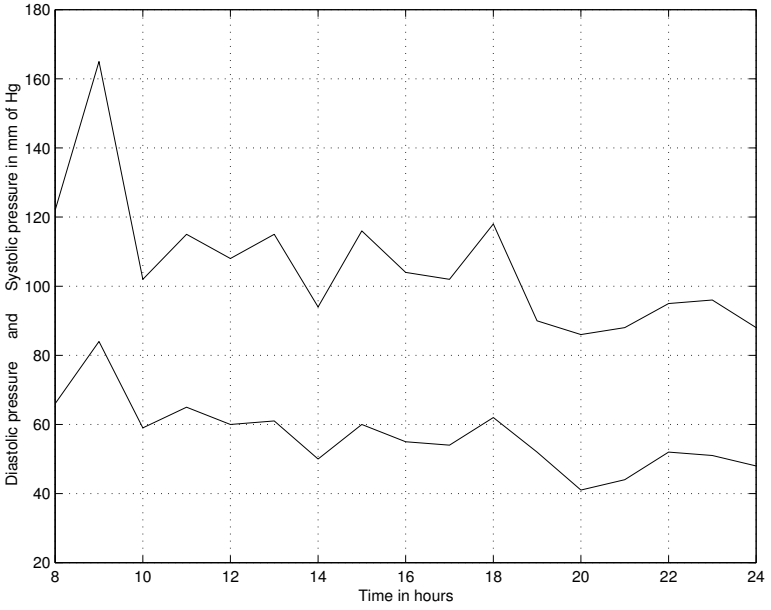


(c)

**Figure 1.3** Measurements of the BP of a patient presented as (a) a single pair or vector of systolic and diastolic measurements $\mathbf{x}$ in *mm of Hg* at an unspecified instant of time, (b) an array $\mathbf{x}(n)$ made up of several measurements at different instants of time, and (c) a signal $\mathbf{x}(t)$ or $\mathbf{x}(n)$. Note the use of boldface $\mathbf{x}$ to indicate that each measurement is a vector with two components. The horizontal axis of the plot represents time in *hours*; the vertical axis gives the systolic pressure (upper trace) and the diastolic pressure (lower trace) in *mm of Hg*. Data courtesy of Foothills Hospital, Calgary.

## 1.2 Examples of Biomedical Signals

The preceding example of body temperature as a signal is a simple example of a *biomedical signal*. Regardless of its simplicity, we can appreciate its importance and value in the assessment of the well-being of a child with a fever or that of a critically ill patient in a hospital. The origins and nature of a few other biomedical signals of various types are described in the following sections, with brief indications of their usefulness in diagnosis. Further detailed discussions on some of the signals are provided in the context of their analysis for various purposes in the chapters that follow.

This book is limited to the analysis of commonly encountered biomedical signals expressed as functions of time. Signals encountered in molecular biology and nanobioscience are not included. The topics of biomedical imaging and the analysis of biomedical images [9, 10] are not considered.

### 1.2.1 The action potential of a cardiac myocyte

The action potential is the basic component of all bioelectrical signals. It provides information on the nature of physiological activity at the single-cell level.

The action potential is the electrical signal that accompanies the mechanical contraction of a single muscle cell when stimulated by an electrical current (neural or external) [11–18]. The action potential is caused by the flow of sodium ($Na^+$), potassium ($K^+$), chloride ($Cl^-$), and other ions across the cell membrane.

Action potentials are also associated with signals and messages transmitted in the nervous system with no accompanying contraction. Hodgkin and Huxley [11, 12] conducted pioneering work on recording action potentials from a nerve fiber; see Sections 1.2.2 and 7.8.1. Recording an action potential requires the isolation of a single cell, and microelectrodes with tips of the order of a few micrometers to stimulate the cell and record the response [13].

**Resting potential:** A nerve or muscle cell is encased in a semipermeable membrane that permits selected substances to pass through while others are kept out. Body fluids surrounding cells are conductive solutions containing charged atoms known as ions. Figure 1.4 gives a schematic illustration of a cell and its characteristics.

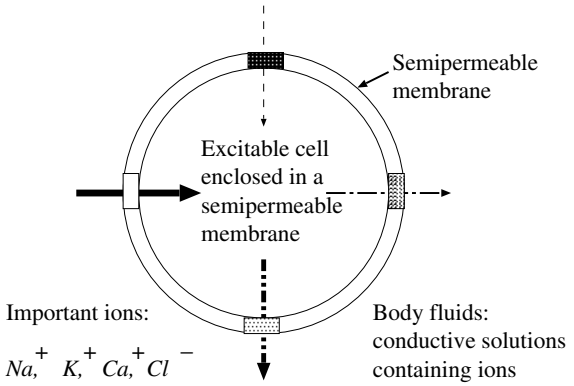


**Figure 1.4** Schematic representation of a cell and its characteristics. The parts of the cell membrane with different shades and the corresponding arrows of different types and thickness represent, in a schematic manner, the variable permeability of the membrane to different ions.

In their resting state, the membranes of excitable cells readily permit the entry of $K^+$ and $Cl^-$ ions, but effectively block the entry of $Na^+$ ions (the permeability for $K^+$ is 50–100 times that for $Na^+$). Various ions seek to establish a balance between the inside and the outside of a cell according to charge and concentration. The inability of $Na^+$ to penetrate a cell membrane results in the following [14]:

- $Na^+$ concentration inside the cell is far less than that outside.
- The outside of the cell is more positive than the inside of the cell.
- To balance the charge, additional $K^+$ ions enter the cell, causing higher $K^+$ concentration inside the cell than outside.

- Charge balance cannot be reached due to differences in membrane permeability for the various ions.
- A state of equilibrium is established with a potential difference, with the inside of the cell being negative with respect to the outside.

Figure 1.5 shows a schematic representation of a cell in its resting state. A cell in its resting state is said to be *polarized*. Most cells maintain a *resting potential* of the order of $-60$ to $-100\ mV$ until some disturbance or stimulus upsets the equilibrium.

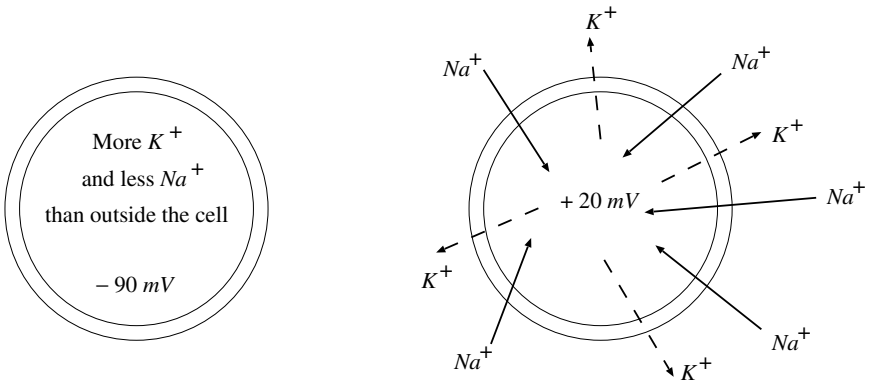


(a) At rest: permeability for $K^+$ 50 to 100 times that for $Na^+$. The cell is polarized.

(b) Depolarization: triggered by a stimulus; fast $Na^+$ channels open.

**Figure 1.5** Schematic representation (a) of a cell in its resting or polarized state and (b) the process of depolarization of the cell due to a stimulus.

**Depolarization:** When a cell is excited by ionic currents or an external stimulus, the membrane changes its characteristics and begins to allow $Na^+$ ions to enter the cell. This movement of $Na^+$ ions constitutes an ionic current, which further reduces the membrane barrier to $Na^+$ ions. This leads to an avalanche effect: $Na^+$ ions rush into the cell. $K^+$ ions try to leave the cell as they were in higher concentration inside the cell in the preceding resting state, but cannot move as fast as the $Na^+$ ions. The net result is that the inside of the cell becomes positive with respect to the outside due to an imbalance of $K^+$ ions. A new state of equilibrium is reached after the rush of $Na^+$ ions stops. This change represents the beginning of the *action potential*, with a peak value of about $+20\ mV$ for most cells. An excited cell displaying an action potential is said to be *depolarized*; the process is called *depolarization.* Figure 1.5 shows a schematic representation of a cell undergoing the process of depolarization.

**Repolarization:** After a certain period of being in the depolarized state the cell becomes polarized again and returns to its resting potential via a process known as *repolarization.* Repolarization occurs by processes that are analogous to those of depolarization, except that instead of $Na^+$ ions, the principal ions involved in repolarization are $K^+$ ions [16]. Membrane depolarization, while increasing the permeability for $Na^+$ ions, also increases the permeability of the membrane for $K^+$ ions via a specific class of ion channels known as voltage-dependent $K^+$ channels. Although this may appear to be paradoxical at first glance, the key to the mechanism for repolarization lies in the time-dependence and voltage-dependence of the membrane permeability changes for $K^+$ ions compared with those for $Na^+$ ions. The permeability changes for $K^+$ during depolarization occur considerably more slowly than those for $Na^+$ ions; hence, the initial depolarization is caused

by an inrush of $Na^+$ ions. However, the membrane permeability changes for $Na^+$ spontaneously decrease near the peak of the depolarization process, while those for $K^+$ ions are beginning to increase. Hence, during repolarization, the predominant membrane permeability is for $K^+$ ions. Because $K^+$ concentration is much higher inside the cell than outside, there is a net efflux of $K^+$ from the cell, which makes the inside more negative, thereby effecting repolarization back to the resting potential.

It should be noted that the voltage-dependent $K^+$ permeability change is due to a distinctly different class of ion channels than those that are responsible for setting the resting potential. A mechanism known as the $Na^+ - K^+$ pump extrudes $Na^+$ ions in exchange for transporting $K^+$ ions back into the cell. However, this transport mechanism carries very little current in comparison with ion channels, and therefore, makes a minor contribution to the repolarization process. The $Na^+ - K^+$ pump is essential to reset the $Na^+ - K^+$ balance of the cell, but the process occurs on a longer time scale than the duration of an action potential.

Nerve and muscle cells repolarize rapidly, with an action potential duration of about $1 - 5\ ms$. Heart muscle cells repolarize slowly, with an action potential duration of $150 - 300\ ms$.

The action potential is always the same for a given cell, regardless of the method of excitation or the intensity of the stimulus beyond a threshold: This is known as the *all-or-none* or all-or-nothing phenomenon. After an action potential, there is a period during which a cell cannot respond to any new stimulus, known as the *absolute refractory period* (about $1\ ms$ in nerve cells [19]). This is followed by a *relative refractory period* ($3 - 5\ ms$ in nerve cells), when another action potential may be triggered by a much stronger stimulus than in the normal situation [19]. Figure 1.6 shows the various phases or intervals of the action potential of a cardiac (ventricular) myocyte.

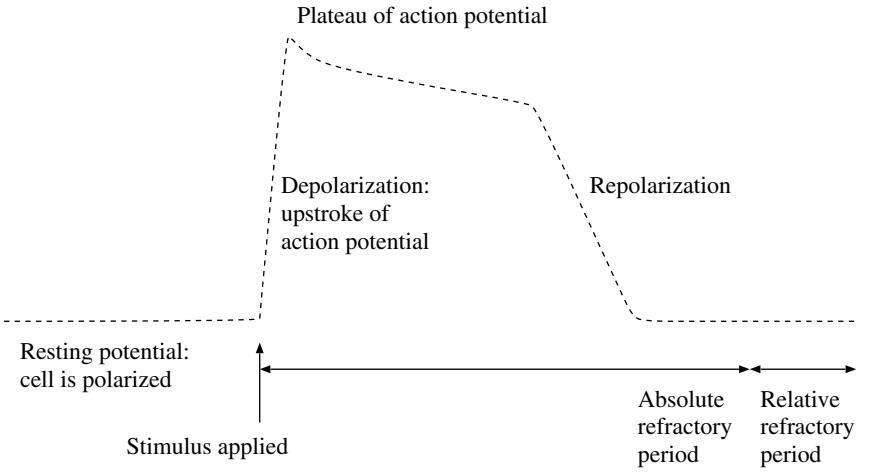


**Figure 1.6** Illustration of the various phases or intervals of the action potential of a cardiac (ventricular) myocyte. The absolute refractory period includes the duration of the action potential.

Figure 1.7 shows action potentials recorded from individual rabbit ventricular and atrial myocytes (muscle cells) [16]. Figure 1.8 shows a ventricular myocyte in its relaxed and fully contracted states. The tissues were first incubated in digestive enzymes, principally collagenase, and then dispersed into single cells using gentle mechanical agitation. The recording electrodes were glass patch pipettes; a whole-cell, current-clamp recording configuration was used to obtain the action potentials. The cells were stimulated at low rates (once per $8\ s$); this is far less than physiological rates. Moreover, the cells were maintained at $20\ ^\circ C$, rather than at body temperature. Nevertheless, the major features of the action potentials shown are similar to those recorded under physiological conditions.

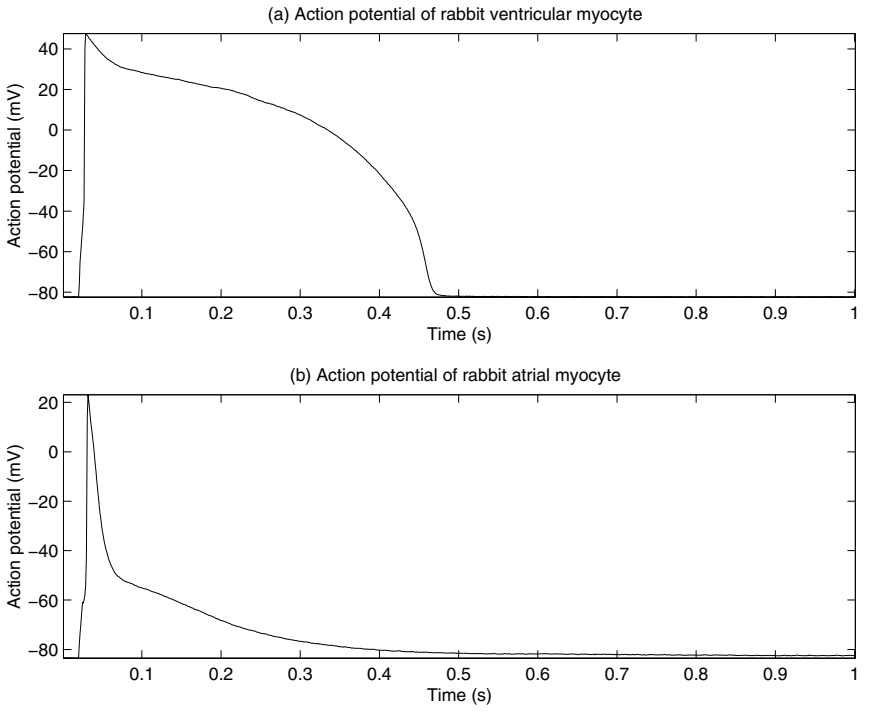


**Figure 1.7** Action potentials of rabbit ventricular and atrial myocytes. Data courtesy of R. Clark, Department of Physiology and Biophysics, University of Calgary.

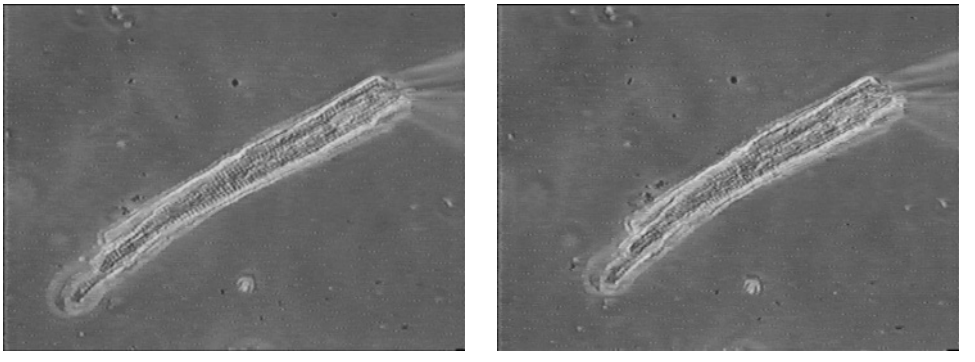

(a) (b)

**Figure 1.8** A single ventricular myocyte of a rabbit in its (a) relaxed state and (b) fully contracted state. The length of the myocyte is approximately 25 $\mu m$. The tip of the glass pipette, faintly visible at the upper-right end of the myocyte, is approximately 2 $\mu m$ wide. Images courtesy of R. Clark, Department of Physiology and Biophysics, University of Calgary.

The resting membrane potential of the cells (from 0 to 20 $ms$ in the plots in Figure 1.7) is about $-83\ mV$. A square pulse of current, 3 $ms$ in duration and 1 $nA$ in amplitude, was passed through the recording electrode and across the cell membrane, causing the cell to depolarize rapidly. The ventricular myocyte exhibits a depolarized potential of about $+40\ mV$; it then slowly declines back to the resting potential level over an interval of about $500\ ms$. The initial rapid depolarization of the atrial cell is similar to that of the ventricular cell, but does not overshoot zero membrane potential as much as the ventricular action potential; repolarization occurs much more quickly than the case for the ventricular cell.

Figure 1.9 shows a schematic representation of a cell as a system. When a stimulus is applied, the cell provides a response or output. Depending on the nature of the cell, such as a nerve cell or a muscle cell, the output could be an action potential, a twitch, or contraction (change in length). When several muscle cells are stimulated, the net result is the development of force.

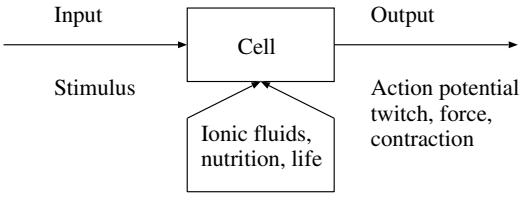


**Figure 1.9** Schematic representation of a cell as a system. Upon receiving an input of a stimulus, the cell provides a response that could cause an action potential, a twitch, contraction, or force. The term "life" indicates that the cell must be alive naturally, or maintained so under laboratory conditions, in order to function. Ionic fluids and nutrition provide the support and environment that are essential for the cell.

See Section 7.8 for further discussions on this subject.

### 1.2.2 The action potential of a neuron

The neuron is one of the basic units or structures of the nervous system. The basic function of a neuron may be considered to be information processing and transmission. Figure 1.10 shows a schematic representation of a neuron and its constituent parts. A neuron receives inputs from other neurons or cells through its dendrites. When adequate inputs or stimuli are received, the neuron is triggered and generates an action potential. The signal generated by the neuron is communicated to other neurons or cells through its axon. A few examples of the functions of networks of neurons are: collection of signals from sensors, such as the eyes and ears, followed by coding and transmission to the brain; processing, analysis, and interpretation of signals and information received in the brain; and communication of activation or control signals from the brain and spinal cord to muscles and other systems.

In studies of the central nervous system (CNS), it is desirable to record the action potentials of isolated neurons *in situ*. Hodgkin and Huxley [11, 12] conducted pioneering studies on recording action potentials from the giant axon of the squid; they proposed mathematical and electrical circuit models for the generation of action potentials. Figure 1.11 shows the first recording of the action potential of a neuron published by Hodgkin and Huxley [11]. While the action potential demonstrates the upstroke of depolarization and the return to resting potential via repolarization, the shape and duration are different from those of the action potentials of the cardiac myocytes shown in Figure 1.7. Hodgkin and Huxley also noted variations in the characteristics of the action potentials of neurons due to temperature. See Section 7.8.1 for further related discussions.

Drake et al. [20] described the design and performance of a multisite microprobe system to record isolated and interrelated neuronal activity *in vivo*. Figure 1.12 shows a sample recording obtained from a rat's brain (cerebral cortex) using the microprobe. It was observed that the waveforms and

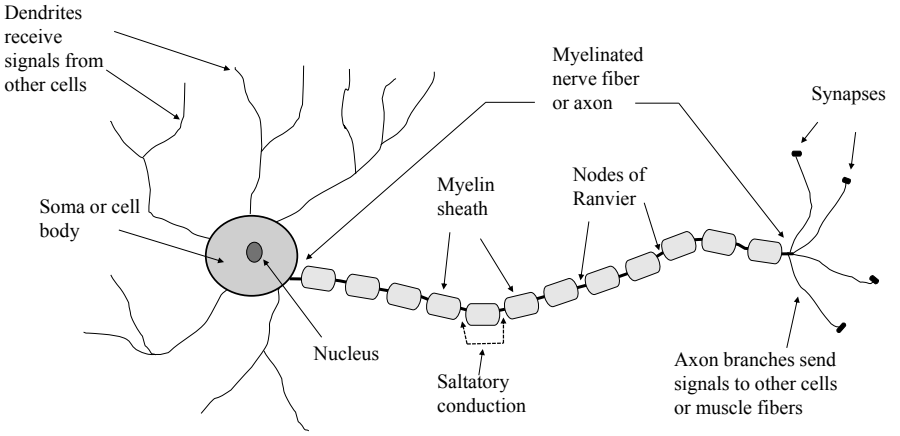


**Figure 1.10** Schematic representation of a neuron.

durations of neuronal action potentials recorded with the microprobe were similar to those measured using single-needle microelectrodes [21]. Note that the durations of the neuronal action potentials are much shorter than those of cardiac myocytes. The study demonstrated the possibility of observing simultaneous spatiotemporal patterns of extracellular single-unit action potentials, which could be used to investigate the columnar organization and layering of cortical tissue. Furthermore, it was indicated that the microprobe could be useful in the exploration of the characteristics of extracellular fields around an active neuron.

**Propagation of an action potential:** An action potential propagates along a muscle fiber or an unmyelinated nerve fiber as explained in the following sentences [22]. Once initiated by a stimulus, the action potential propagates along the whole length of a fiber without decrease in amplitude by progressive depolarization of the membrane. Current flows from a depolarized region through the intracellular fluid to adjacent inactive regions, thereby depolarizing them. Current also flows through the extracellular fluids, through the depolarized membrane, and back into the intracellular space, completing the local circuit. The energy to maintain conduction is supplied by the fiber itself.

Myelinated nerve fibers are covered by an insulating sheath of *myelin*; see Figure 1.10. The sheath is interrupted every few millimeters by spaces known as the *nodes of Ranvier*, where the fiber is exposed to the interstitial fluid. Sites of excitation and changes of membrane permeability exist only at the nodes, and current flows by jumping from one node to the next in a process known as *saltatory conduction*.

### 1.2.3 The electroneurogram (ENG)

The ENG is an electrical signal observed as a stimulus and the associated action potential propagate over the length of a nerve. It may be used to measure the velocity of propagation (or conduction velocity) of a stimulus or action potential in a nerve [13, 23, 24]. ENGs may be recorded using concentric needle electrodes or silver–silver-chloride electrodes ($Ag - AgCl$) at the surface of the body.

The conduction velocity in a peripheral nerve may be measured by stimulating a motor nerve and measuring the related activity at two points that are a known distance apart along its course. In order to minimize muscle contraction and other undesired effects, the experimental limb is held in

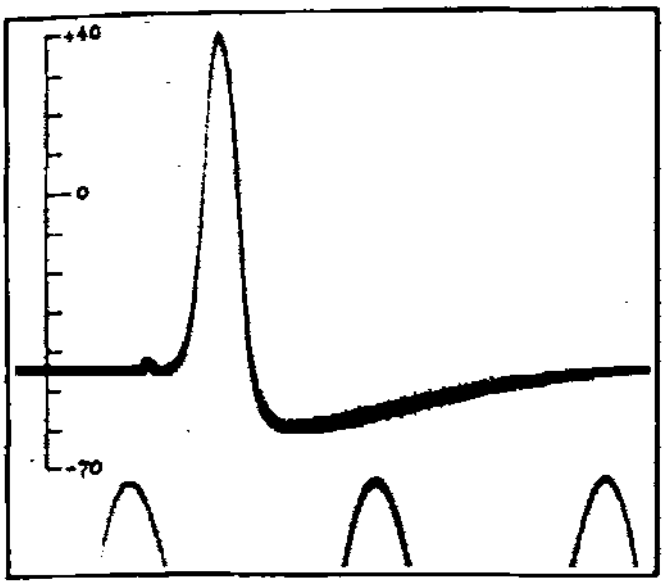


**Figure 1.11** First known tracing of an action potential recorded from the axon of a squid by Hodgkin and Huxley [11]. The vertical axis is in the range $-70$ to $+40$ $mV$ and the time calibration waveform shown at the bottom is a sinusoid of frequency $500$ $Hz$. Reproduced with permission from A.L. Hodgkin and A.F. Huxley. Action potentials recorded from inside a nerve fibre, *Nature*, 144:710–711, 1939. ©Springer Nature.

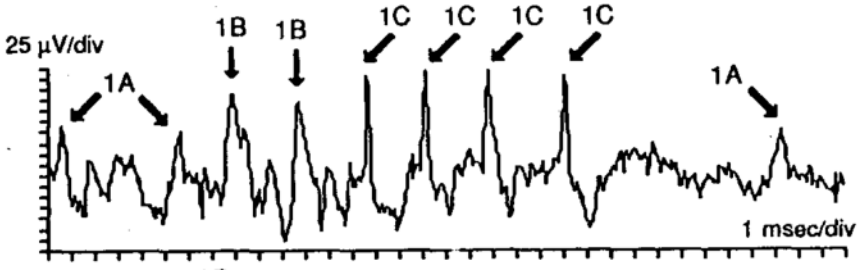


**Figure 1.12** Neuronal action potentials recorded from a rat's brain using a multisite microprobe system. The action potentials marked 1A have low amplitude, just above the baseline neural noise level. The action potentials marked 1B possess broader waveforms and could possibly be composed of two superimposed action potentials. The action potentials marked 1C are clearly isolated, have the same amplitude, and are likely from the same cell. Reproduced with permission from K.L. Drake, K.D. Wise, J. Farraye, D.J. Anderson, and S.L. BeMent, Performance of planar multisite microprobes in recording extracellular single-unit intracortical activity, *IEEE Transactions on Biomedical Engineering*, 35(9):719–732, 1988. ©IEEE.

a relaxed posture and a strong but short stimulus is applied in the form of a pulse of about $100$ $V$ amplitude and $100 - 300$ $\mu s$ duration [13, 23, 24]. The difference in the latencies of the ENGs recorded over the associated muscle gives the conduction time. Knowing the separation distance between the stimulating and recording sites, it is possible to determine the conduction velocity in the nerve [13,23,24]. ENGs have amplitudes of the order of $10$ $\mu V$ and are susceptible to power-line interference and instrumentation noise.

Figure 1.13 illustrates the ENGs recorded in a study of nerve conduction velocity. The stimulus was applied to the ulnar nerve near the wrist. The ENGs were recorded at the wrist (marked "Wrist" in the figure), just below the elbow (BElbow), and just above the elbow (AElbow) using surface

electrodes, amplified with a gain of $2,000$, and filtered to the bandwidth $10 - 10,000\ Hz$. The three traces in the figure indicate increasing latencies with respect to the stimulus time point, which is at the left-hand margin of the plots. The responses shown in the figure are normal, indicate a BElbow–Wrist latency of $3.23\ ms$, and result in a nerve conduction velocity of $64.9\ m/s$.

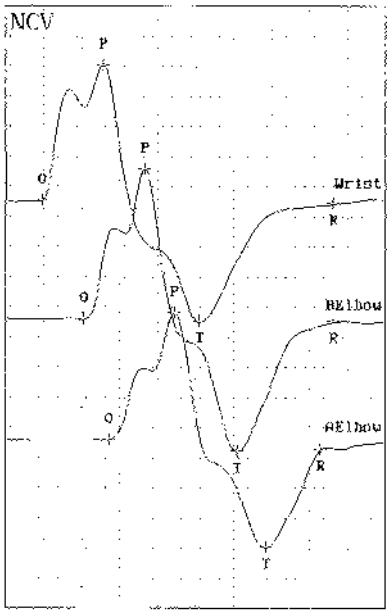


**Figure 1.13** Nerve conduction velocity (NCV) measurement via electrical stimulation of the ulnar nerve. The grid boxes represent $3\ ms$ in width and $2\ \mu V$ in height. AElbow: above the elbow. BElbow: below the elbow. O: onset. P: Peak. T: trough. R: recovery of baseline. Courtesy of M. Wilson and C. Adams, Alberta Children's Hospital, Calgary.

Typical values of propagation rate or nerve conduction velocity are [13, 22, 25]:

- $45 - 70\ m/s$ in nerve fibers;
- $0.2 - 0.4\ m/s$ in heart muscle;
- $0.03 - 0.05\ m/s$ in the time-delay fibers between the atria and the ventricles (AV node).

Neural diseases may cause a decrease in conduction velocity.

### 1.2.4 The electromyogram (EMG)

Skeletal muscle fibers are considered to be twitch fibers because they produce a mechanical twitch response for a single stimulus and generate a propagated action potential. Skeletal muscles are made up of collections of *motor units*, each of which consists of an anterior horn cell (motoneuron or motor neuron), its axon, and all muscle fibers innervated by that axon [26–28]. A motor unit is the smallest muscle unit that can be activated by volitional effort. The constituent fibers of a motor unit are activated synchronously. Component fibers of a motor unit extend lengthwise in loose bundles along the muscle. In cross-section, the fibers of a given motor unit are interspersed with the fibers of other motor units [13,22,29]. Figure 1.14 shows a schematic representation of two motor units. Figure 1.15 (top panel) illustrates a motor unit in schematic form along with related models [29]. When stimulated by a neural signal, each motor unit contracts and causes an electrical

signal that is the summation of the action potentials of all of its constituent cells. This is known as the *single-motor-unit action potential* (SMUAP, or simply MUAP) and may be recorded using needle electrodes inserted into the muscle or region of interest.

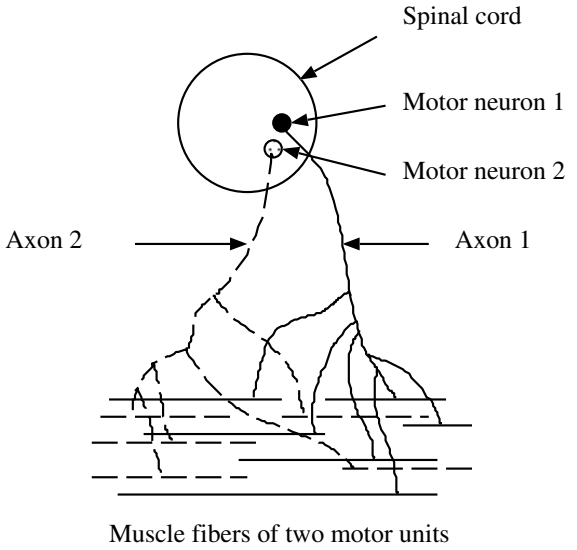


**Figure 1.14** Schematic representation of two motor units, one in solid line and the other in dashed line.

Muscles for gross movement or large force have hundreds of muscle fibers per motor unit; muscles for precise or fine movement have fewer fibers per motor unit. The number of muscle fibers per motor nerve fiber (or motor unit) is known as the *innervation ratio.* The mechanical output (contraction) of a muscle is the net result of stimulation and contraction of several of its motor units.

Various experiments have been conducted to estimate the innervation ratios of several muscles in animals and human beings, *in vivo* and using autopsy samples, with some variations in the methods and definitions used. Goodgold and Eberstein [22] and Kimura [19] provide tables including the following examples. The platysma (a large sheet-like muscle spanning parts of the pectoral muscle, deltoid, clavicle, and neck) has $1,826$ large nerve fibers controlling $27,100$ muscle fibers in $1,096$ motor units, leading to an estimate of about $25$ muscle fibers per motor unit. The first dorsal interosseus (FDI) muscle (on the back of the palm of the hand and the index finger) has $199$ large nerve fibers and $40,500$ muscle fibers in $119$ motor units, with about $340$ muscle fibers per motor unit. The medial gastrocnemius (calf muscle of the leg) has $965$ large nerve fibers and $1,120,000$ muscle fibers in $579$ motor units, with about $1,934$ muscle fibers per motor unit.

Laryngeal muscles have been estimated to have only two or three muscle fibers per motor unit [22]. Gath and Stålberg [30] used a multielectrode probe for *in situ* measurement of the innervation ratios of human muscles; they estimated the number of muscle fibers per motor unit to be $72$ in the brachial biceps, $70$ in the deltoid, and $124$ in the tibialis anterior. Brown and Harvey [27] studied the muscles of cats' eyes and noted that not more than $10$ muscle fibers are supplied by a single nerve fiber in the extrinsic ocular muscles. See Goodgold and Eberstein [22], Kimura [19], Buchthal and Schmalbruch [26], and Brown et al. [28] for related discussions.

Normal SMUAPs are usually biphasic or triphasic, $3-15\ ms$ in duration, $100-300\ \mu V$ in amplitude, and appear with frequency in the range of $6-30/s$ [13, 22]. Schematic representations of monophasic, biphasic, and triphasic waveforms are shown in Figure 1.16. The shape of a recorded SMUAP depends on the type of the needle electrode used, its position with respect to the active

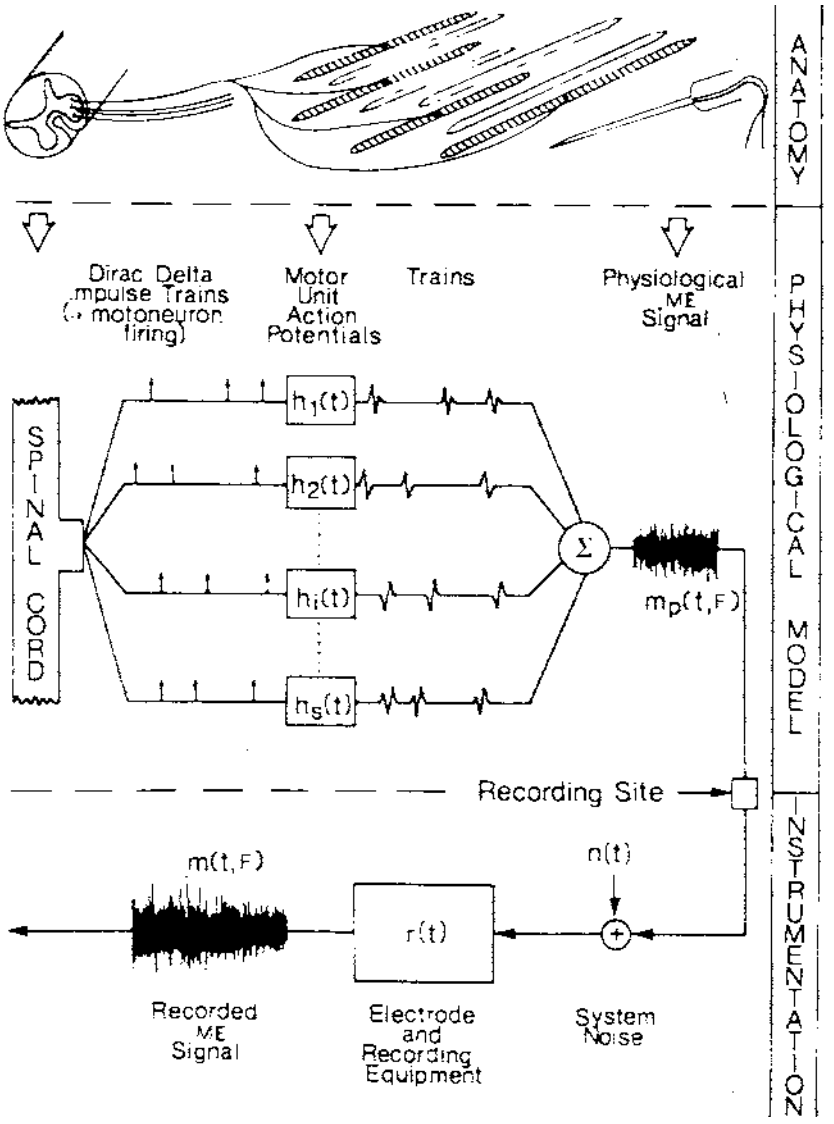


**Figure 1.15** Schematic representation of a motor unit and model for the generation of EMG signals. Top panel: A motor unit includes an anterior horn cell or motor neuron (illustrated in a cross-section of the spinal cord), an axon, and several connected muscle fibers. The hatched fibers belong to one motor unit; the nonhatched fibers belong to other motor units. A needle electrode is also illustrated. Middle panel: The firing pattern of each motor neuron is represented by an impulse train. Each system $h_i(t)$ shown represents a motor unit that is activated and generates a train of SMUAPs. The net EMG is the sum of several SMUAP trains. Bottom panel: Effects of instrumentation on the EMG signal acquired. The observed EMG is a function of time $t$ and muscular force produced $F$. ME: myoelectric. Reproduced with permission from C.J. de Luca, Physiology and mathematics of myoelectric signals, *IEEE Transactions on Biomedical Engineering,* 26:313–325, 1979. ©IEEE.

motor unit, and the projection of the electrical field of the activity on to the electrodes. Figure 1.17 illustrates simultaneous recordings of the activities of a few motor units from three channels of needle electrodes [31]. Although the SMUAPs are biphasic or triphasic, the same SMUAP displays variable shape from one channel to another. (*Note:* The action potentials in Figure 1.7 are monophasic; the first two SMUAPs in Channel 1 in Figure 1.17 are biphasic, and the third SMUAP in the same signal is triphasic.)

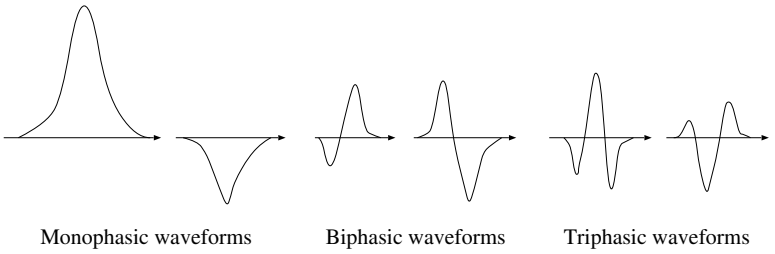


**Figure 1.16** Schematic representations of monophasic, biphasic, and triphasic waveforms.

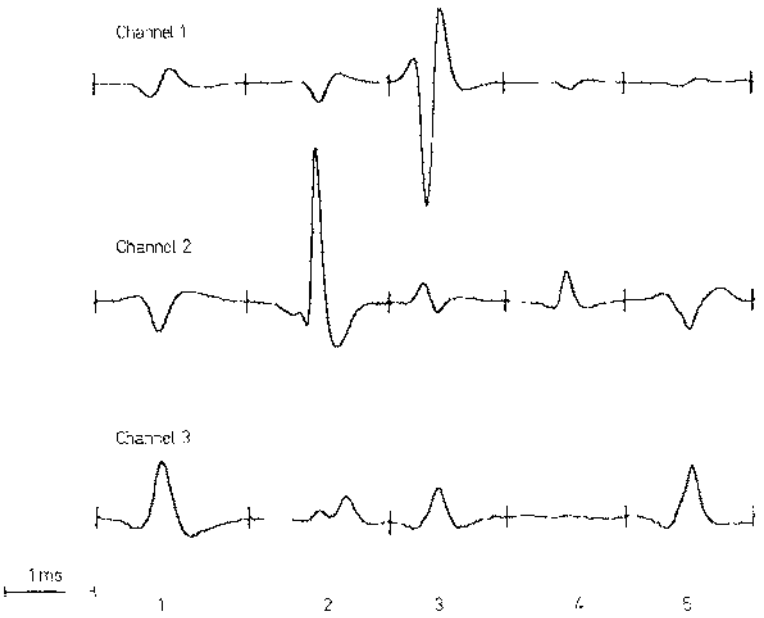


**Figure 1.17** SMUAP trains recorded simultaneously from three channels of needle electrodes. Observe the different shapes of the same SMUAPs (aligned vertically across the three channels) projected on to the axes of the three channels. Three different motor units are active over the duration of the signals illustrated. Reproduced with permission from B. Mambrito and C.J. de Luca, Acquisition and decomposition of the EMG signal, in *Progress in Clinical Neurophysiology*, Volume 10: *Computer-aided Electromyography*, Editor: J.E. Desmedt, pp 52–72, 1983. ©S. Karger AG, Basel, Switzerland.

The shape of SMUAPs is affected by disease. Figure 1.18 illustrates SMUAP trains of a normal subject and those of patients with neuropathy and myopathy. Neuropathy causes slow conduction and/or desynchronized activation of the fibers within a motor unit, and a polyphasic SMUAP with an amplitude that is larger than normal. The same motor unit may be observed to fire at higher rates than normal before more motor units are recruited. Myopathy involves loss of muscle fibers

in motor units, with the related motoneuron and nerves presumably intact. *Splintering* of SMUAPs occurs due to asynchrony in activation as a result of patchy destruction of fibers (such as the case in muscular dystrophy), leading to polyphasic SMUAPs. More motor units may be observed to be recruited at low levels of effort.

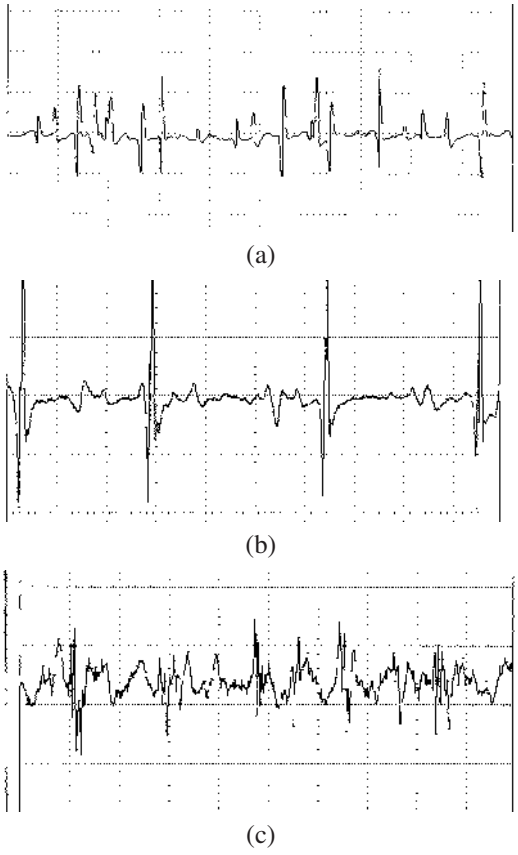


**Figure 1.18** Examples of SMUAP trains. (a) From the right deltoid of a normal subject, male, 11 years; the SMUAPs are mostly biphasic, with duration in the range $3-5\ ms$. (b) From the deltoid of a six-month-old male patient with brachial plexus injury (neuropathy); the SMUAPs are polyphasic and large in amplitude ($800\ \mu V$), and the same motor unit is firing at a relatively high rate at low-to-medium levels of effort. (c) From the right biceps of a 17-year-old male patient with myopathy; the SMUAPs are polyphasic and indicate early recruitment of more motor units at a low level of effort. The signals were recorded with gauge 20 needle electrodes. The width of each grid box represents a duration of $20\ ms$; its height represents an amplitude of $200\ \mu V$. Courtesy of M. Wilson and C. Adams, Alberta Children's Hospital, Calgary.

**Gradation of muscular contraction:** Muscular contraction levels are controlled in two ways:

- *Spatial recruitment,* by activating new motor units with increasing effort; and
- *Temporal recruitment,* by increasing the frequency of discharge (firing rate) of each motor unit with increasing effort.

Figure 1.19 gives a schematic illustration of spatiotemporal recruitment of motor units and the related EMG signals. Motor units are activated at different times and at different frequencies causing asynchronous contraction. The twitches of individual motor units sum and fuse to form tetanic contraction and increased force. Weak volitional effort causes motor units to fire at about $5-15\ pps$

(pulses per second). As greater tension is developed, an *interference pattern* EMG is obtained, with the constituent and active motor units firing in the range of $25 - 50\ pps$. Grouping of MUAPs has been observed as fatigue develops, leading to decreased high-frequency content and increased amplitude in the EMG [29].

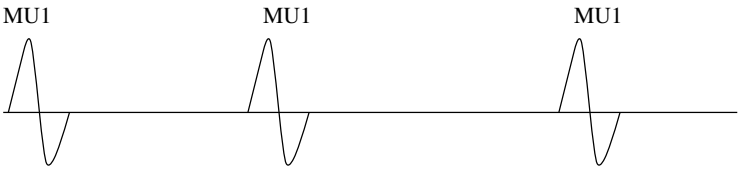


(a) At the beginning with low effort, only motor unit MU1 is firing at a low rate.

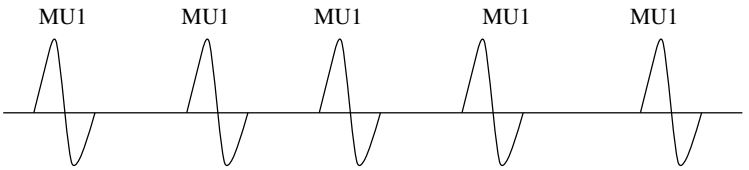


(b) At a slightly higher level of effort, with temporal recruitment, the firing rate of MU1 is increased. No other motor unit has been recruited yet.

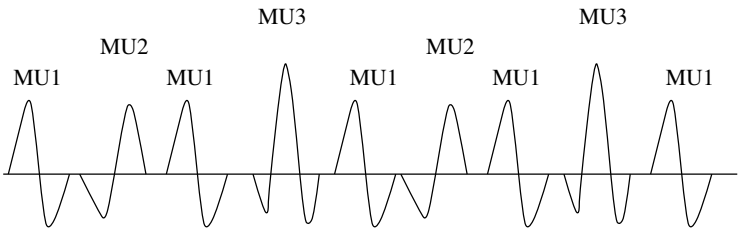


(c) At an even higher level of effort, with spatial recruitment, new motor units MU2 and MU3 have been brought into action. MU1 continues to fire at the same rate as in (b).

**Figure 1.19** Schematic representation of spatiotemporal recruitment of motor units and the resulting EMG signals. To keep the illustration simple, it is assumed that the MUAPs do not overlap.

Spatiotemporal summation of the MUAPs of all of the active motor units gives rise to the EMG of the muscle; see Figure 1.19. EMG signals recorded using surface electrodes are complex signals including interference patterns of several MUAP trains and are difficult to analyze. An EMG signal indicates the level of activity of a muscle, and may be used to diagnose neuromuscular diseases such as neuropathy and myopathy.

Figure 1.20 illustrates an EMG signal recorded from the crural diaphragm of a dog using fine-wire electrodes sewn in-line with the muscle fibers and placed $10\ mm$ apart [32]. The signal represents one period of breathing (inhalation being the active part as far as the muscle and EMG are concerned). It is seen that the overall level of activity in the signal increases during the initial phase of inhalation. Figure 1.21 shows the early parts of the same signal on an expanded time scale. SMUAPs are seen at the beginning stages of contraction, followed by increasingly complex interference patterns of several MUAPs.

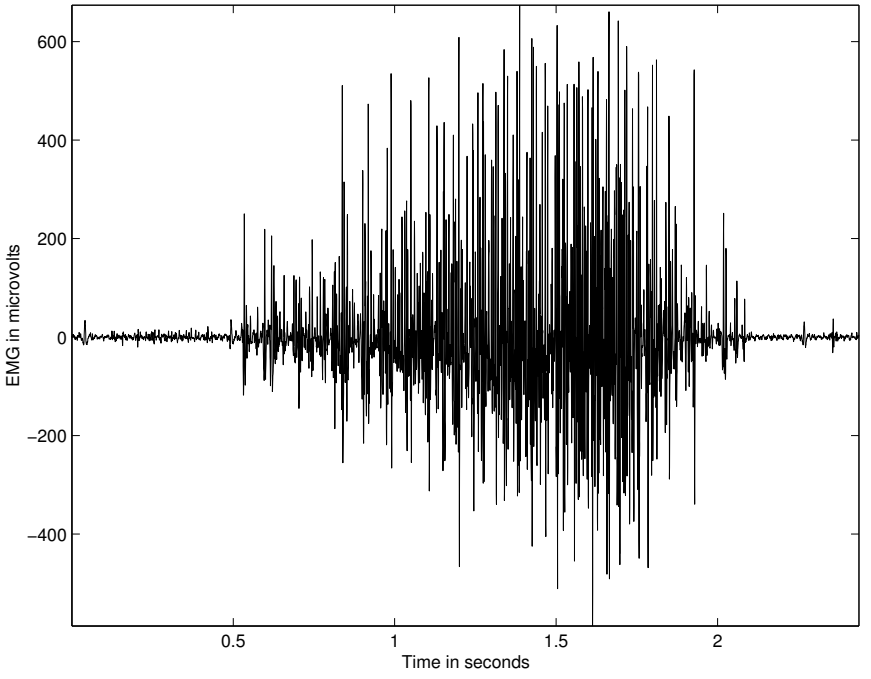


**Figure 1.20** EMG signal recorded from the crural diaphragm muscle of a dog using implanted fine-wire electrodes; see also Figure 1.21. Data courtesy of R.S. Platt and P.A. Easton, Department of Clinical Neurosciences, University of Calgary.

Figure 1.22 shows an EMG signal recorded using surface electrodes placed on the forearm of a subject. In this experiment, designed to study the variation of the EMG signal with respect to the force exerted by a muscle, the subject performed a series of contractions using a gripping device equipped with a force transducer. (The output of the transducer was not calibrated in units of force.) The subject was instructed to squeeze the gripping device to the maximum extent possible; the corresponding output was noted as the level of maximal voluntary contraction (MVC). The subject was then asked to relax the muscle, and squeeze the device again in five steps, between approximately $20\%$ and $100\%$ MVC, each contraction lasting for about $2-3\ s$, with resting periods of about $2-3\ s$ between each contraction. The EMG and force signals were lowpass filtered with the cutoff frequency at $1\ kHz$, highpass filtered with the cutoff frequency at $10\ Hz$, and recorded at the sampling rate of $2\ kHz$ per channel. In the plot shown in Figure 1.22, the force signal has been normalized such that the minimum is zero and the maximum is $100$; thus, the force exerted is expressed in %MVC. It is evident that the dynamic range (peak-to-peak swing) and power of the EMG signal increase as the level of force exerted increases. Figure 1.23 shows as expanded view of the period $10-12\ s$ of the force and EMG signals, where the increasing trend of the EMG signal with increasing force is clearly seen.

Signal processing techniques for the analysis of EMG signals are described in Sections 5.2.4, 5.6, 5.9, 5.10, 5.11, 5.13.4, 7.2.1, and 7.3. See Nikolic and Krarup [33] for the description of methods for decomposition of EMG signals into their constituent MUAPs and firing patterns for quantitative analysis. EMG signals are useful in the control of prosthetic devices [34, 35].

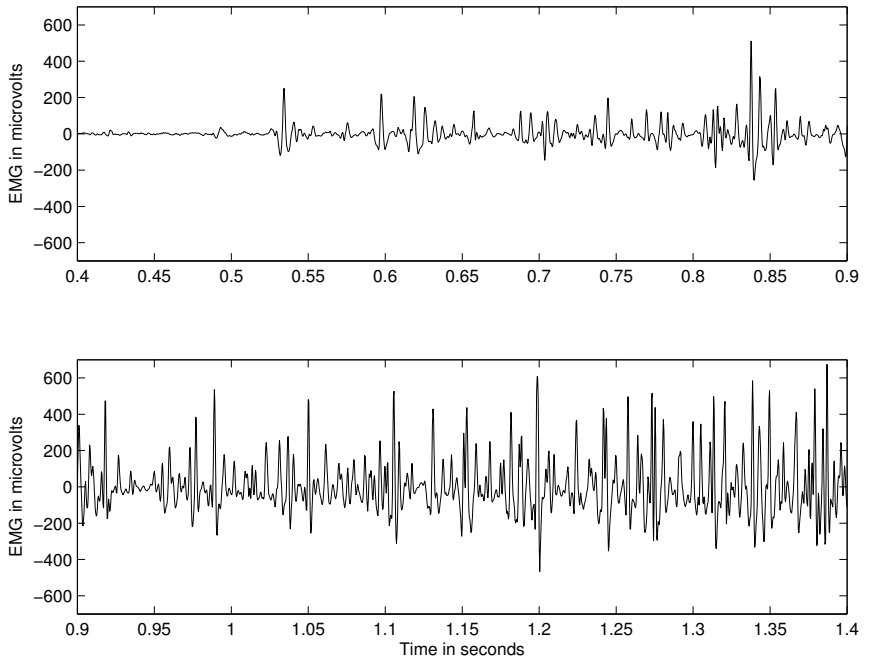


**Figure 1.21** The initial part of the EMG signal in Figure 1.20 shown on an expanded time scale. Observe the SMUAPs at the initial stages of contraction, followed by increasingly complex interference patterns of several MUAPs. Data courtesy of R.S. Platt and P.A. Easton, Department of Clinical Neurosciences, University of Calgary.

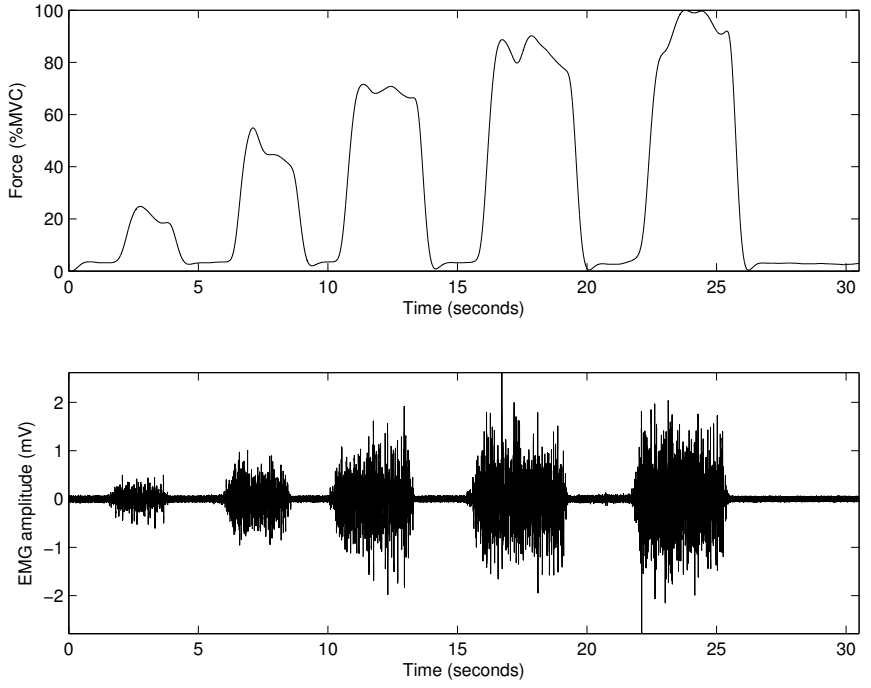


**Figure 1.22** Force signal (upper plot) and the EMG signal (lower plot) recorded from the forearm muscle of a subject using surface electrodes; see also Figure 1.23. Data courtesy of Shantanu Banik.

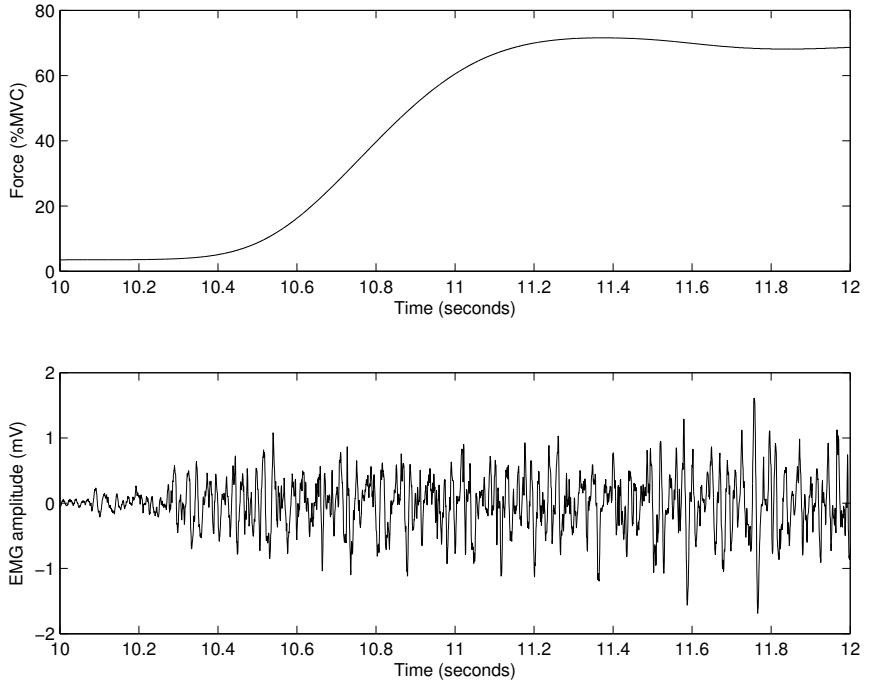


**Figure 1.23** Expanded view of the part of the EMG (lower plot) and force signals (upper plot) in Figure 1.22 over the period $10 - 12$ $s$. Observe the increasing levels of the range and power of the EMG signal at the initial stages of contraction. Data courtesy of Shantanu Banik.

### 1.2.5 The electrocardiogram (ECG)

The ECG is the electrical manifestation of the contractile activity of the heart and can be recorded fairly easily with surface electrodes on the limbs or chest. The ECG is the most commonly known, recognized, and used biomedical signal. Original investigations on recording of the human ECG were conducted by Waller [36] and Einthoven [37] in the late 1800s and the early 1900s.

The rhythm of the heart in terms of beats per minute (*bpm*) may be easily estimated by counting the readily identifiable waves in the ECG signal. More important is the fact that the ECG waveshape is altered by cardiovascular diseases and abnormalities, such as myocardial ischemia, myocardial infarction, ventricular hypertrophy, and conduction problems.

**The heart:** The heart is a four-chambered pump with two atria for collection of blood and two ventricles to pump out blood. Figure 1.24 shows a schematic representation of the four chambers and the major vessels connecting to the heart. The resting or filling phase of a cardiac chamber is called *diastole*; the contracting or pumping phase is called *systole*.

The right atrium (or auricle) collects deoxygenated blood from the superior and inferior vena cavae. During atrial contraction, blood is passed from the right atrium to the right ventricle through the tricuspid valve. During ventricular systole, the deoxygenated blood in the right ventricle is pumped out through the pulmonary valve to the lungs for oxygenation.

The left atrium receives oxygenated blood from the lungs, which is passed on during atrial contraction to the left ventricle via the mitral valve. The left ventricle is the largest and most important cardiac chamber. The left ventricle contracts the strongest among the cardiac chambers, as it has to pump out the oxygenated blood through the aortic valve and the aorta against the pressure of the rest of the vascular system of the body. Due to the higher level of importance of contraction of the ventricles, the terms systole and diastole are applied to the ventricles by default.

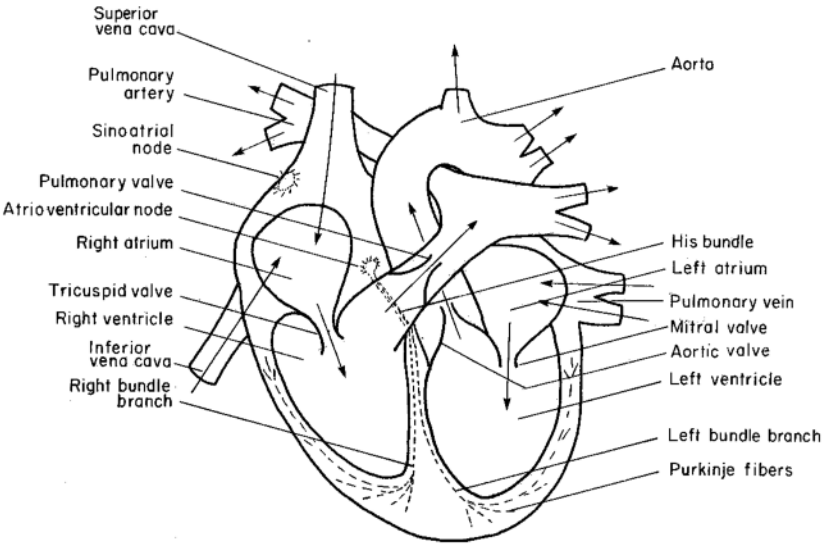


**Figure 1.24** Schematic representation of the chambers, valves, vessels, and conduction system of the heart.

The heart rate (HR) or cardiac rhythm is controlled by specialized pacemaker cells that form the sinoatrial (SA) node located at the junction of the superior vena cava and the right atrium [25]. The firing rate of the SA node is controlled by the autonomic nervous system (ANS) leading to the delivery of the neurotransmitters acetylcholine (for vagal stimulation, causing a reduction in heart rate) or epinephrine (for sympathetic stimulation, causing an increase in the heart rate). The normal (resting) heart rate is about $70\ bpm$. The heart rate is lower during sleep, but abnormally low heart rates below $60\ bpm$ during activity could indicate a disorder called *bradycardia*. The instantaneous heart rate could reach values as high as $200\ bpm$ during vigorous exercise or athletic activity; a high resting heart rate could be due to illness, disease, or cardiac abnormalities, and is termed *tachycardia*.

**The electrical system of the heart:** Coordinated electrical events and a specialized conduction system intrinsic and unique to the heart play major roles in the rhythmic contractile activity of the heart. The SA node is the basic, natural, cardiac pacemaker that triggers its own train of action potentials. The action potential of the SA node propagates through the rest of the heart, causing a particular pattern of excitation and contraction (see Figure 1.25). A schematic ECG signal is shown in Figure 1.26 with labels showing the names and durations of the various component waves. Also shown in the figure are representations of the action potentials of the atrial and ventricular myocytes. The sequence of events and waves in a cardiac cycle is as follows [25]:

1. The SA node fires.

2. Electrical activity is propagated through the atrial musculature at comparatively low rates, causing slow-moving depolarization (contraction) of the atria. This results in the P wave in the ECG (see Figures 1.26 and 1.27). Due to the slow contraction of the atria and their relatively small size, the P wave is a slow, low-amplitude wave, with an amplitude of about $0.1-0.2\ mV$ and a duration of about $60-80\ ms$.

3. The excitation wave faces a propagation delay at the atrioventricular (AV) node, which results in a normally isoelectric segment of about $60-80\ ms$ after the P wave in the ECG, known as

the PQ segment. The pause assists in the completion of the transfer of blood from the atria to the ventricles.

4. The AV node fires.

5. The His bundle, the bundle branches, and the Purkinje system of specialized conduction fibers propagate the stimulus to the ventricles at a high rate.

6. The wave of stimulus spreads rapidly from the apex (at the bottom) of the heart upwards, causing rapid depolarization (contraction) of the ventricles. This results in the QRS wave of the ECG — a sharp biphasic or triphasic wave of about $1\ mV$ amplitude and $80\ ms$ duration (see Figure 1.27).

7. The plateau portion of the action potential causes a normally isoelectric segment of about $100 - 120\ ms$ after the QRS, known as the ST segment; see Figure 1.26. This is because ventricular muscle cells possess a relatively long action potential duration of $300 - 350\ ms$ (see Figure 1.7).

8. Repolarization (relaxation) of the ventricles causes the slow T wave, with an amplitude of $0.1 - 0.3\ mV$ and duration of $120 - 160\ ms$ (see Figure 1.27).

A summary of the various events described above, represented as parts of a cardiac cycle in relation to an ECG signal, is given in Figure 1.28.

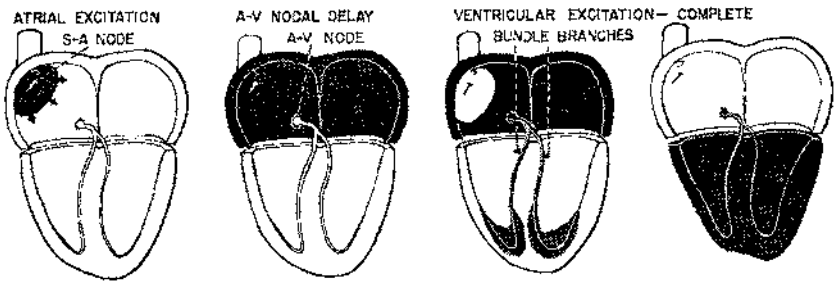


**Figure 1.25** Propagation of the excitation pulse through the heart. Reproduced with permission from R.F. Rushmer, *Cardiovascular Dynamics*, 4th edition, ©W.B. Saunders, Philadelphia, PA, 1976.

It should be noted that, whereas Figure 1.26 shows only one representative action potential each of an atrial myocyte and a ventricular myocyte, multitudes of such action potentials are produced in rapid succession. The action potentials of various cardiac myocytes project on to the axis of the ECG being recorded with varying scale factors (including negative values or reversal) and phase (or time delay). Thus, the shapes of various action potentials as projected on to the recording axis could be widely different (see Figure 1.17). For the same reasons, the waveform of an externally recorded ECG varies with the positions of the leads used, which essentially determine the recording axis.

Any disturbance in the regular rhythmic activity of the heart is called *arrhythmia*. Cardiac arrhythmia may be caused by irregular firing patterns from the SA node, or by abnormal and additional pacing activity from other parts of the heart. Many parts of the heart possess inherent rhythmicity and pacemaker properties, for example, the SA node, the AV node, the Purkinje fibers, atrial tissue, and ventricular tissue. If the SA node is inactive or depressed, any one of the above tissues may take over the role of the pacemaker or introduce *ectopic* beats. Different types of abnormal rhythm (arrhythmia) result from variations in the site and frequency of impulse formation. Premature ventricular contractions (PVCs) caused by ectopic foci on the ventricles upset the regular rhythm and may lead to ventricular dissociation and fibrillation — a state of disorganized contraction of the

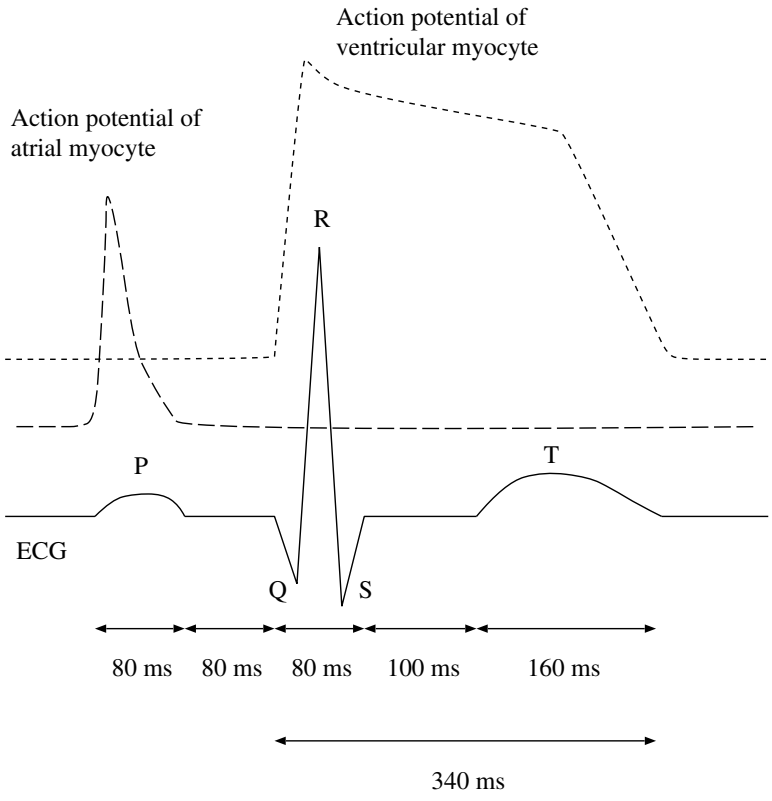


**Figure 1.26** Schematic representations of an ECG signal and the action potentials of atrial and ventricular myocytes. See also Figure 1.7.

ventricles independent of the atria — resulting in no effective pumping of blood and possibly death. The waveshapes of PVCs are usually substantially different from those of the normal beats of the same subject due to the different conduction paths of the ectopic impulses and the associated abnormal contraction events. Figure 1.29 shows an ECG signal with a few normal beats and two PVCs. (See Figure 10.10 for an illustration of ventricular bigeminy, where every second pulse from the SA node is replaced by a PVC with a full compensatory pause.)

The QRS waveshape is affected by conduction disorders; for example, bundle-branch block causes a widened and possibly jagged QRS. Figure 1.30 shows the ECG signal of a patient with right bundle-branch block. Observe the wider-than-normal QRS complex, which also displays a waveshape that is significantly different from normal QRS waves. Ventricular hypertrophy (enlargement) could also cause a wider-than-normal QRS.

The ST segment, which is normally isoelectric (flat and in-line with the PQ segment) may be elevated or depressed due to myocardial ischemia (reduced blood supply to a part of the heart muscles caused by a block in the coronary arteries) or due to myocardial infarction (total lack of blood supply leading to dead myocardial tissue or scar incapable of contraction). Many other diseases cause specific changes in the ECG waveshape: the ECG is an important signal that is useful in heart-rate (rhythm) monitoring and the diagnosis of cardiovascular diseases.

**ECG signal acquisition:** In clinical practice, the standard 12-lead ECG is obtained using four limb leads and chest leads in six positions [25, 38]. The right leg is used to place the reference (ground) electrode. The left arm, right arm, and left leg are used to obtain leads I, II, and III. The illustration in Figure 1.31 shows the limb leads used to acquire the commonly used lead II ECG.

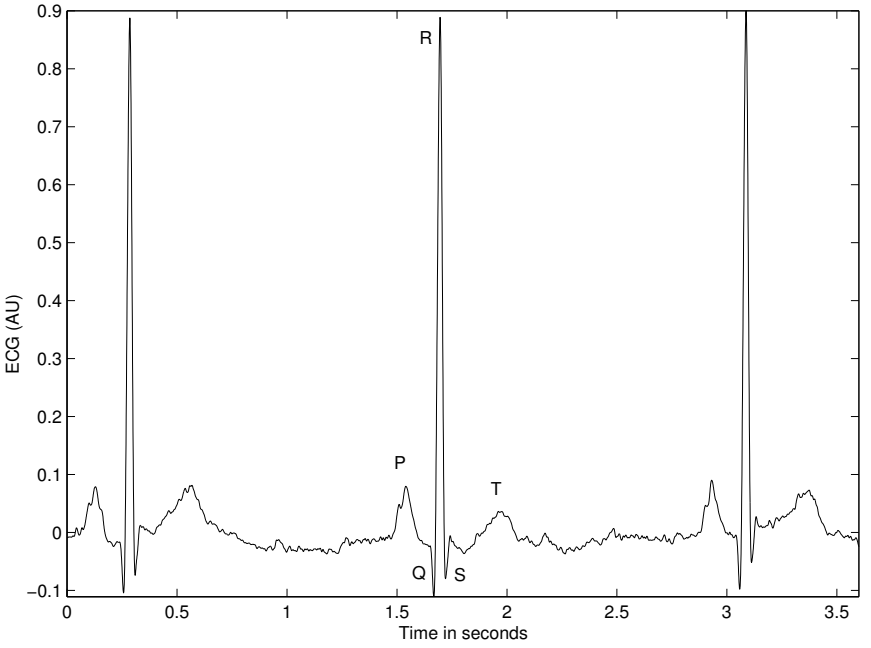


**Figure 1.27** A typical ECG signal (male subject of age 24 years). (*Note:* Signal values may not be calibrated, that is, specified in actual units, in some situations. Sometimes, the calibration details may be lost in the acquisition and processing steps. As is the case in this plot, signal values in plots in this book are in arbitrary units (AU) or normalized units unless specified.)

A combined reference known as *Wilson's central terminal* is formed by combining the left arm, right arm, and left leg leads; it is used as the reference for chest leads. The *augmented* limb leads known as aVR, aVL, and aVF (aV for augmented vector, R for the right arm, L for the left arm, and F for the left leg or foot) are obtained by using the exploring electrode on the limb indicated by the name of the lead, with the reference being Wilson's central terminal without the exploring limb lead.

Figure 1.32 shows the directions of the axes formed by the six limb leads. The hypothetical equilateral triangle formed by leads I, II, and III is known as *Einthoven's triangle.* The center of the triangle represents Wilson's central terminal. Schematically, the heart is assumed to be placed at the center of the triangle. The six leads measure projections of the three-dimensional (3D) cardiac electrical vector on to the axes illustrated in Figure 1.32. The six axes sample the $0^\circ - 180^\circ$ range in steps of approximately $30^\circ$. The projections facilitate viewing and analysis of the electrical activity of the heart from different perspectives in the frontal plane.

The six chest leads (written as V1–V6) are obtained from six standardized positions on the chest [25] with Wilson's central terminal as the reference. The positions for placement of the precordial (chest) leads are indicated in Figure 1.33. The V1 and V2 leads are placed at the fourth intercostal space just to the right and left of the sternum, respectively. V4 is recorded at the fifth intercostal space at the left midclavicular line. The V3 lead is placed half-way between the V2 and V4 leads. The V5 and V6 leads are located at the same level as the V4 lead, but at the anterior axillary line and the midaxillary line, respectively. The six chest leads permit viewing the cardiac electrical vector from different orientations in a cross-sectional plane: V5 and V6 are most sensitive to left-ventricular activity; V3 and V4 depict septal activity best; V1 and V2 reflect well activity in the right-half of the heart.

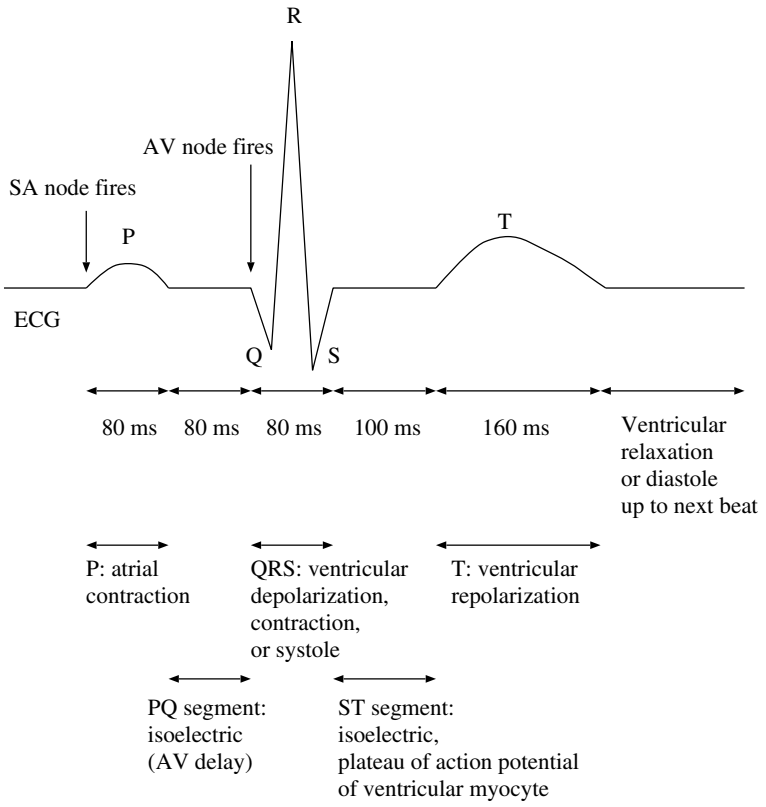


**Figure 1.28** Summary of the parts and waves of a cardiac cycle as seen in an ECG signal.

In spite of being redundant, the 12-lead system serves as the basis of the standard clinical ECG. Clinical ECG interpretation is mainly empirical. A compact and efficient system has been proposed for *vectorcardiography* or VCG [25, 39], where loops inscribed by the 3D cardiac electrical vector in three mutually orthogonal planes, namely, the frontal, horizontal, and sagittal planes, are plotted and analyzed. Regardless, the 12-lead scalar ECG is the most commonly used procedure in clinical practice.

Because an external ECG is a projection of the internal 3D cardiac electrical vector, external ECG recordings are not unique. Some of the lead interrelationships are [25, 38]:

- II = I + III,
- aVL = ( I − III ) / 2,

which are depicted in Figures 1.34 and 1.35.

Some of the important features of the standard clinical ECG are:

- A rectangular calibration pulse of $1\ mV$ amplitude and $200\ ms$ duration is applied to produce a pulse of $1\ cm$ height on the plot.
- The typical recording speed used is $25\ mm/s$, resulting in a graphical scale of $0.04\ s/mm$ or $40\ ms/mm$. Then, the width of the calibration pulse is $5\ mm$.
- The ECG signal peak value is normally about $1\ mV$.

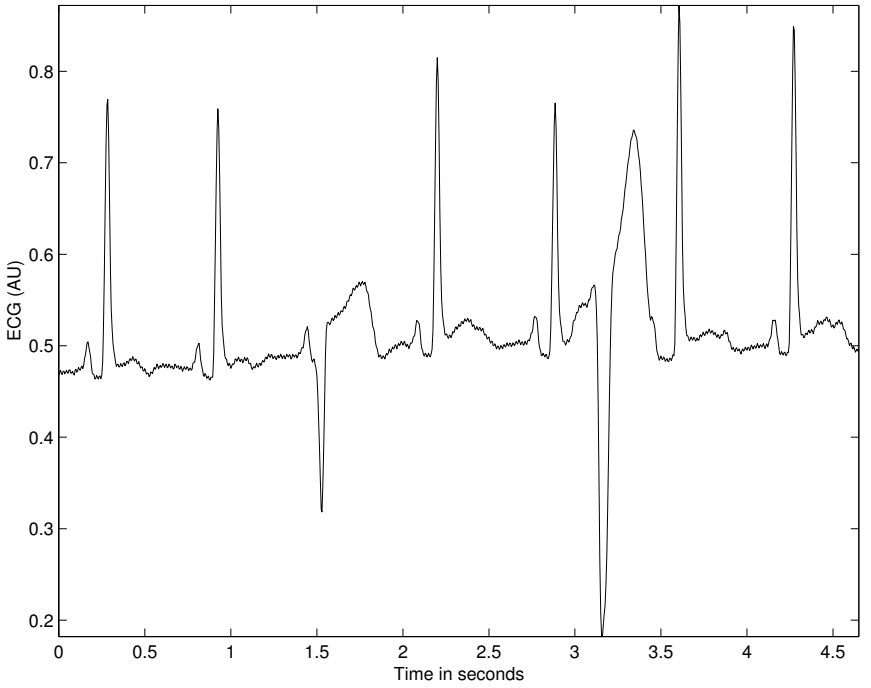


**Figure 1.29** ECG signal with PVCs. The third and sixth beats are PVCs. The first PVC has blocked the normal beat that would have appeared at about the same time instant, but the second PVC has not blocked any normal beat triggered by the SA node. Data courtesy of G. Groves and J. Tyberg, Department of Physiology and Biophysics, University of Calgary.

- The amplifier gain used is 1,000.
- Clinical ECG is usually filtered to a bandwidth of about $0.05 - 100\ Hz$, with a recommended sampling rate of $500\ Hz$ for diagnostic ECG. Distortions in the shape of the calibration pulse may indicate improper filter settings or a poor signal acquisition system.
- ECG for heart-rate monitoring could use a reduced bandwidth $0.5 - 50\ Hz$ and a lower sampling rate $100\ Hz$.
- High-resolution ECG requires a greater bandwidth of $0.05 - 500\ Hz$.

Some of the features mentioned above are related to recording of the ECG on paper and may not be relevant to digital or computer recording of the ECG.

For details of other systems of ECG leads and electrodes, see Rushmer [25], Friedman [40], Goldberger [39], Malmivuo and Plonsey [41], Webster [13], and Draper et al. [42].

Figure 1.36 shows the 12-lead ECG of a normal male adult. The system used to obtain the illustration records three channels at a time: leads I, II, III; aVR, aVL, aVF; V1, V2, V3; and V4, V5, V6 are recorded in the three available channels simultaneously. Other systems may record one channel at a time. Observe the variable shapes of the ECG waves from one lead to another. A well-trained cardiologist is able to deduce the 3D orientation of the cardiac electrical vector by analyzing the waveshapes in the six limb leads. Cardiac defects, if any, may be localized by analyzing the waveshapes in the six chest leads.

Figure 1.37 shows the 12-lead ECG of a patient with right bundle-branch block with secondary repolarization changes. The increased QRS width and distortions in the QRS shape indicate the effects of asynchronous activation of the ventricles due to the bundle-branch block.

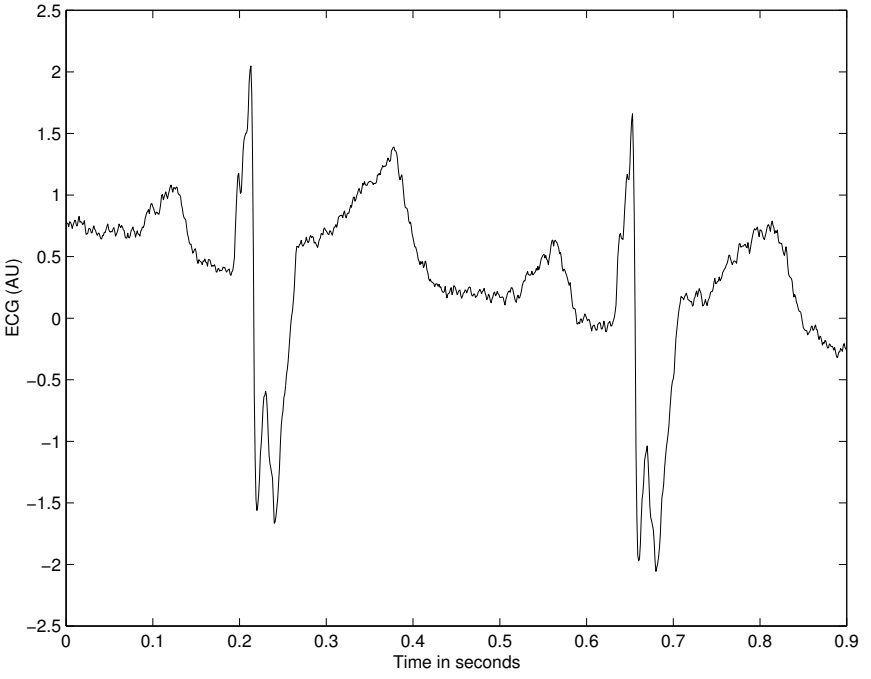


**Figure 1.30** ECG signal of a patient with right bundle-branch block and hypertrophy (male patient of age 3 months). The QRS complex is wider than normal, and displays an abnormal, jagged waveform due to desynchronized contraction of the ventricles. (The signal also has a baseline drift, which has not been corrected.)

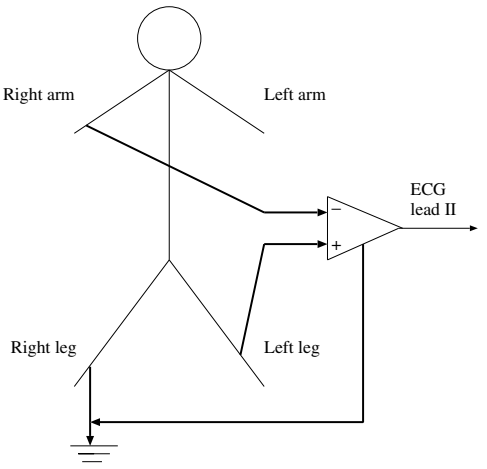


**Figure 1.31** Limb leads used to acquire the commonly used lead II ECG. *Note:* The labeling of the left or right side refers to the corresponding side of the patient or subject, as in medical convention, and not the side of the reader.

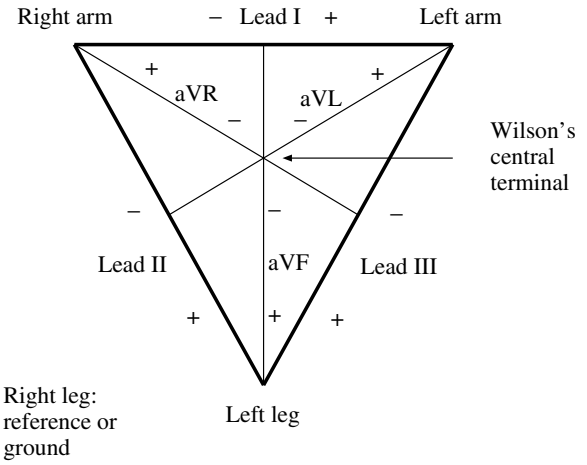


**Figure 1.32** Einthoven's triangle and the axes of the six ECG leads formed by using four limb leads.

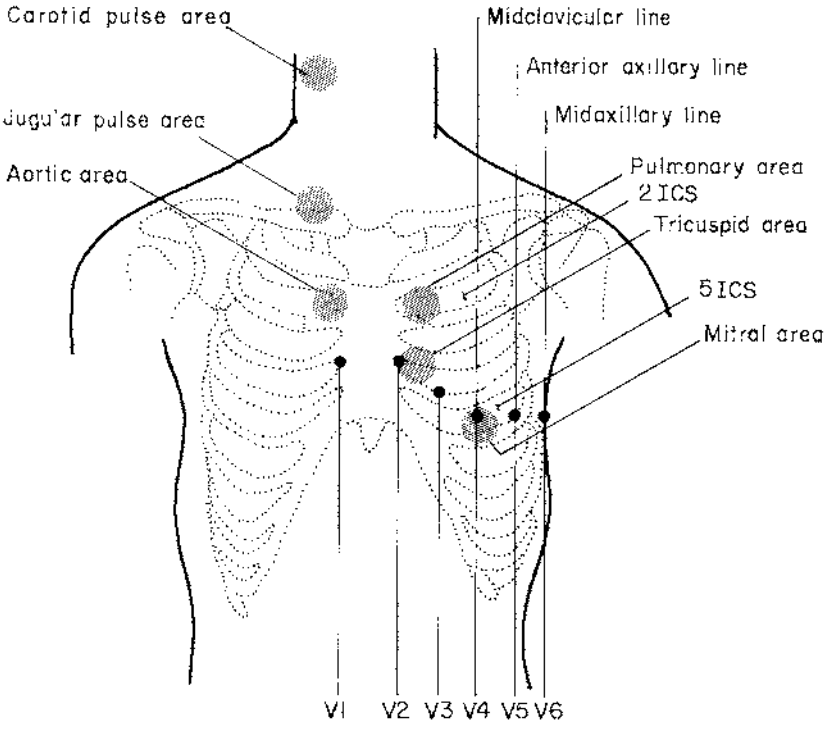


**Figure 1.33** Positions for placement of the precordial (chest) leads V1–V6 for ECG, auscultation areas for heart sounds, and pulse transducer positions for the carotid and jugular pulse signals. ICS: intercostal space.

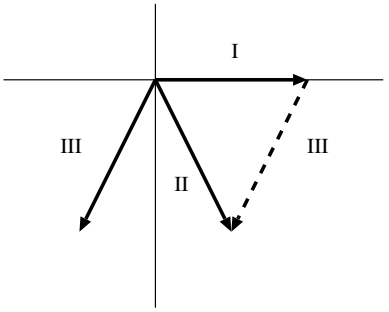


**Figure 1.34** Vectorial relations between ECG leads I, II, and III. See also Figure 1.32.

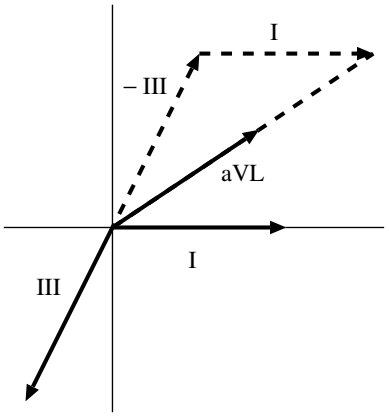


**Figure 1.35** Vectorial relations between ECG leads I, III, and aVL. See also Figure 1.32.

See Section 7.8 for discussions on electrophysiological modeling of the heart. Signal processing techniques to filter ECG signals are presented in Sections 3.3, 3.6, 3.7, 3.9, and 3.13. Detection of ECG waveforms is discussed in Sections 4.2.1, 4.3.2, 4.3.3, and 4.8. Analysis of ECG waveform shape and classification of beats are dealt with in Sections 5.2.1, 5.2.2, 5.2.3, 5.4, 5.7, 5.8, 10.2.1, and 10.11. Analysis of heart-rate variability (HRV) is described in Sections 7.2.2, 7.9, and 8.12. See Sections 3.14, 9.7.2, and 9.11 for discussions on fetal and maternal ECG. For reviews of computer applications in ECG analysis, see Jenkins [43, 44] and Cox et al. [45].

### 1.2.6 The electroencephalogram (EEG)

The EEG (popularly known as *brain waves*) represents the electrical activity of the brain [46–48]. A few important aspects of the organization of the brain are as follows. The main parts of the brain are the cerebrum, the cerebellum, the brain stem (including the midbrain, pons medulla, and the reticular formation), and the thalamus (between the midbrain and the hemispheres). Figure 1.38 gives a schematic representation of the various parts and functional areas of the human brain. The cerebrum is divided into two hemispheres, separated by a longitudinal fissure across which there is a large connective band of fibers known as the corpus callosum. The outer surface of the cerebral hemispheres, known as the cerebral cortex, is composed of neurons (gray matter) in convoluted patterns, and separated into regions by fissures (sulci). Beneath the cortex lie nerve fibers that lead to other parts of the brain and the body (white matter).

Cortical potentials are generated due to excitatory and inhibitory postsynaptic potentials developed by cell bodies and dendrites of pyramidal neurons. Physiological control processes, thought

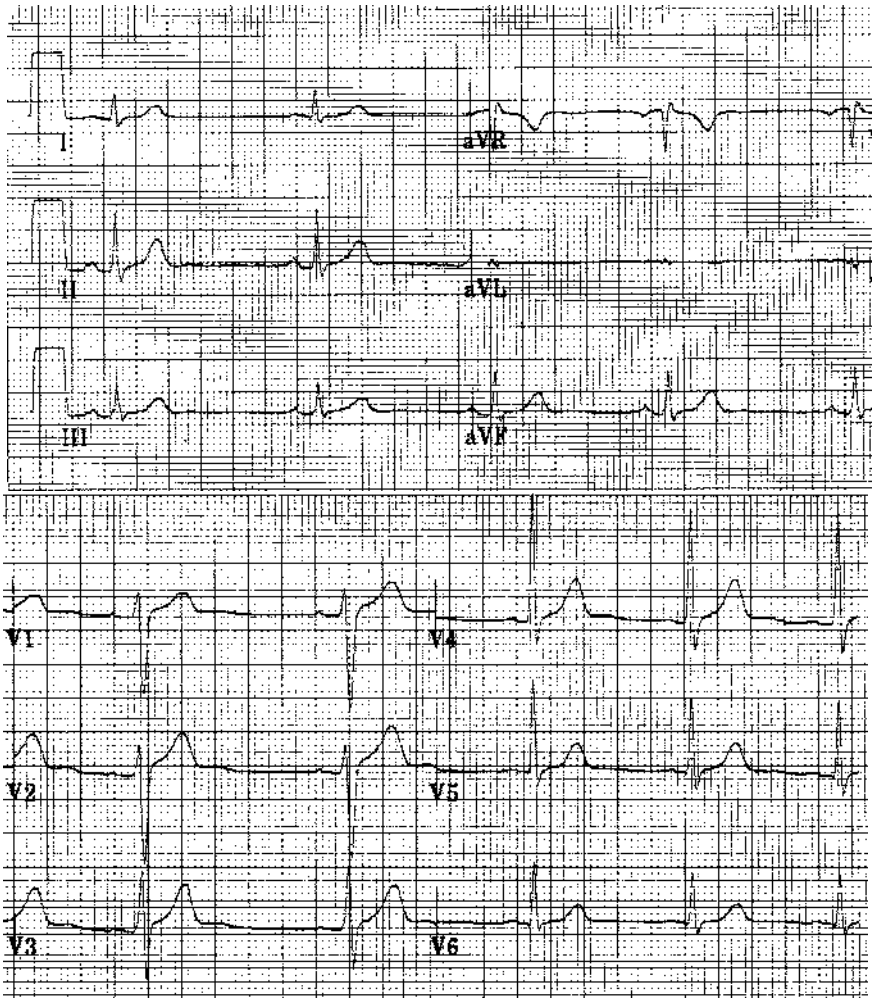


**Figure 1.36** Standard 12-lead ECG of a normal male adult. Signal courtesy of E. Gedamu and L.B. Mitchell, Foothills Hospital, Calgary.

processes, and external stimuli generate signals in the corresponding parts of the brain that may be recorded using electrodes placed on the surface of the scalp. The scalp EEG is an average of the multifarious activities of many small zones of the cortical surface beneath the electrodes used.

In clinical practice, several channels of the EEG are recorded simultaneously from various locations on the scalp for comparative analysis of activities in different regions of the brain. The International Federation of Societies for Electroencephalography and Clinical Neurophysiology recommended the $10-20$ system of electrode placement for clinical EEG recording [46], which is schematically illustrated in Figure 1.39. The name $10-20$ indicates the fact that the electrodes along the midline are placed at $10\%, 20\%, 20\%, 20\%, 20\%$, and $10\%$ of the total nasion–inion distance; the other series of electrodes are also placed at similar fractional distances of the corresponding reference distances [46]. The interelectrode distances are equal along any anteroposterior or transverse line, and electrode positioning is symmetrical. EEG signals may be used to study the nervous system, to monitor sleep stages [49, 50], for biofeedback and control, for brain–computer interfacing (BCI) [51], and for detection or diagnosis of epilepsy (seizure) [52–54].

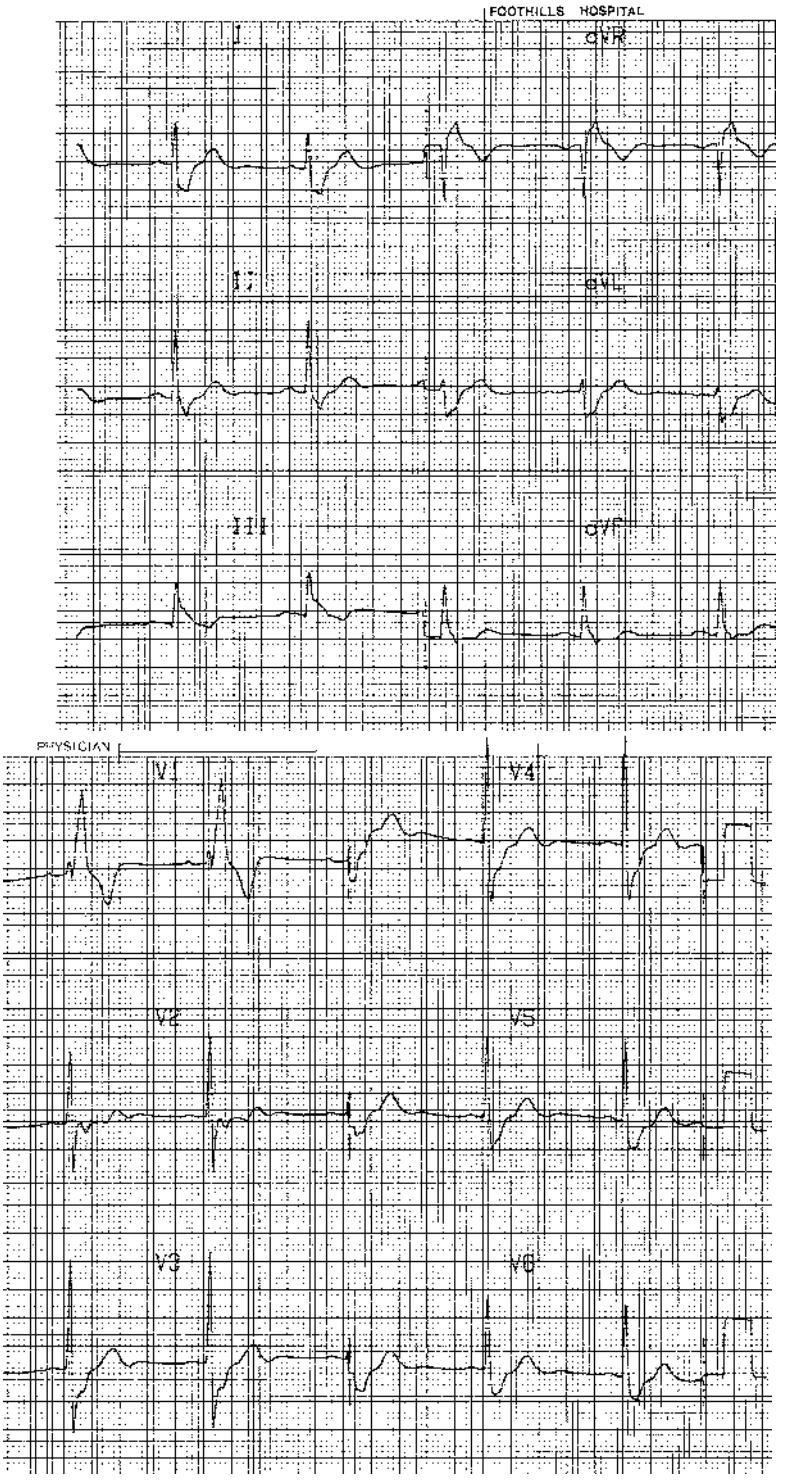


**Figure 1.37** Standard 12-lead ECG of a patient with right bundle-branch block. Signal courtesy of L.B. Mitchell, Foothills Hospital, Calgary.

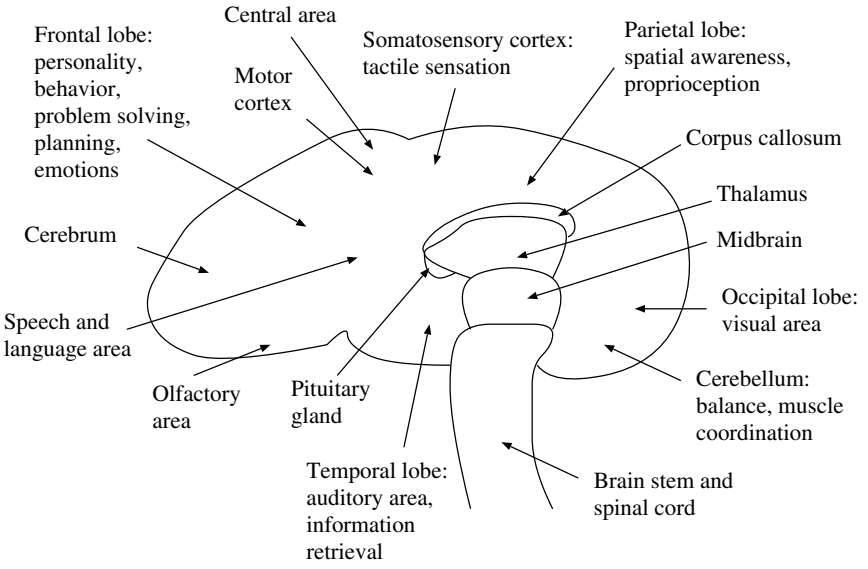


**Figure 1.38** Schematic diagram showing the various parts and functional areas of the human brain.

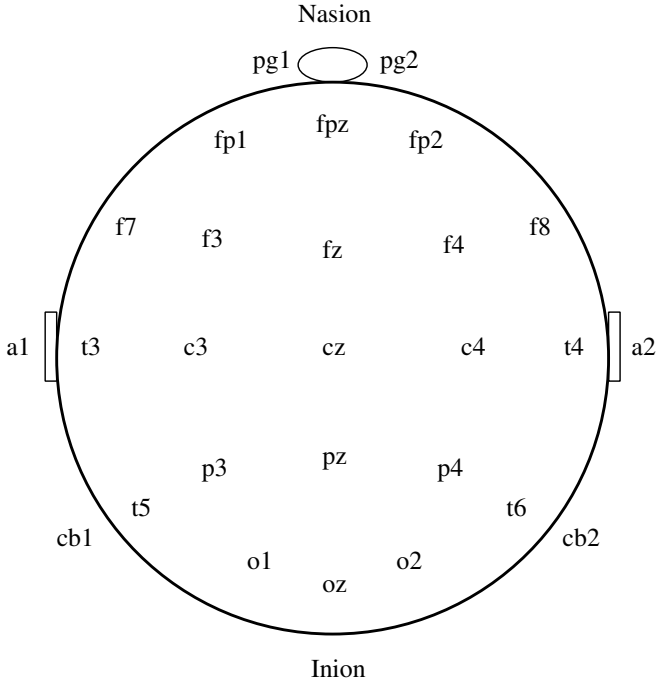


**Figure 1.39** The $10-20$ system of electrode placement for EEG recording [46]. Notes regarding channel labels: pg, nasopharyngeal; a, auricular (earlobes); fp, prefrontal; f, frontal; p, parietal; c, central; o, occipital; t, temporal; cb, cerebellar; z, midline; odd numbers on the left, even numbers on the right of the subject.

Typical EEG instrumentation settings used are lowpass filtering at $75\ Hz$, and recording at $100\ \mu V/cm$ and $30\ mm/s$ for $10-20$ minutes over $8-16$ simultaneous channels. Monitoring of sleep EEG and detection of transients related to epileptic seizures may require multichannel EEG acquisition over several hours. Special EEG techniques include the use of needle electrodes and nasopharyngeal electrodes, recording the electrocorticogram (ECoG) from an exposed part of the cortex, and the use of intracerebral electrodes. Evocative techniques for recording the EEG include initial recording at rest (eyes open and eyes closed), hyperventilation (after breathing at 20 respirations per minute for $2-4$ minutes), photic stimulation (with $1-50$ flashes of light per second), auditory stimulation with loud clicks, sleep (different stages), and pharmaceuticals or drugs.

EEG signals exhibit several patterns of rhythmic or periodic activity. (*Note:* The term *rhythm* stands for different phenomena or events in the ECG and the EEG.) The commonly used terms for EEG frequency ($f$) bands are:

- Delta ($\delta$): $0.5 \leq f < 4\ Hz$;
- Theta ($\theta$): $4 \leq f < 8\ Hz$;
- Alpha ($\alpha$): $8 \leq f \leq 13\ Hz$; and
- Beta ($\beta$): $f > 13\ Hz$.

Figure 1.40 illustrates traces of EEG signals with the rhythms listed above.

EEG rhythms are associated with various physiological and mental processes [47,48]. The alpha rhythm is the principal resting rhythm of the brain; it is common in wakeful, resting adults, especially in the occipital area, with bilateral synchrony. Auditory and mental arithmetic tasks with the eyes closed lead to strong alpha waves, which are suppressed when the eyes are opened (that is, by a visual stimulus); see Figure 1.40 (e) [46].

In addition to the commonly studied rhythms mentioned above, the gamma rhythm is defined as activity in the range $30-80\ Hz$. The gamma rhythm is considered to be related to responses induced by various types of sensory input or stimuli, active sensory processes involving attention, and short-term memory processes [55]; see Mantini et al. [56] and Rennie et al. [57] for related discussions.

The alpha wave is replaced by slower rhythms at various stages of sleep. Theta waves appear at the beginning stages of sleep; delta waves appear at deep-sleep stages. High-frequency beta waves appear as background activity in tense and anxious subjects. The depression or absence of the normal (expected) rhythm in a certain state of a subject could indicate abnormality. The presence of delta or theta (slow) waves in a wakeful adult may be considered to be abnormal. Focal brain injury and tumors lead to abnormal slow waves in the corresponding regions. Unilateral depression (left–right asymmetry) of a rhythm could indicate disturbances in cortical pathways. Spikes and sharp waves could indicate the presence of epileptogenic regions in the corresponding parts of the brain.

Figure 1.41 shows an example of eight channels of the EEG recorded simultaneously from the scalp of a subject. All channels display high levels of alpha activity. Figure 1.42 shows 10 channels of the EEG of a subject with spike-and-wave complexes. Observe the distinctly different waveshape and sharpness of the spikes in Figure 1.42 as compared to the smooth waves in Figure 1.41.

EEG signals also include spikes, transients, and other waves and patterns associated with various disorders of the nervous system (see Figure 4.1 and Section 4.2.4). Figure 1.43 shows a 21-channel record of a patient with a seizure starting at about the $50$-$s$ mark [58]. The signal is characterized by a recruiting theta rhythm at about $5\ Hz$ in the channels labeled as T2, F8, T4, and T6. Artifacts are evident in the signal due to muscle activity (in T3, C3, and C4) and blinking of the eye (in Fp1 and Fp2). Increased amounts of relatively high-frequency activity are seen in several channels after the $50$-$s$ mark related to the seizure.

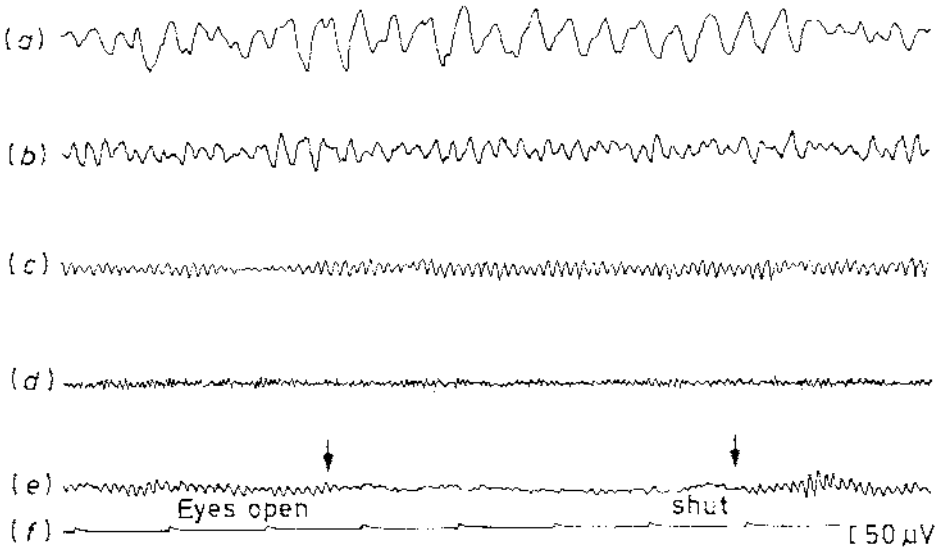


**Figure 1.40** From top to bottom: (a) delta rhythm; (b) theta rhythm; (c) alpha rhythm; (d) beta rhythm; (e) blocking of the alpha rhythm by eye opening; (f) 1 $s$ time markers and 50 $\mu V$ marker. Reproduced with permission from R. Cooper, J.W. Osselton, and J.C. Shaw, *EEG Technology*, 3rd Edition, 1980. ©Butterworth Heinemann Publishers, a division of Reed Educational & Professional Publishing Ltd., Oxford, UK.

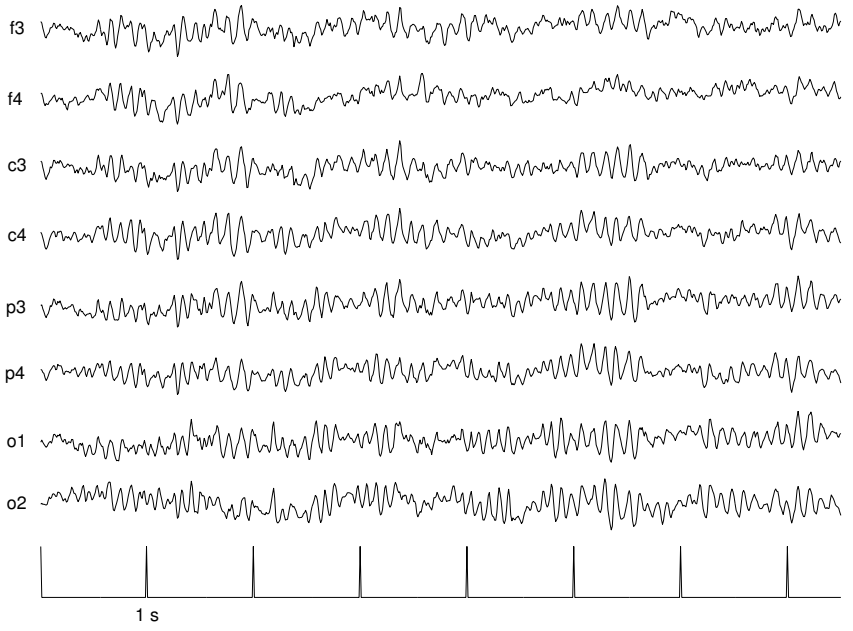


**Figure 1.41** Eight channels of the EEG of a subject displaying alpha rhythm. See Figure 1.39 for details regarding channel labels. Data courtesy of Y. Mizuno-Matsumoto, Osaka University Medical School, Osaka, Japan.

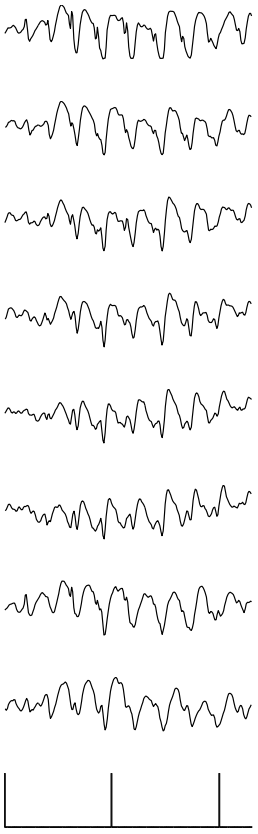

**Figure 1.42** Ten channels of the EEG of a subject displaying spike-and-wave complexes. The channels shown are, from top to bottom: c3, c4, p3, p4, o1, o2, t3, t4, and time (1 $s$ per mark). See Figure 1.39 for details regarding channel labels. Data courtesy of Y. Mizuno-Matsumoto, Osaka University Medical School, Osaka, Japan.

Detection of events and rhythms in EEG signals is discussed in Sections 4.4, 4.5, and 4.6. Spectral analysis of EEG signals is dealt with in Sections 6.3.4, 6.7, and 7.5.2. Adaptive segmentation of EEG signals is described in Sections 8.2.2, 8.5, and 8.10. Detection of seizures is discussed in Sections 8.17 and 9.8. See Section 9.12 for a discussion on EEG channel selection for BCI.

### 1.2.7 Event-related potentials (ERPs)

The term *event-related potential* is more general than and preferred to the term *evoked potential*, and includes the ENG or the EEG in response to light, sound, electrical, or other external stimuli. Short-latency ERPs are predominantly dependent on the physical characteristics of the stimulus, whereas longer-latency ERPs are predominantly influenced by the conditions of presentation of the stimuli.

Somatosensory evoked potentials (SEPs) are useful for noninvasive evaluation of the nervous system from a peripheral receptor to the cerebral cortex. Median nerve short-latency SEPs are obtained by placing stimulating electrodes about $2 - 3$ $cm$ apart over the median nerve at the wrist with electrical stimulation at $5 - 10$ $pps$, each stimulus pulse being of duration less than $0.5$ $ms$ with an amplitude of about $100$ $V$ (producing a visible thumb twitch). The SEPs are recorded from the surface of the scalp. The latency, duration, and amplitude of the response are measured.

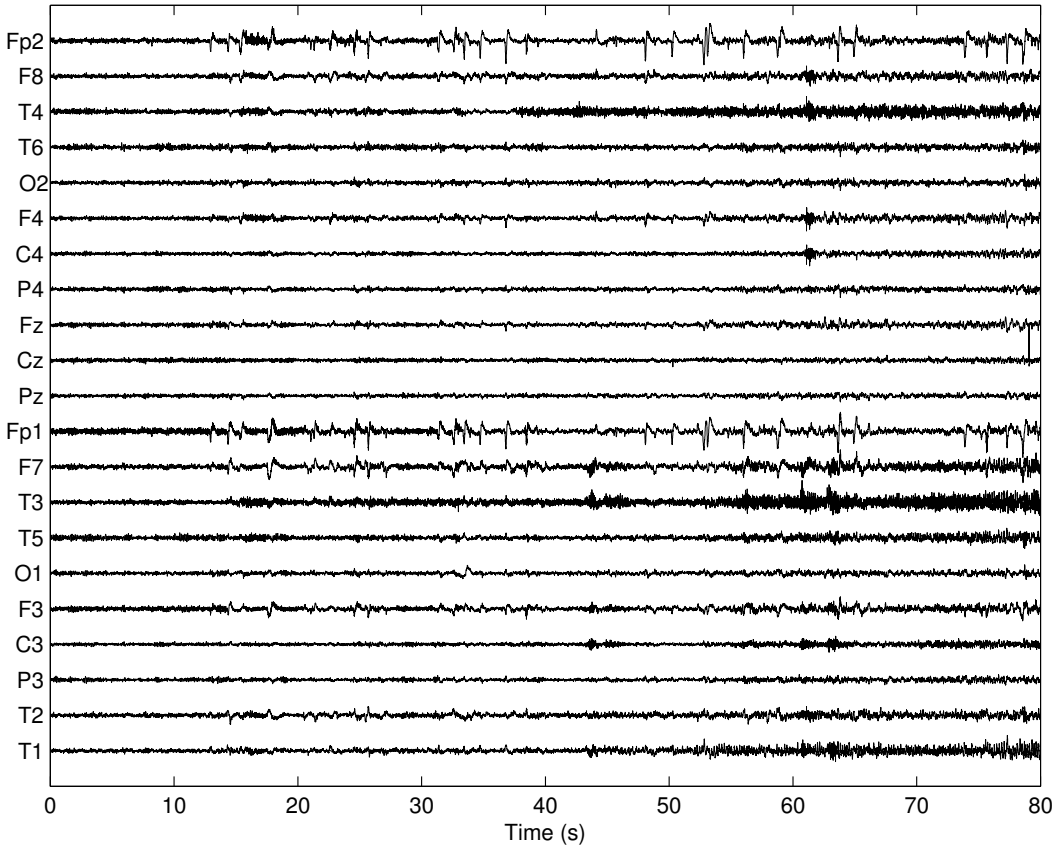


**Figure 1.43** 21 channels of the EEG of a subject displaying seizure activity. Data courtesy of M. De Vos, Katholieke Universiteit Leuven, Leuven, Belgium. T1 and T2 are sphenoidal electrodes.

ERPs and SEPs are weak signals typically buried in ongoing activity of the associated systems. Examples of ERPs are provided in Figures 3.2 and 3.43. Improvement of signal-to-noise ratio ($SNR$) is usually achieved by synchronized averaging and filtering. See Sections 3.5, 3.12, 8.18, and 9.12 for examples of ERPs and related signal processing methods.

### 1.2.8 The electrogastrogram (EGG)

The electrical activity of the stomach consists of rhythmic waves of depolarization and repolarization of its constituent smooth muscle cells [59–61]. The activity originates in the midcorpus of the stomach, with intervals of about 20 $s$ in humans. The waves of activity are always present and are not directly associated with contractions; they are related to the spatial and temporal organization of gastric contractions.

External (cutaneous) electrodes can record the signal known as the electrogastrogram (EGG). Chen et al. [62] used the following procedures to record cutaneous EGG signals. With the subject in the supine position and remaining motionless, the stomach was localized using a $5 - MHz$ ultrasound transducer array, and the orientation of the distal stomach was marked on the abdominal surface. Three active electrodes were placed on the abdomen along the antral axis of the stomach with an interelectrode spacing of 3.5 $cm$. A common reference electrode was placed 6 $cm$ away in the upper-right quadrant. Three bipolar signals were obtained from the three active electrodes in

relation to the common reference electrode. The signals were amplified and filtered to the bandwidth of $0.02 - 0.3\ Hz$ with $6\ dB/octave$ transition bands, and sampled at $2\ Hz$.

The surface EGG is believed to reflect the overall electrical activity of the stomach, including the electrical control activity and the electrical response activity. Chen et al. [62] indicated that gastric dysrhythmia or arrhythmia may be detected via analysis of the EGG. Other researchers suggest that the diagnostic potential of the signal has not yet been established [59, 60]. Accurate and reliable measurement of the electrical activity of the stomach requires implantation of electrodes within the stomach [63], which limits its practical applicability.

### 1.2.9 The phonocardiogram (PCG)

The heart sound signal is perhaps the most traditional biomedical signal, as indicated by the fact that the stethoscope is the primary instrument carried and used by physicians. The PCG is a vibration or sound signal related to the contractile activity of the cardiohemic system (the heart and blood together) [25, 64–69]; it represents a recording of the heart sound signal. Recording of the PCG signal requires a transducer to convert the vibration or sound signal into an electronic signal: Microphones, pressure transducers, or accelerometers may be placed on the chest surface for this purpose. The normal heart sounds provide an indication of the general state of the heart in terms of rhythm and contractility. Cardiovascular diseases and defects cause changes to the heart sounds or additional sounds and murmurs that could be useful in their diagnosis.

**The genesis of heart sounds:** The externally recorded heart sounds are not caused by valve leaflet movements *per se*, as believed earlier, but by vibrations of the whole cardiovascular system triggered by pressure gradients [25]. The cardiohemic system may be compared to a fluid-filled balloon, which, when stimulated at any location, vibrates as a whole. Externally, however, heart sound components are best heard at certain locations on the chest individually, and this localization has led to the concept of *secondary sources* on the chest related to the well-known auscultatory areas: the mitral, aortic, pulmonary, and tricuspid areas [25]. The standard auscultatory areas are indicated in Figure 1.33. The mitral area is near the apex of the heart. The aortic area is to the right of the sternum, in the second intercostal space. The tricuspid area is in the fourth intercostal space on either side of the sternum. The pulmonary area lies at the left parasternal line in the second or third intercostal space [25].

A normal cardiac cycle contains two major sounds — the first heart sound (S1) and the second heart sound (S2). Figure 1.44 shows a normal PCG signal, along with the ECG and carotid pulse tracings. S1 occurs at the onset of ventricular contraction, and corresponds in timing to the QRS complex in the ECG signal.

The initial vibrations in S1 occur when the first myocardial contractions in the ventricles move blood toward the atria, sealing the AV (mitral and tricuspid) valves (see Figure 1.45). The second component of S1 begins with abrupt tension of the closed AV valves, decelerating the blood. At this stage, known as isovolumic contraction, all four of the cardiac valves are closed. Next, the semilunar (aortic and pulmonary) valves open, and the blood is ejected out of the ventricles. The third component of S1 may be caused by oscillation of blood between the root of the aorta and the ventricular walls. This is followed by the fourth component of S1, which may be due to vibrations caused by turbulence in the ejected blood flowing rapidly through the ascending aorta and the pulmonary artery.

Following the systolic pause in the PCG of a normal cardiac cycle, the second sound S2 is caused by the closure of the semilunar valves. While the primary vibrations occur in the related arteries due to deceleration of blood, the ventricles and atria also vibrate, due to transmission of vibrations through the blood, the valves, and the valve rings. S2 has two components, one due to closure of the aortic valve (A2) and the other due to closure of the pulmonary valve (P2). The aortic valve normally closes before the pulmonary valve, and hence A2 precedes P2 by a few milliseconds. The A2–P2 gap is widened in normal subjects during inspiration. The pulmonary impedance is lower during

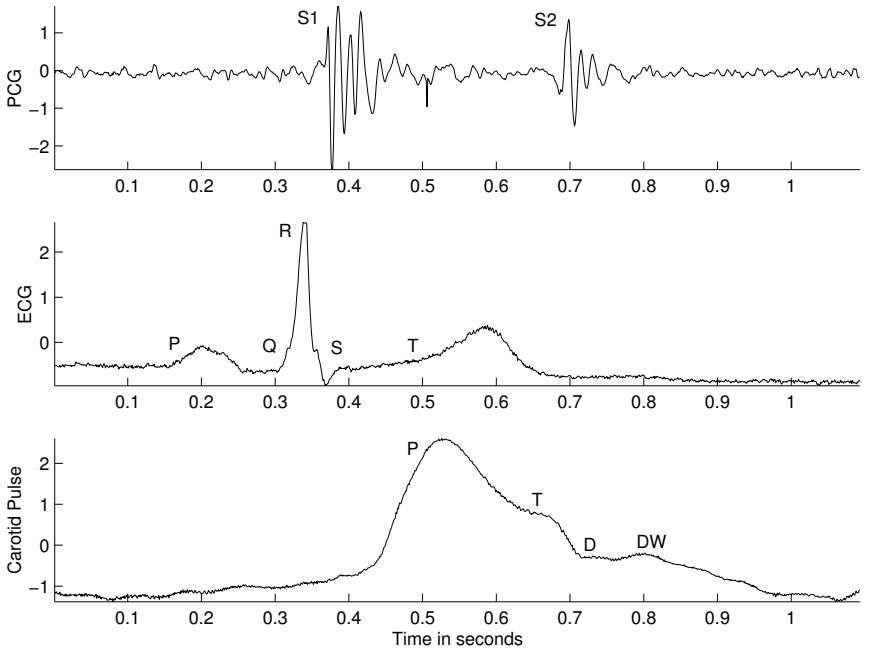


**Figure 1.44** Three-channel simultaneous record of the PCG, ECG, and carotid pulse signals of a normal male adult.

inspiration as compared to the condition during expiration. The compliance of the pulmonary vessels is increased during inspiration because they are dilated due to negative thoracic pressure. These conditions cause P2 to be delayed during inspiration as compared to the situation during expiration. (*Note:* The PCG signal in Figure 1.44 does not show the A2 and P2 components separately.) A wide gap is sustained during expiration in the case of pulmonary hypertension. Bundle-branch block could cause the A2–P2 gap to widen, or may even reverse the order of occurrence of A2 and P2.

In some cases, a third heart sound (S3) may be heard, corresponding to sudden termination of the ventricular rapid-filling phase. Because the ventricles are filled with blood and their walls are relaxed during this part of diastole, the vibrations of S3 contain much lower frequencies than S1 and S2. In late diastole, a fourth heart sound (S4) may be heard sometimes, caused by atrial contractions displacing blood into the distended ventricles. In addition to these sounds, valvular clicks and snaps are occasionally heard.

**Heart murmurs:** The intervals between S1 and S2, and S2 and S1 of the next cycle (corresponding to ventricular systole and diastole, respectively), are normally silent. Murmurs, which are caused by certain cardiovascular defects and diseases, may occur in these intervals. Murmurs are high-frequency noise-like sounds that arise when the velocity of blood becomes high as it flows through an irregularity, such as a constriction, an orifice, or a baffle. Typical conditions in the cardiovascular system that cause turbulence in blood flow are valvular stenosis and insufficiency. A valve is said to be stenosed when, due to the deposition of calcium or other reasons, the valve leaflets are stiffened and do not open completely, thereby causing an obstruction or baffle in the path of the blood being ejected. A valve is said to be insufficient when it cannot close effectively and causes reverse leakage or regurgitation of blood through a narrow gap.

Systolic murmurs are caused by conditions such as ventricular septal defect (a hole in the septum or wall between the left ventricle and the right ventricle), aortic stenosis, pulmonary stenosis, mitral insufficiency, and tricuspid insufficiency. Semilunar valvular stenosis (aortic stenosis and

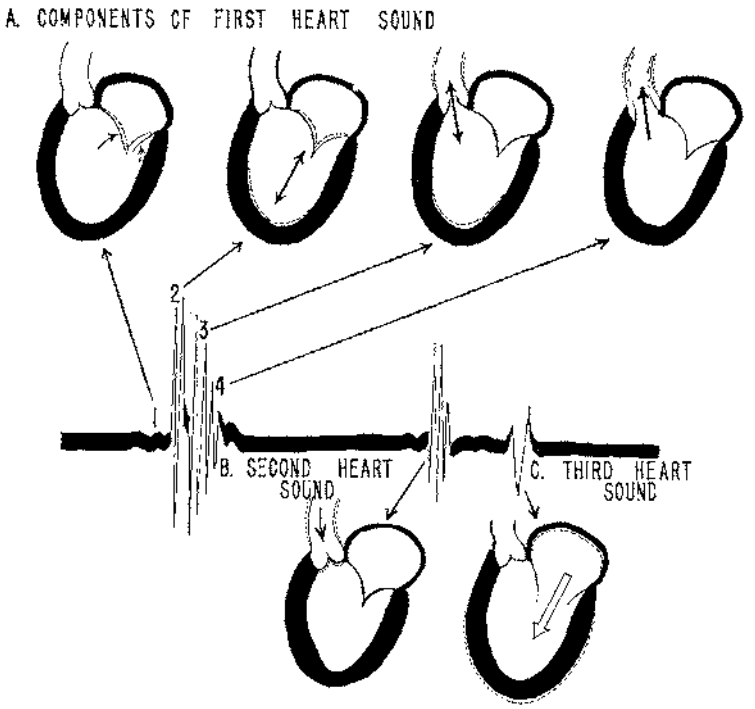


**Figure 1.45** Schematic representation of the genesis of heart sounds. Only the left portion of the heart is illustrated as it is the major source of the heart sounds. The corresponding events in the right portion also contribute to the sounds. The atria do not directly contribute much to the heart sounds. Reproduced with permission from R.F. Rushmer, *Cardiovascular Dynamics*, 4th edition, ©W.B. Saunders, Philadelphia, PA, 1976.

pulmonary stenosis) causes an obstruction in the path of blood being ejected during systole. AV valvular insufficiency (mitral insufficiency and tricuspid insufficiency) causes regurgitation of blood to the atria during ventricular contraction.

Diastolic murmurs are caused by conditions such as aortic insufficiency, pulmonary insufficiency, mitral stenosis, and tricuspid stenosis. Other conditions causing murmurs are atrial septal defect and patent ductus arteriosus (an abnormal connection or shunt between the aorta and the pulmonary artery), as well as certain physiological or functional conditions that result in increased cardiac output or blood velocity.

Various features of heart sounds and murmurs, such as intensity, frequency content, and timing, are affected by many physical and physiological factors, including the recording site on the thorax, intervening thoracic structures, ventricular contractility, positions of the cardiac valves at the onset of systole, the degree of the defect present, the heart rate, and blood velocity. For example, S1 is loud and delayed in mitral stenosis; right bundle-branch block causes wide splitting of S2; left bundle-branch block results in reversed splitting of S2; acute myocardial infarction causes a pathologic S3; and severe mitral regurgitation leads to an increased S4 [64–68]. Although murmurs are noise-like events, their features aid in distinguishing between different causes. For example, aortic stenosis causes a diamond-shaped midsystolic murmur, whereas mitral stenosis causes a decrescendo–crescendo type of diastolic–presystolic murmur. Figure 1.46 illustrates the PCG, ECG, and carotid pulse signals of a patient with aortic stenosis; the PCG displays the typical diamond-shaped murmur in systole.

**Recording of PCG signals:** PCG signals are normally recorded using piezoelectric contact sensors that are sensitive to displacement or acceleration at the skin surface. The PCG signals illustrated in this section were obtained using a Hewlett Packard HP21050A transducer, which has a nominal bandwidth of $0.05 - 1,000\ Hz$. The carotid pulse signals shown in this section were recorded using the HP21281A pulse transducer, which has a nominal bandwidth of $0 - 100\ Hz$. PCG recording is normally performed in a quiet room, with the patient in the supine position with the head resting on a pillow. The PCG transducer is placed firmly at the desired position on the chest using a suction ring and/or a rubber strap.

The use of the ECG and carotid pulse signals in the analysis of PCG signals is described in Sections 2.2.1, 2.2.2, and 2.3. Segmentation of the PCG based on events detected in the ECG and carotid pulse signals is discussed in Section 4.9. A particular type of synchronized averaging to detect A2 in S2 is the topic of Section 4.10. Spectral analysis of the PCG and its applications are presented in Sections 6.2.1, 6.3.6, 6.5, and 7.11. Parametric modeling and detection of S1 and S2 are described in Sections 7.5.2 and 7.10. Modeling of sound generation in stenosed coronary arteries is discussed in Section 7.7.2. Adaptive segmentation of PCG signals with no other reference signal is considered in Section 8.11.

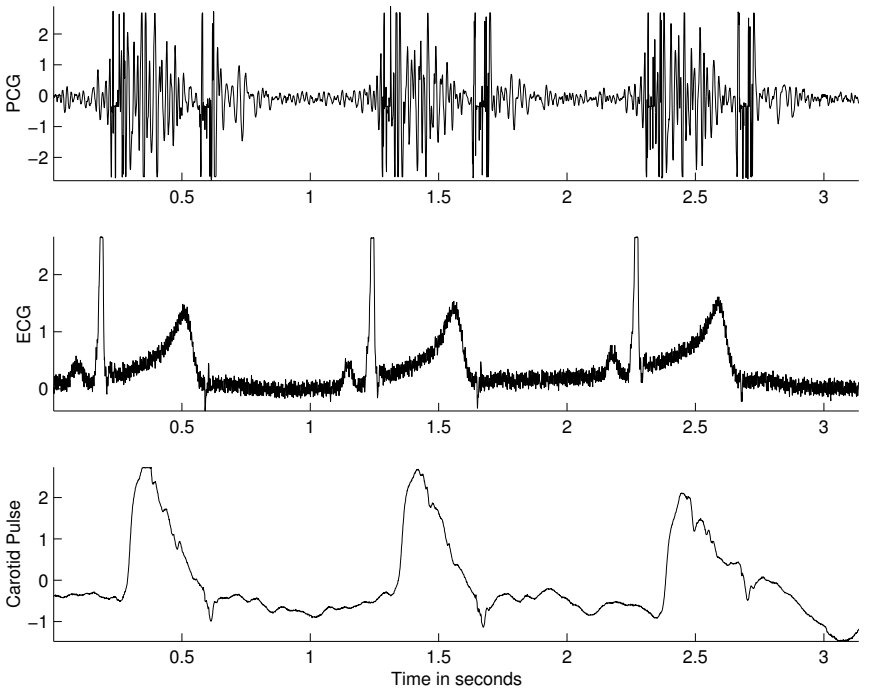


**Figure 1.46** Three-channel simultaneous record of the PCG, ECG, and carotid pulse signals of a patient (female, 11 years) with aortic stenosis. Note the presence of the typical diamond-shaped systolic murmur and the split nature of S2 in the PCG.

### 1.2.10 The carotid pulse

The carotid pulse is a pressure signal recorded over the carotid artery as it passes near the surface of the body at the neck. It provides a pulse signal indicating the variations in arterial BP and volume with each heart beat. Because of the proximity of the recording site to the heart, the carotid pulse signal closely resembles the morphology of the pressure signal at the root of the aorta; however, it

cannot be used to measure absolute pressure [65]. The carotid pulse is a useful adjunct to the PCG and can assist in the identification of S2 and its components.

The carotid pulse rises abruptly with the ejection of blood from the left ventricle to the aorta, reaching a peak called the percussion wave (marked as P in Figure 1.44). This is followed by a plateau or a secondary wave known as the tidal wave (marked as T in Figure 1.44), caused by a reflected pulse returning from the upper body. Next, closure of the aortic valve causes a notch known as the dicrotic notch (marked as D in Figure 1.44). The dicrotic notch may be followed by the dicrotic wave (marked as DW in Figure 1.44) due to a reflected pulse from the lower body [65]. The carotid pulse trace is affected by valvular defects such as mitral insufficiency and aortic stenosis [65]. In the case of aortic stenosis, obstruction of blood flow across the aortic valve leads to prolongation of ejection, which, in turn, causes an abnormally slow initial upstroke of the carotid pulse and longer ejection time [65]. In the case of mitral insufficiency, the dicrotic wave is accentuated [65]. Regardless of some benefits provided by the carotid pulse in the diagnosis of cardiovascular defects and diseases, it is not commonly used in current clinical practice.

The carotid pulse signals shown in this section were recorded using the HP21281A pulse transducer, which has a nominal bandwidth of $0 - 100\ Hz$. The carotid pulse signal is usually recorded with the PCG and ECG signals. Placement of the carotid pulse transducer requires careful selection of a location on the neck as close to the carotid artery as possible, where the pulse is felt the strongest, usually by a trained technician (see Figure 1.33).

Details on intervals that may be measured from the carotid pulse and their use in segmenting the PCG are presented in Sections 2.2.2 and 2.3. Signal processing techniques for the detection of the dicrotic notch are described in Section 4.3.5. The use of the dicrotic notch for segmentation of PCG signals is explored in Sections 4.9 and 4.10. The use of the carotid pulse to average PCG spectra in systole and diastole is described in Section 6.3.6.

### 1.2.11 The photoplethysmogram (PPG)

The term plethysmography is used to indicate techniques used to measure volume and related changes in a part of the body of interest [70, 71]. Typically, changes over time in the volume of air or blood in a certain part of the body are of interest; examples include measuring changes in the volume of air in the lungs to study respiration and study of flow of blood in the arteries in the legs to diagnose atherosclerosis (hardening of the arteries that impedes flow of blood). Impedance plethysmography involves the measurement of the electrical conductivity or resistance of a part of the body; variations in the impedance may then be related to changes in volume of the body part or its fluid content [70, 71].

An optically produced plethysmogram called a photoplethysmogram (PPG) [72] can be used to identify changes in blood volume in a microvascular bed of tissue. A PPG signal can be recorded noninvasively by attaching a pulse oximeter device at the skin surface of an earlobe or a fingertip. Figure 1.47 shows plots of PPG signals obtained from multiple bilateral sites from a patient with unilateral peripheral artery occlusive disease of the lower extremity. The PPG signals illustrate the damping, relative delay between the legs, and reduction in amplitude of the affected side's toe pulse. The bilateral similarity of the ear and finger PPG signals is indicative of the absence of severe proximal artery dysfunction [72].

The PPG signal consists of pulsatile and superimposed (low-frequency or DC) components. The cardiac-synchronized fluctuations in blood volume caused by heart beats contribute to the AC component. Sympathetic nervous system (SNS) activity, respiration, and thermoregulation influence the DC component. The PPG can be used to monitor respiration as well as hypovolemia and other circulatory disorders because of their influence on the blood flow under the skin.

In terms of the physical principles, the interaction of light with biological tissues causes reflection, scattering, and absorption, resulting in certain PPG signal characteristics. Melanin significantly absorbs light with shorter wavelengths; red and near-infrared light easily flow through water,

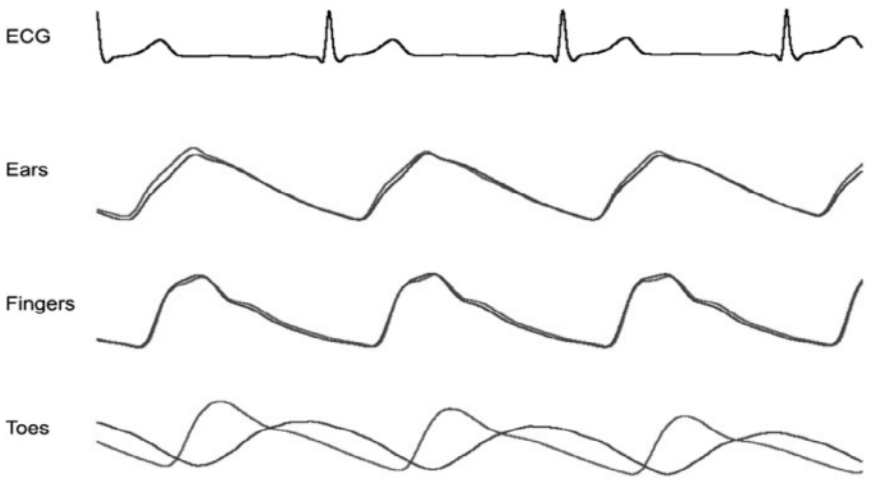


**Figure 1.47** PPG signals obtained from multiple body sites (left and right earlobes, index fingers, and toes) of a patient; the corresponding ECG is also shown. Reproduced with permission from J. Allen, Photoplethysmography and its application in clinical physiological measurement. *Physiological Measurement*, 28(3), p.R1, 2007. ©IOP.

but ultraviolet and longer infrared light are absorbed. Therefore, PPG sensors typically use infrared wavelengths. A photodetector located opposite the light emitting diode (LED) source detects light that is transmitted through the material in the transmission mode, whereas in the reflection mode, the photodetector detects light that is backscattered or reflected off tissue, bone, and/or blood vessels. Although the transmission mode can get a usable signal, suitable measurement sites might be limited: the fingertip, nasal septum, face, tongue, and earlobe are examples of body parts where transmitted light can be easily detected and where the sensors may be easily placed for optimal performance. Effective PPG acquisition at the nasal septum, cheek, or tongue may require a topical anesthetic. The preferred PPG monitoring locations are the earlobe and fingertip, but there is little blood flow at these locations. Furthermore, the earlobe and fingertip are sensitive to the environment, such as low temperature. A fingertip sensor's interference with regular activates is its biggest drawback.

The reflection mode obviates sensor location issues, allowing for the utilization of numerous measurement sites. However, motion artifacts and pressure anomalies affect the PPG in the reflection mode. Any movement, including physical activity, can produce motion artifacts that corrupt the PPG signal and reduce the precision with which physiological parameters may be measured. Compressional deformation of the underlying arteries can occur as a result of the pressure or contact force between a PPG sensor and the measurement site. As a result, the pressure applied to the skin may have an impact on the AC component of the reflected PPG signal.

Clinical applications of PPG signals [72] include measurement of blood oxygen saturation [73], estimation of the heart rate [74, 75], measurement of BP [76], and diagnosis of arterial disease [77]. PPG signals may also be used to measure respiratory activity without the need for an additional sensor. Figure 1.48 shows a PPG signal, the respiratory signal obtained using a strain gauge in a chest belt, and the respiratory signal derived from the PPG signal [78]. Madhav et al. [78] showed that the PPG-derived respiratory signal had low error values, high correlation, and similar morphological characteristics as compared to the respiratory signal obtained using a strain gauge on the chest. The PPG signal is useful in monitoring sleep apnea (see Section 2.4). Wavelet analysis of PPG is Section 8.14.

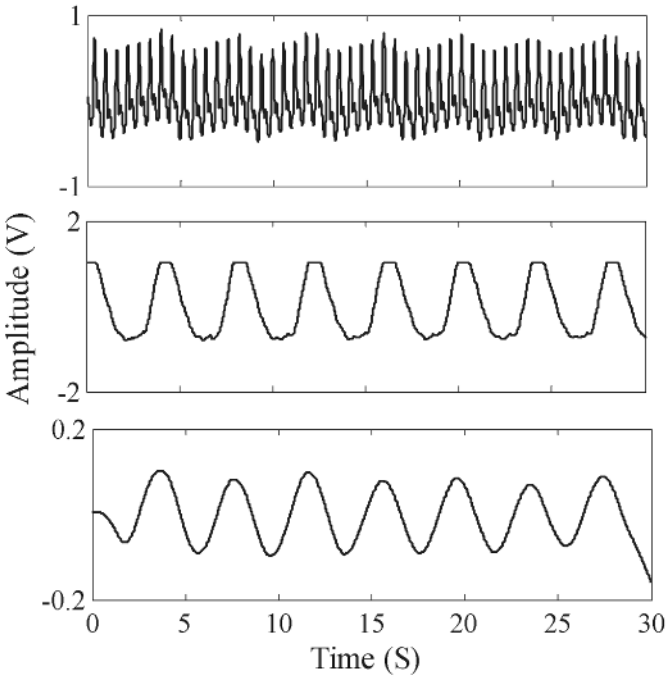


**Figure 1.48** From top to bottom: PPG signal; respiratory signal obtained using a strain gauge in a chest belt; respiratory signal derived from the PPG signal. Reproduced with permission from K.V. Madhav, M.R. Ram, E.H. Krishna, N.R. Komalla, and K.A. Reddy, Robust extraction of respiratory activity from PPG signals using modified MSPCA. *IEEE Transactions on Instrumentation and Measurement*, 62(5), pp 1094-1106, 2013 ©IEEE.

### 1.2.12 Signals from catheter-tip sensors

For specific and detailed monitoring of cardiac function, sensors placed on catheter tips may be inserted into the cardiac chambers. It then becomes possible to acquire several signals such as left ventricular pressure, right atrial pressure, aortic pressure, and intracardiac sounds [67, 68]. While these signals provide valuable and accurate information, the procedures are invasive and are associated with certain risks.

Figures 1.49 and 1.50 illustrate multichannel aortic, left ventricular, and right ventricular pressure recordings from a dog using catheter-tip sensors. The ECG signal is also shown. Observe in Figure 1.49 that the right ventricular and left ventricular pressures increase exactly at the instant of each QRS complex. The aortic pressure peaks slightly after the corresponding increase in the left ventricular pressure. The notch (incisura) in the aortic pressure signal is due to closure of the aortic valve. (The same notch propagates through the vascular system and appears as the dicrotic notch in the carotid pulse signal.) The left ventricular pressure range ($10 - 110\ mm\ of\ Hg$) is much larger than the right ventricular pressure range ($5 - 25\ mm\ of\ Hg$). The aortic pressure range is limited to the vascular BP range of $80 - 120\ mm\ of\ Hg$.

The signals in Figure 1.50 display the effects of PVCs. Observe the depressed ST segment in the ECG signal in the figure, likely due to myocardial ischemia. (It should be noted that the PQ and ST segments of the ECG signal in Figure 1.49 are isoelectric, even though the displayed values indicate a nonzero level. On the other hand, in the ECG in Figure 1.50, the ST segment stays below the corresponding isoelectric PQ segment.) The ECG complexes appearing just after the $2\ s$ and $3\ s$ markers are PVCs arising from different ectopic foci, as evidenced by their markedly different waveforms. Although the PVCs cause a less-than-normal increase in the left ventricular pressure,

they do not cause a rise in the aortic pressure, as not much blood is effectively pumped out of the left ventricle during the ectopic beats.

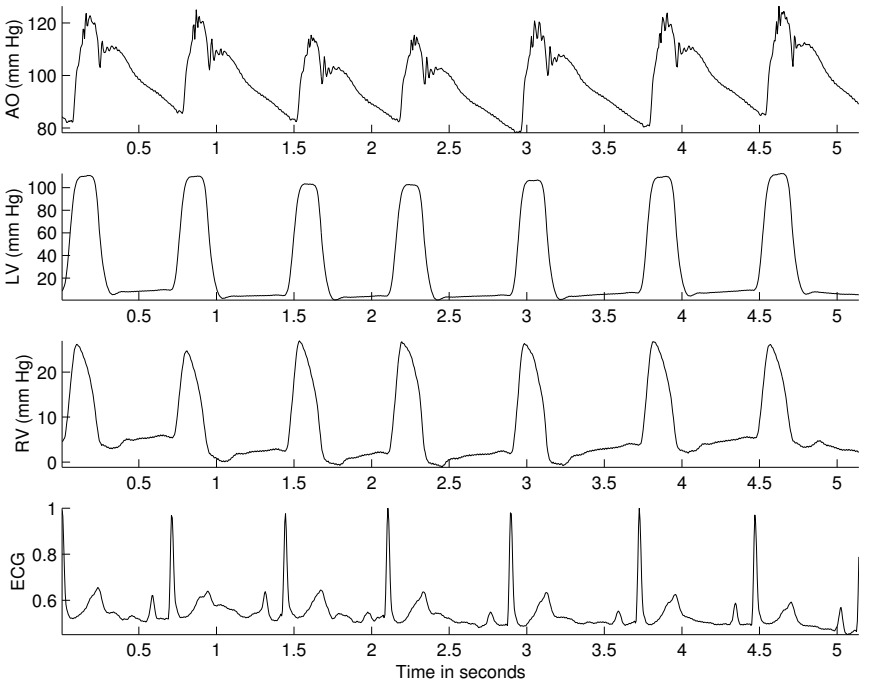


**Figure 1.49** Normal ECG and intracardiac pressure signals from a dog. The pressure signals shown are AO, near the aortic valve; LV, in the left ventricle; and RV, in the right ventricle. Data courtesy of R. Sas and J. Tyberg, Department of Physiology and Biophysics, University of Calgary.

### 1.2.13 The speech signal

Human beings are social creatures by nature and have an innate need to communicate. Humans are endowed with a sophisticated vocal system. The speech signal is an important signal, although it is more commonly considered as a communication signal than a biomedical signal. However, the speech signal can serve as a diagnostic signal when speech and vocal-tract disorders need to be investigated [79, 80].

Speech sounds are produced by transmitting puffs of air from the lungs through the oral tract as well as the nasal tract for certain sounds [81]. Figure 1.51 shows a schematic diagram of the anatomy of the vocal tract; Figure 1.52 gives a schematic representation of the parts of the speech production system. The vocal tract starts at the vocal cords or glottis in the throat and ends at the lips and the nostrils. The shape of the vocal tract is varied to produce different types of sound units or *phonemes* which, when concatenated, form speech. In essence, the vocal tract acts as a filter that modulates the spectral characteristics of the input puffs of air. It is evident that the system is dynamic; therefore, the filter and the speech signal produced have time-varying characteristics, that is, they are nonstationary (see Section 3.2.4).

Speech sounds may be classified as voiced, unvoiced, and plosive sounds [81]. Voiced sounds involve the participation of the glottis: air is forced through the vocal cords held at a certain tension. The vocal cords vibrate and the result is a series of quasiperiodic pulses of air which is passed through the vocal tract; see Figure 1.53. The input to the vocal tract may be treated as a train of impulses or pulses that is almost periodic. The vocal tract acts as a filter: Upon convolution

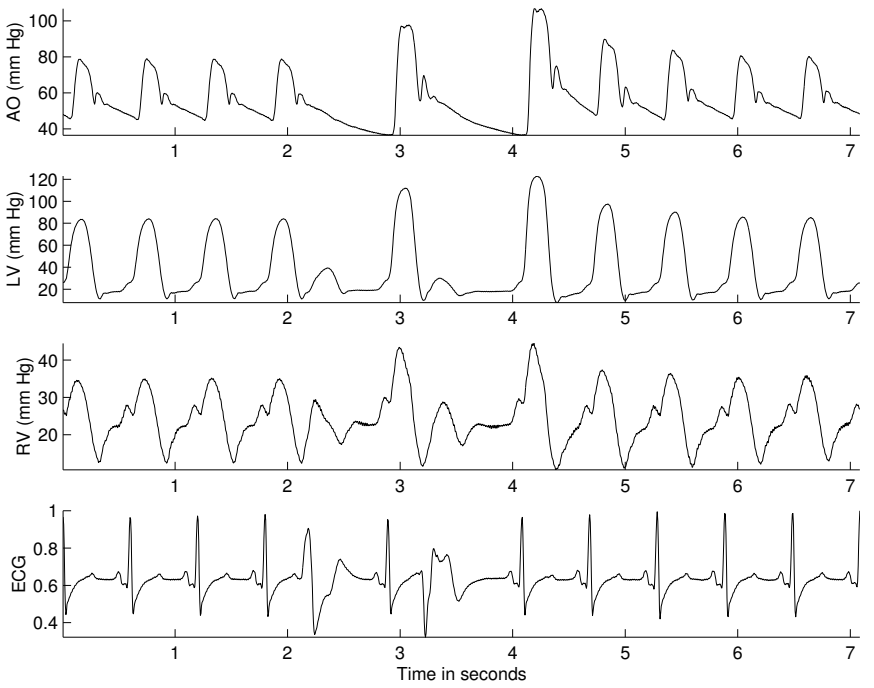


**Figure 1.50** ECG and intracardiac pressure signals from a dog with PVCs. The pressure signals shown are AO, near the aortic valve; LV, in the left ventricle; and RV, in the right ventricle. Data courtesy of R. Sas and J. Tyberg, Department of Physiology and Biophysics, University of Calgary.

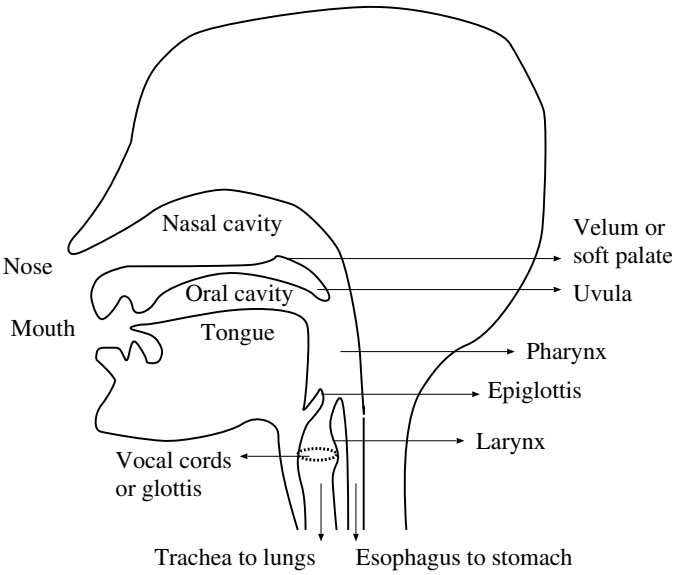


**Figure 1.51** Schematic diagram of the anatomy of the vocal tract.

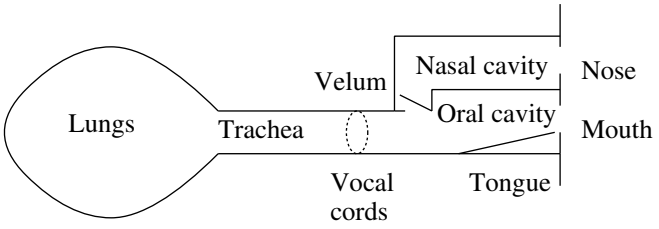


**Figure 1.52** Schematic representation of the speech production system.

with the impulse response of the vocal tract, which is held steady in a certain configuration for the duration of the voiced sound desired, a quasiperiodic signal is produced with a characteristic waveshape that is repeated. All vowels are voiced sounds. Figure 1.54 shows the speech signal of the word "safety" spoken by a male subject. Figure 1.55 shows, in the upper trace, a portion of the signal corresponding to the phoneme /E/ (the letter "a" in the word). The quasiperiodic nature of the signal is evident. Features of interest in voiced signals are the pitch (average interval between the repetitions of the vocal-tract impulse response or basic wavelet) and the resonance or formant frequencies of the vocal-tract system.

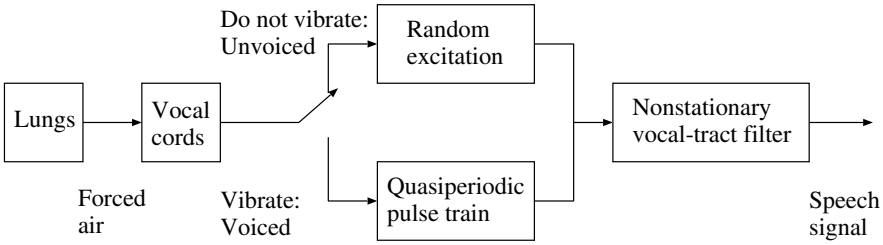


**Figure 1.53** Schematic representation of the production of voiced and unvoiced speech.

An unvoiced sound (or fricative) is produced by forcing a steady stream of air through a narrow opening or constriction formed at a specific position along the vocal tract. The vocal cords do not vibrate for such sounds; see Figure 1.53. The result is a turbulent signal that appears like random noise. The input to the vocal tract is a broadband random signal, which is filtered by the vocal tract to yield the desired sound. Fricatives are unvoiced sounds, as they do not involve any activity (vibration) of the vocal cords. The phonemes /S/, /SH/, /Z/, and /F/ are examples of fricatives. The lower trace in Figure 1.55 shows a portion of the speech signal corresponding to the phoneme /S/ in the word "safety." The signal has no identifiable structure and appears to be random (see also Figures 3.1, 3.3, and 3.4, as well as Section 3.2.4). The transfer function of the vocal tract, as evidenced by the Fourier spectrum of the signal itself, would be of interest in analyzing a fricative.

Plosives, also known as stops, involve complete closure of the vocal tract, followed by an abrupt release of built-up pressure. The phonemes /P/, /T/, /K/, and /D/ are examples of plosives. The sudden burst of activity at about 1.1 $s$ in Figure 1.54 illustrates the plosive nature of /T/. Plosives are difficult to characterize as they are transients; their properties are affected by the preceding phoneme as well. For more details on the speech signal, see Rabiner and Schafer [81].

Parkinson's disease, which causes tremor, rigidity, and loss of muscle control, is also known to affect speech. The changes in speech caused by the disease include reduced loudness, increased vocal tremor, and breath-related noise. Vocal impairment caused by the disease are labeled as dysphonia, which refers to the inability to produce normal vocal sounds, and dysarthria, which relates to difficulty in pronouncing words [80]. Tsanas et al. [80] and Rueda et al. [82] describe several techniques for the analysis of speech signals for the classification of Parkinson's disease. Maciel

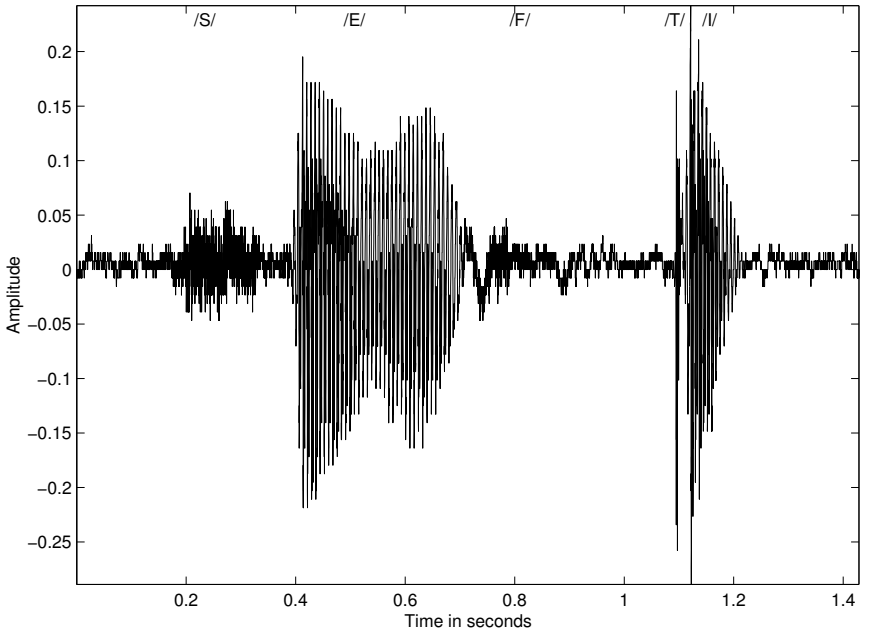


**Figure 1.54** Speech signal of the word "safety" uttered by a male speaker. Approximate time intervals of the various phonemes in the word are /S/: $0.2 - 0.35$ $s$; /E/: $0.4 - 0.7$ $s$; /F/: $0.75 - 0.95$ $s$; /T/: transient at $1.1$ $s$; /I/: $1.1 - 1.2$ $s$. Background noise is also seen in the signal before the beginning and after the termination of the speech segment, as well as during the stop interval before the plosive /T/.

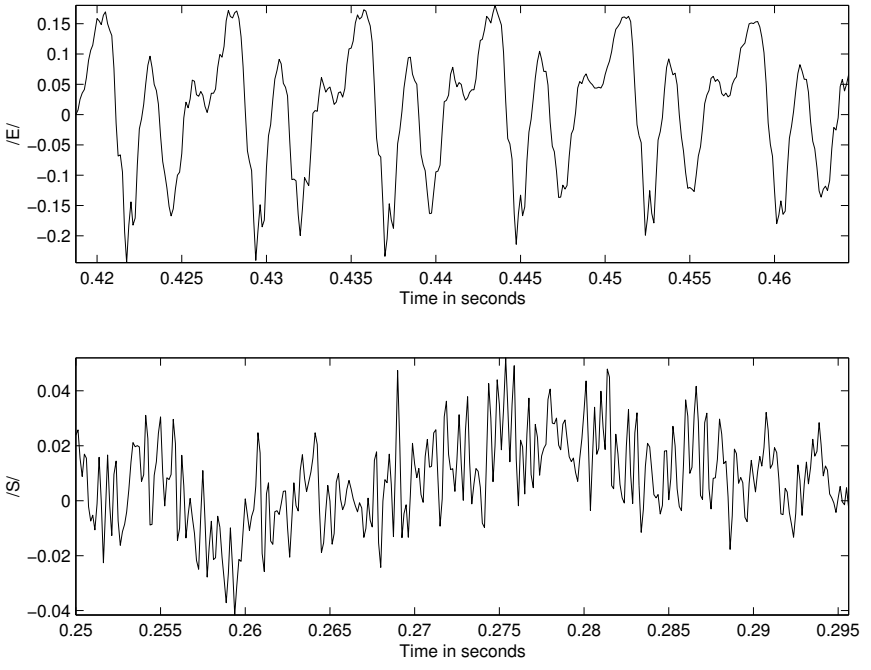


**Figure 1.55** Segments of the speech signal in Figure 1.54 on an expanded scale to illustrate the quasiperiodic nature of the voiced sound /E/ in the upper trace and the almost random nature of the fricative /S/ in the lower trace.

et al. [83] describe techniques used to derive diagnostically useful parameters from speech signals. In the case of voiced speech segments, some of such measures represent temporal or spectral variations over time, perturbation of pitch, perturbation of frequency, and jitter. While most methods for the analysis of speech abnormalities use signals of sustained vowels, Umapathy et al. [84] proposed methods to decompose continuous speech signals and extract features for classification of speech pathology. See also Umapathy and Krishnan [85], Ghoraani et al. [86], and Arias-Londoño et al. [87] for additional related material.

Signal processing techniques for extraction of the vocal-tract response from voiced speech signals are described in Section 4.7.3. Frequency-domain characteristics of speech signals are illustrated in Sections 7.6.3 and 8.4.1. See Section 10.14 for discussions on multimodal signal analysis procedures for the diagnosis of Parkinson's disease.

### 1.2.14 The vibroarthrogram (VAG)

Several processes related to aging and arthritis cause deterioration of various joints in the body, accompanied by pain and sounds. The following paragraphs provide descriptions of the knee joint, a few related disorders, and the nature of the related sounds.

**The knee joint:** As illustrated in Figure 1.56, the knee joint is formed between the femur, the patella, and the tibia. The knee joint is the largest articulation in the human body that can effectively move from $0^\circ$ extension to $135^\circ$ flexion, together with $20^\circ$ to $30^\circ$ rotation of the flexed leg on the femoral condyles. The joint has four important features: a joint cavity, articular cartilage, a synovial membrane, and a fibrous capsule [88, 89]. The knee joint is known as a synovial joint, as it contains a lubricating substance called the synovial fluid. The patella (knee cap), a sesamoid bone, protects the joint, and is precisely aligned to slide in the groove (trochlea) of the femur during leg movement. The knee joint is made up of three compartments: the patellofemoral, the lateral tibiofemoral, and the medial tibiofemoral compartments. The patellofemoral compartment is classified as a synovial gliding joint, and the tibiofemoral as a synovial hinge joint [90]. The anterior and posterior cruciate ligaments as well as the lateral and medial ligaments bind the femur and tibia together, give support to the knee joint, and limit movement of the joint. The various muscles around the joint help in the movement of the joint and contribute to its stability.

The knee derives its physiological movement and its typical rolling–gliding mechanism of flexion and extension from its six degrees of freedom: three in translation and three in rotation. The translations of the knee take place on the anterior–posterior, medial–lateral, and proximal–distal axes. The rotational motion consists of flexion–extension, internal–external rotation, and abduction–adduction.

Although the tibial plateaus are the main load-bearing structures in the knee, the cartilage, menisci, and ligaments also bear loads. The patella aids knee extension by lengthening the lever arm of the quadriceps muscle throughout the entire range of motion, and allows a better distribution of compressive stresses on the femur [91].

**Articular cartilage:** Two types of cartilage are present in the knee joint: the *articular cartilage*, which covers the ends of bones, and the wedge-shaped fibrocartilaginous structure called the *menisci*, located between the femur and the tibia [92]. The shock-absorbing menisci are composed of the medial meniscus and the lateral meniscus, which are two crescent-shaped plates of fibrocartilage that lie on the articular surface of the tibia.

The articular surfaces of the knee joint are the large curved condyles of the femur, the flattened condyles (medial and lateral plateaus) of the tibia, and the facets of the patella. There are three types of articulation: an intermediate articulation between the patella and the femur, as well as lateral and medial articulation between the femur and the tibia. The articular surfaces are covered by cartilage, as in all of the major joints of the body. Cartilage is vital to joint function because it protects the underlying bone during movement. Loss of cartilage function leads to pain, decreased mobility, and, in some instances, deformity and instability.

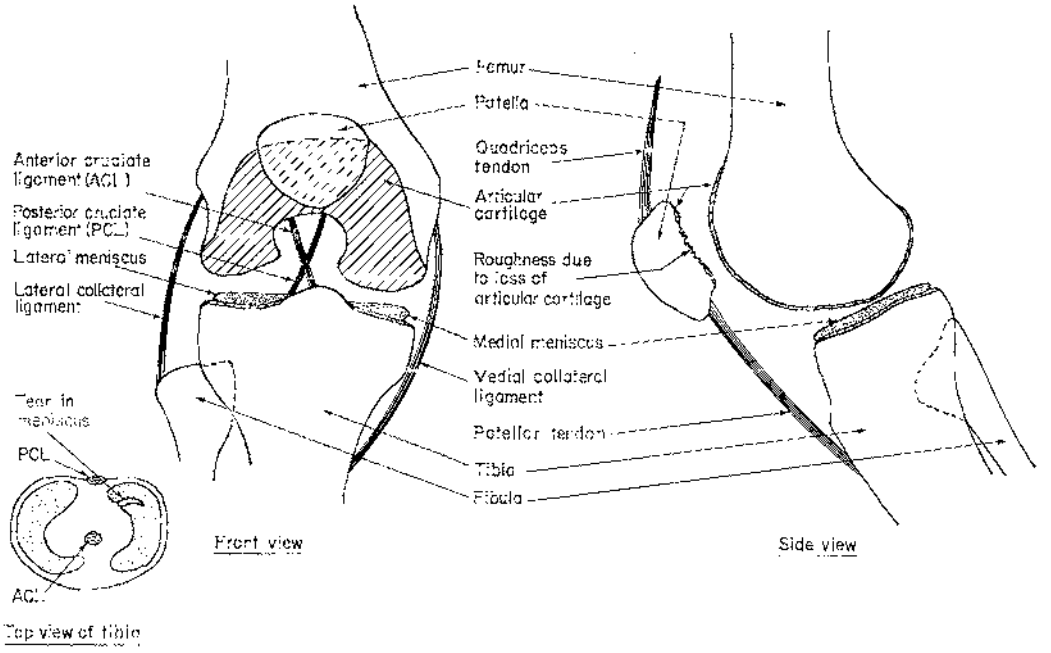


**Figure 1.56** Front and side views of the knee joint (the two views are not mutually orthogonal). The inset shows the top view of the tibia with the menisci.

**Knee-joint disorders:** The knee is a commonly injured joint in the body. Arthritic degeneration of injured knees is a well-known phenomenon and is known to result from a variety of traumatic causes. Damage to the stabilizing ligaments of the knee or to the shock-absorbing fibrocartilaginous pads (the menisci) are two of the most common causes of deterioration of knee-joint surfaces. Impact trauma to the articular cartilage surfaces could lead to surface deterioration and secondary osteoarthritis.

Nontraumatic conditions of the knee joint include the common idiopathic condition known as chondromalacia patella (soft cartilage of the patella), in which articular cartilage softens, fibrillates, and sheds off the undersurface of the patella. Similarly, the meniscal fibrocartilage of the knee can soften, which could lead to degenerative tears and secondary changes in the regional hyaline surfaces; see Figure 8.2 for related illustrations.

**Knee-joint sounds:** Considerable noise is often associated with degeneration of knee-joint surfaces. The VAG is a vibration signal recorded from a joint during movement (articulation) of the joint. Normal joint surfaces are smooth and produce little or no sound, whereas joints affected by osteoarthritis and other degenerative diseases may have suffered cartilage loss and produce palpable and audible grinding vibration and sound.

Figure 1.57 shows the experimental setup used by Rangayyan et al. [93] to record VAG signals. In their studies, the subject sat on a rigid table in a relaxed position with the leg to be tested being freely suspended in air. An accelerometer (model 3115a, Dytran, Chatsworth, CA) was placed at the midpatella (knee cap) position on the surface of the knee joint. The VAG signal was recorded as the subject swung the leg over an approximate angle range of $135^\circ$ (approximately full flexion) to $0^\circ$ (full extension) and back to $135^\circ$ in $4\ s$. The first half of each VAG signal corresponds, approximately, to extension, and the second half corresponds to flexion of the leg. The VAG signals were prefiltered to the bandwidth of $10\ Hz$ to $1\ kHz$ and digitized at the sampling rate of $2.5\ kHz$.

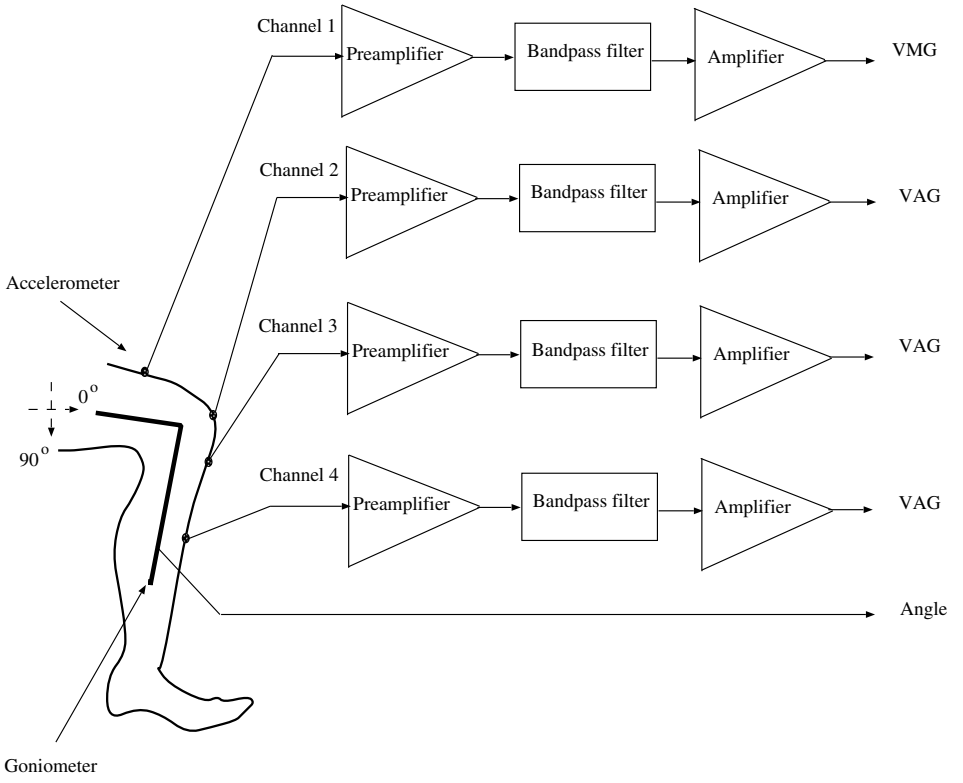


**Figure 1.57** Experimental setup to measure VAG and the related muscle-contraction interference signals at various positions along the leg [93, 94]. Channels 1 to 4 correspond, in order, to the distal rectus femoris (thigh), midpatella (knee cap), tibial tuberosity, and midtibial shaft positions.

In related studies by Zhang et al. [94], additional accelerometers were placed at the distal rectus femoris (thigh), tibial tuberosity, and midtibial shaft positions to study the possibility of muscle-contraction interference in VAG signals; see Figure 1.57 as well as Sections 1.2.15, 2.2.7, and 3.3.6. The muscle-contraction or vibration signal from the rectus femoris was referred to as the vibromyogram (VMG).

The left-hand column in Figure 1.58 shows VMG signals recorded at the distal rectus femoris (thigh), midpatella, tibial tuberosity, and midtibial shaft positions of a subject during isometric contraction of the rectus femoris muscle (with no leg or knee movement). The right-hand column of the figure shows VAG signals recorded at the same positions using the same accelerometers, but during isotonic contraction (swinging movement of the leg). The top signal (a) in the right-hand column indicates the VMG signal generated at the rectus femoris during acquisition of the VAG signals; parts (b)–(d) of the right-hand column show the VAG signals.

Rangayyan et al. [93] observed substantial differences between normal and abnormal VAG signals, with the latter including grinding and clicking sounds; see also Frank et al. [95] and Wu et al. [96]. VAG signals are difficult to analyze because they have no well-defined or recognizable waveforms and have complex nonstationary characteristics. Detection of knee-joint problems via the analysis of VAG signals could help avoid unnecessary exploratory surgery and also aid better selection of patients who would benefit from surgery [93, 95, 97–102]. Further details on the VAG signal are provided in Sections 2.2.7, 3.3.6, 5.12.1, and 8.2.3. Modeling of a specific type of VAG signal known as patellofemoral crepitus is presented in Sections 7.2.4, 7.3, and 7.7.3. Adaptive filtering of the VAG signal to remove muscle-contraction interference is described in Sections 3.10.2,

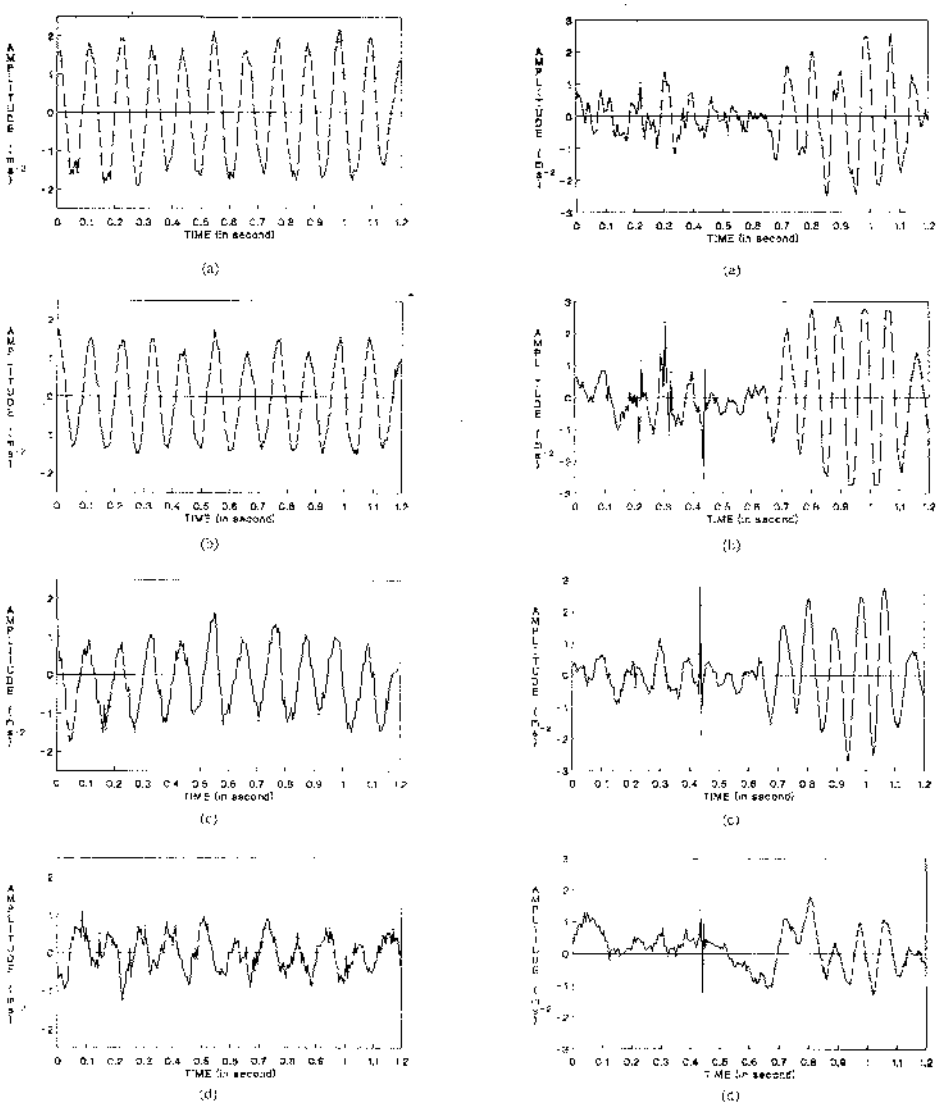

**Figure 1.58** Left-hand column: VMG signals recorded simultaneously at (top-to-bottom) (a) the distal rectus femoris, (b) midpatella, (c) tibial tuberosity, and (d) midtibial shaft positions during isometric contraction (no leg or knee movement). Right-hand column: Vibration signals recorded simultaneously at the same positions as above during isotonic contraction (swinging movement of the leg). Observe the muscle-contraction interference appearing in the extension parts (second halves) of each of the VAG signals [plots (b)–(d)] in the right-hand column [94]. The recording setup is shown in Figure 1.57. Reproduced with permission from Y.T. Zhang, R.M. Rangayyan, C.B. Frank, and G.D. Bell, Adaptive cancellation of muscle-contraction interference from knee joint vibration signals, *IEEE Transactions on Biomedical Engineering,* 41(2):181–191, 1994. ©IEEE.

3.10.3, and 3.15. Adaptive segmentation of VAG signals into quasistationary segments is illustrated in Sections 8.6.1 and 8.6.2. The role of VAG signal analysis in the detection of articular cartilage pathology is discussed in Sections 5.12, 6.6, 9.9, and 10.12.

### 1.2.15 The vibromyogram (VMG)

The VMG is the direct mechanical manifestation of contraction of a skeletal muscle and is a vibration signal that accompanies the EMG. The signal has also been named the sound myogram, acoustic myogram, or phono-myogram. Muscle sounds or vibrations are related to variations in the dimensions (contraction) of the constituent muscle fibers (see Figure 1.8) and may be recorded using contact microphones or accelerometers placed on the muscle surface [103, 104]; see Section 1.2.14. The frequency and intensity of the VMG have been shown to vary in direct proportion to the contraction level [103, 104]. The VMG, along with the EMG, may be useful in studies related to neuromuscular control, muscle contraction, athletic training, biofeedback, and rehabilitation. VMG signal analysis, however, is not as well established or common as EMG analysis.

Simultaneous analysis of the VMG and EMG signals is discussed in Section 2.2.6. Adaptive cancellation of the VMG from knee-joint vibration signals is the topic of Sections 3.10.2, 3.10.3, and 3.15. Analysis of muscle contraction using the VMG is described in Section 5.11.

### 1.2.16 Otoacoustic emission (OAE) signals

The OAE signal represents the acoustic energy emitted by the cochlea either spontaneously or in response to an acoustic stimulus. The existence of this signal indicates that the cochlea not only receives sound but also produces acoustic energy [105]. The OAE signal could provide objective information on the micromechanical activity of the preneural or sensory components of the cochlea that are distal to the nerve-fiber endings. Analysis of the OAE signal could lead to improved noninvasive investigative techniques to study the auditory system. The signal may also assist in screening of hearing function and in the diagnosis of hearing impairment.

### 1.2.17 Bioacoustic signals

Several systems and parts of the human body produce sounds and vibrations in various bands of frequencies under both normal physiological and pathological conditions. In the preceding sections, we have studied the PCG, VMG, VAG, and OAE signals. A few other bioacoustic signals that have been studied by several researchers are breathing, tracheal, lung, and chest sounds [106–114]; snoring sounds [115, 116]; swallowing sounds [117]; gastrointestinal or bowel sounds [118]; sounds of the shoulder, temporomandibular, and hip joints [119]; cough sounds [120]; and crying sounds of infants [121]. Kompis et al. [108] describe methods for acoustic imaging of the chest using multiple transducers. Kaniusas et al. [122] proposed techniques for integrated analysis of sound signals related to the cardiac system, respiration, and snoring. See Section 8.13 for a discussion on analysis of crying sounds of infants.

## 1.3 Objectives of Biomedical Signal Analysis

The representation of biomedical signals in electronic form facilitates computer processing and analysis of the data. Figure 1.59 illustrates the typical steps and processes involved in computer-aided diagnosis (CAD) and therapy based on biomedical signal analysis.

Some of the major objectives of biomedical instrumentation and signal analysis [13, 14, 123–126] are the following:

- *Information gathering* — measurement and analysis of phenomena to interpret a system.

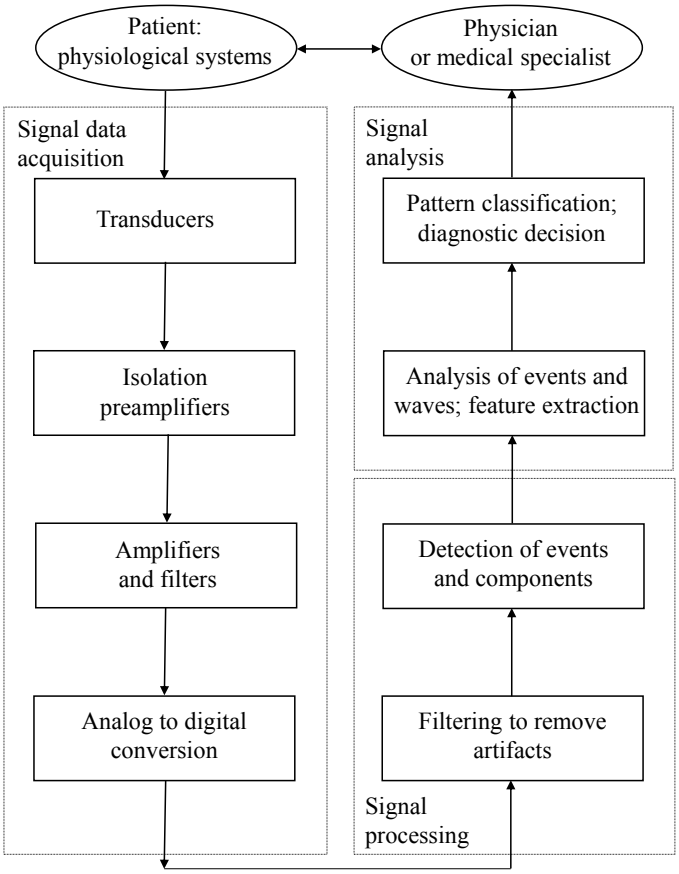


**Figure 1.59** Computer-aided diagnosis and therapy based on biomedical signal analysis.

- *Diagnosis* — detection of malfunction, pathology, or abnormality.
- *Monitoring* — obtaining continuous or periodic information about a system.
- *Therapy and control* — modification of the behavior of a system based on the outcome of the activities listed above to ensure a specific result.
- *Evaluation* — objective analysis to determine the ability to meet functional requirements, obtain proof of performance, perform quality control, or measure the effect of treatment.

Signal acquisition procedures may be categorized as being invasive or noninvasive, and active or passive.

**Invasive versus noninvasive procedures:** Invasive procedures involve the placement of transducers or other devices inside the body, such as needle electrodes to record MUAPs, or insertion of catheter-tip sensors into the heart to record intracardiac signals. Noninvasive procedures are desirable in order to minimize risk to the subject. Recording of the ECG using limb or chest electrodes, the EMG with surface electrodes, or the PCG with microphones or accelerometers placed on the chest are noninvasive procedures.

Note that making measurements or imaging with X rays or ultrasound may be classified as invasive procedures, as they involve penetration of the body with externally administered radiation, even though the radiation is invisible and there is no visible puncturing or invasion of the body.

**Active versus passive procedures:** Active data acquisition procedures require external stimuli to be applied to the subject, or require the subject to perform a certain activity to stimulate the system of interest in order to elicit the desired response or signal. For example, recording an EMG signal requires contraction of the muscle of interest, such as clenching a fist; recording the VAG signal from the knee requires flexing of the leg over a certain joint angle range; and recording visual ERP signals requires the delivery of flashes of light to the subject. While these stimuli may appear to be innocuous, they do carry risks in certain situations for some subjects: Flexing the knee beyond a certain angle may cause pain for some subjects, and strobe lights may trigger epileptic seizures in some subjects. The investigator should be aware of such risks, factor them in a *risk–benefit analysis*, and be prepared to manage adverse reactions.

Passive procedures do not require the subject to perform any activity. Recording of the ECG using limb or chest electrodes, the EEG during sleep using scalp-surface electrodes, or the PCG with microphones or accelerometers placed on the chest are passive procedures, but require contact between the subject and the transducers or instruments. Note that although the procedure is passive, the system of interest is active under its own natural control in these procedures. Acquiring an image of a subject with reflected natural light (with no flash from the camera) or with the natural infrared (thermal) emission could be categorized as a passive and noncontact procedure.

Most organizations require ethics approval by specialized committees for experimental procedures involving human or animal subjects, with the aim of minimizing the risk and discomfort to the subject and maximizing the benefits to both the subjects and the investigator.

**The human–instrument system:** Some of the components of a *human–instrument system* [13, 14, 123–126] are the following:

- *The subject or patient:* It is important always to bear in mind that the main purpose of biomedical instrumentation and signal analysis is to provide a certain benefit to the subject or patient. All systems and procedures should be designed so as not to cause undue inconvenience to the subject and not to cause any harm or danger. In applying invasive or risky procedures, it is extremely important to perform a risk–benefit analysis and determine if the anticipated benefits of the procedure are worth placing the subject at the risks involved.

- *Stimulus or procedure of activity:* Application of stimuli to the subject in active procedures requires instruments such as strobe light generators, sound generators, and electrical pulse generators. Procedures in which the subject is required to perform some specified actions or activities should include standardized protocols of the desired activities to ensure repeatability and consistency of the experiment and the results. Such procedures require ethics approval by specialized committees.

- *Transducers:* electrodes, sensors.

- *Signal conditioning equipment:* preamplifiers, amplifiers, filters.

- *Display equipment:* oscilloscopes, strip-chart or paper recorders, computer monitors, printers.

- *Recording, data acquisition, data transmission, and data processing equipment:* analog instrumentation tape recorders, analog-to-digital converters (ADCs), digital-to-analog converters (DACs), telemetry systems, wireless data transmission and reception devices, digital tapes, compact disks (CDs), data storage devices, computers.

- *Control devices:* power supply stabilizers and isolation equipment, patient intervention systems.

The science of measurement of physiological variables and parameters is known as *biometrics*. Some of the aspects to be considered in the design, specification, or use of biomedical instruments [13, 14, 123–126] are the following:

- *Isolation of the subject or patient* — Safety is of paramount importance so that the subject is not placed at the risk of electrocution or any other harm.
- *Dynamic range of operation* — The dynamic range is defined as the minimum to the maximum values of the signal or parameter being measured.
- *Sensitivity* — This can be represented by the smallest signal variation measurable and determines the resolution of the system.
- *Linearity* — Linear transfer characteristics are desired over at least a portion of the range of operation. Any nonlinearity present may need to be corrected or taken into account at later stages of signal processing.
- *Hysteresis* — A lag in measurement due to the direction of variation of the entity being measured indicates hysteresis, which may add a bias to the measurement.
- *Frequency response* — This represents the variation of sensitivity with frequency. Most systems encountered in practice exhibit a lowpass behavior, that is, the sensitivity of the system decreases as the frequency of the input signal increases. Signal restoration techniques may be required to compensate for reduced high-frequency sensitivity.
- *Stability* — An unstable system could preclude repeatability and consistency of measurements.
- $SNR$ — Artifacts due to power-line interference, grounding problems, thermal noise, and other sources could compromise the quality of the signal being acquired. A good understanding of the signal-degrading phenomena affecting the system is necessary in order to design appropriate filtering and correction procedures.
- *Accuracy* — The accuracy of a measurement could be affected by errors due to component tolerance; movement or mechanical errors; drift due to changes in temperature, humidity, or pressure; reading errors due to parallax; and zeroing or calibration errors.

The scientific and technological aspects of biomedical signal acquisition have advanced substantially over the past few decades. Systems are now available to acquire a few dozen to a few hundred channels of signals; wearable and portable systems are also available to facilitate wireless signal data acquisition from untethered and mobile subjects engaged in various activities [127–131]. Junnila et al. [132] developed a ballistocardiographic (BCG) chair, designed to look like a normal office chair, with a lightweight and flexible electromechanical film sensor to record the vibration signal related to cardiac activity along with the ECG and an impedance cardiogram. Guerrero et al. [133] used multiple pressure sensors integrated into a bed to obtain BCG signals. The envelope of the BCG signal was used to derive information related to respiration and detect sleep-related breathing disorders. Peltokangas et al. [134] describe a system with eight embroidered textile electrodes attached to a bed sheet to measure multiple channels of the ECG and facilitate monitoring of patients during sleep. Mikhelson et al. [135] reported on a system with a millimeter-wave sensor, two cameras, and a pan/tilt base not only to detect and track a subject but also to measure the subject's chest displacement and the heart rate in a noncontact manner. See Krishnan [131] for related discussions.

## 1.4 Challenges in Biomedical Signal Acquisition and Analysis

In spite of the long history of biomedical instrumentation and its extensive use in healthcare and research, many practical challenges and difficulties are encountered in biomedical signal acquisition, processing, and analysis [13, 14, 123–126]. The characteristics of the problems, and hence

their potential solutions, are unique to each type of signal. Particular attention should be paid to the following issues.

**Accessibility of the variables to measurement:** Most of the systems and organs of interest, such as the cardiovascular system and the brain, are located well within the body in protective enclosures (for good reasons!). While the ECG may be recorded using limb electrodes, the signal so acquired is only a projection of the true 3D cardiac electrical vector on to the axis of the electrodes. Such a signal may be sufficient for rhythm monitoring, but could be inadequate for more specific analysis of the cardiac system such as atrial electrical activity. Accessing the atrial electrical activity at the source requires the insertion of an electrode close to the atrial surface or within the atria.

Similarly, measurement of BP using a pressure cuff over an arm gives an estimate of the brachial arterial pressure. Detailed study of pressure variations within the cardiac chambers or arteries over a cardiac cycle would require the insertion of catheters with pressure sensors into the heart. Such invasive procedures provide access to the desired signals at their sources and often provide clear and useful signals, but carry high risks.

The surface EMG includes the interference pattern of the activities of several motor units even at low levels of muscular contraction. Acquisition of SMUAPs requires access to the specific muscle layer or unit of interest by insertion of fine-wire or needle electrodes. The procedure carries risks of infection and damage to muscle fibers, and causes pain to the subject during muscular activity.

An investigator should assess the system and variables of interest carefully, and determine the minimal level of intervention that is absolutely essential to the data acquisition procedure. A trade-off between the integrity and quality of the information acquired versus the pain and risks to the subject may be needed.

**Variability of the signal source:** It is evident from the preceding sections that the various systems that comprise the human body are dynamic with several variables or degrees of freedom. Biomedical signals represent the dynamic activity of physiological systems and the states of their constituent variables. The nature of the processes or the variables could be deterministic or random (stochastic); a special case is that of periodicity or quasiperiodicity.

A normal ECG exhibits a regular rhythm with a readily identifiable waveshape (the QRS complex) in each period; under such conditions, the signal may be referred to as a deterministic and periodic signal. However, the cardiovascular system of a heart patient may not stay in a given state over substantial periods, and the waveshape and rhythm may vary over time.

The surface EMG is the summation of the MUAPs of the motor units that are active at the given instant of time. Depending on the level of contraction desired (at the volition of the subject), the number of active motor units varies, increasing with increasing effort. Furthermore, the firing intervals and the firing rate of each motor unit also vary in response to the level of contraction desired, and exhibit stochastic properties. While the individual MUAPs possess readily identifiable and simple monophasic, biphasic, or triphasic waveshapes, the interference pattern of several motor units firing at different rates will appear as an almost random signal with no visually recognizable waves or waveshapes.

The dynamic nature of biological systems causes most signals to exhibit stochastic and non-stationary behavior. This means that signal statistics such as mean, variance, and spectral density change with time. For this reason, signals from a dynamic system should be analyzed over extended periods of time including various possible states of the system, and the results should be placed in the context of the corresponding states.

**Interrelationships and interactions among physiological systems:** The various systems that compose the human body are not mutually independent; rather, they are interrelated and interact in various ways. Some of the interactive phenomena are compensation, feedback, cause-and-effect, collateral effects, ipsilateral and/or contralateral effects, loading, and take-over of function of a disabled system or part by another system or part. For example, the second heart sound exhibits a split during active inspiration in normal subjects due to reduced intrathoracic pressure and decreased venous return to the left side of the heart [65] (but not during expiration); this is due to normal

physiological processes. However, the second heart sound is split in both inspiration and expiration due to delayed right ventricular contraction in right bundle-branch block, pulmonary valvular stenosis or insufficiency, and other conditions [65]. Ignoring this interrelationship could lead to misinterpretation of the signal. See Chapter 2 for more detailed discussions on this topic.

**Effect of the instrumentation or procedure on the system:** The placement of transducers on and connecting a system to instruments could affect the performance or alter the behavior of the system, and could cause spurious variations in the parameters being investigated. The experimental procedure or activity required to elicit the signal may lead to certain effects that could alter signal characteristics. This aspect may not always be obvious unless careful attention is paid. For example, the placement of a relatively heavy accelerometer may affect the vibration characteristics of a muscle and compromise the integrity of the vibration or sound signal being measured. Fatigue may set in after a few repetitions of an experimental procedure, and subsequent measurements may not be indicative of the true behavior of the system; the system may need some rest between procedures or their repetitions.

**Physiological artifacts and interference:** One of the prerequisites for the acquisition of a good ECG signal is for the subject to remain relaxed and still with no movement. Coughing, tensing of muscles, and movement of the limbs cause the corresponding EMG to appear as an undesired artifact. In the absence of any movement by the subject, the only muscular activity in the body would be that of the heart. When chest leads are used, even normal breathing could cause the associated EMG of the chest muscles to interfere with the desired ECG. It should also be noted that breathing causes beat-to-beat variations in the RR interval, which should not be mistaken to be sinus arrhythmia (see Section 2.2.4 for more details and a related illustration). An effective solution would be to record the signal with the subject holding his or her breath for a few seconds. This simple solution is not applicable in long-term monitoring of critically ill patients or in recording the ECG of infants; signal processing procedures would then be required to remove the concomitant artifacts.

A unique situation is that of acquiring the ECG of a fetus through surface electrodes placed over the expectant mother's abdomen: the maternal ECG appears as an interference in this situation. No volitional or external control is possible or desirable to prevent the artifact in this situation, which calls for adaptive cancellation techniques using multiple channels of various signals [136]; see Chapters 3 and 9.

Another example of physiological interference or cross-talk is that of muscle-contraction interference in the recording of the knee-joint VAG signal [94]. The rectus femoris muscle is active (contracting) during the swinging movement of the leg that is required to elicit the knee-joint vibration signal. The VMG of the muscle is propagated to the knee and appears as an interference. Swinging the leg mechanically using a mechanical actuator is a possible solution; however, this represents an unnatural situation and may cause other sound or vibration artifacts from the machine. Adaptive filtering using multichannel vibration signals from various points is a feasible solution [94]; see Chapter 3.

**Energy limitations:** Most biomedical signals are generated at microvolt or millivolt levels at their sources. Recording such signals requires sensitive transducers and instrumentation with low noise levels. The connectors and cables need to be shielded, in order to obviate pickup of ambient electromagnetic (EM) signals. Some applications may require transducers with integrated amplifiers and signal conditioners so that the signal leaving the subject at the transducer is much stronger than ambient sources of potential interference. A Faraday cage or shield, constructed with a wire mesh or foil of a conducting material to enclose the entire data acquisition setup including the subject and all devices, may be used to prevent external EM waves from contaminating the signals being recorded. Whereas such a cage is feasible in a laboratory, it may be impractical in a clinical or hospital setting.

When external stimuli are required to elicit a certain response from a system, the level of the stimulus is constrained due to safety factors and physiological limitations. Electrical stimuli to

record the ENG need to be limited in voltage level so as to not cause local burns or interfere with the electrical control signals of the cardiac or nervous systems. Auditory and visual stimuli are constrained by the lower thresholds of detectability, and upper thresholds related to frequency response, saturation, or pain.

**Patient safety:** Protection of the subject or patient from electrical shock or radiation hazards is an unquestionable requirement of paramount importance. The relative levels of any other risks involved should be assessed when a choice is available between various procedures and should be analyzed against their relative benefits. Patient safety concerns may preclude the use of a procedure that may yield better signals or results than others, or require modifications to a procedure that may lead to inferior signals. Review of experimental procedures by ethics committees should consider all of these issues before providing ethics approval. Further signal processing steps would then become essential in order to improve signal quality or otherwise compensate for the initial loss.

In consideration of the various difficulties encountered in the acquisition of biomedical signals, several institutions and agencies have supported efforts to develop public databases of annotated signals. The PhysioNet [137–139] is one such resource that is useful in education and research activities related to biomedical signals.

## 1.5 Why Use Computer-aided Monitoring and Diagnosis?

Physicians, cardiologists, neuroscientists, and healthcare technologists are highly trained and skilled practitioners. Why then would we want to use computers or electronic instrumentation for monitoring and analysis of biomedical signals? The following points provide some arguments in favor of the application of computers to process and analyze biomedical signals. Further discussions on the strengths and limitations of CAD are provided in Section 10.15.

- Humans are highly skilled and fast in the analysis of visual patterns and waveforms, but are slow in arithmetic operations with large numbers of values. The ECG of a single cardiac cycle (heart beat) could have at least 200 numerical values; the corresponding PCG at least 2,000. If signals need to be processed to remove noise or extract a parameter, it would not be practical for a person to perform such computation. Computers can perform millions of arithmetic operations per second. It should be noted, however, that recognition of waveforms and images using mathematical procedures typically requires huge numbers of operations and procedures that could lead to slow responses in such tasks from low-level computers.

- Humans could be affected by fatigue, boredom, and environmental factors, and are susceptible to committing errors. Long-term monitoring of signals, for example, the heart rate and ECG of a critically ill patient, by a human observer watching an oscilloscope or computer display is neither economical nor feasible. A human observer could be distracted by other events in the surrounding areas and may miss short episodes or transients in the signal. Computers, being inanimate but mathematically accurate and consistent machines, can be designed to perform computationally specific and repetitive tasks.

- Analysis by humans is usually subjective and qualitative. When comparative analysis is required between the signals of a subject and another or a standard pattern, a human observer would typically provide a qualitative response. For example, if the QRS width of the ECG is of interest, a human observer may remark that the QRS of the subject is wider than the reference or normal. More specific or objective comparison to the accuracy of the order of a few milliseconds would require the use of electronic instrumentation or a computer. Derivations of quantitative or numerical features from signals with large numbers of samples would certainly demand the use of computers.

- Analysis by humans is subject to interobserver as well as intraobserver variations. Given that most analyses performed by humans are based on qualitative judgment, they are liable to vary with time for a given observer, or from one observer to another. The former could also be due to lack of diligence or due to inconsistent application of knowledge, and the latter due to variations in training and level of understanding. Computers can apply a given procedure repeatedly and whenever recalled in a consistent manner. It is further possible to encode the knowledge (to be more specific, the logic) of many experts into a single computational procedure, and thereby enable a computer with the collective intelligence of several human experts in the area of interest.
- Most biomedical signals vary slowly over time (that is, they are lowpass signals), with their bandwidth limited to a few tens to a few thousand $Hz$. Typical sampling rates for digital processing of most biomedical signals range from $100\ Hz$ to a few $kHz$; only a few of the signals mentioned in this chapter, such as speech and bioacoustic signals, require higher sampling rates of the order of $5 - 20\ kHz$. Sampling rates as above facilitate *on-line, real-time* analysis of biomedical signals with even low-end computers. The term "on-line" indicates that the patient or subject is connected to the system or computer that is acquiring and analyzing signals. The term "real-time analysis" may be used to indicate the processing of each sample of a signal before the next sample arrives, or the processing of an epoch or episode such as an ECG beat before the next one is received in its entirety in a buffer. Monitoring the heart rate of critically ill patients demands on-line and real-time ECG analysis. However, some applications do not require on-line, real-time analysis: For example, processing a VAG signal to diagnose cartilage degeneration, or analyzing a long-term ECG record obtained over several hours using an ambulatory system, usually does not demand immediate attention and results. In such cases, computers could be used for *off-line* analysis of prerecorded signals with sophisticated signal processing and time-consuming modeling techniques. The speed required for real-time processing and the computational complexities of modeling techniques in the case of off-line applications would both rule out the possibility of performance of the tasks by humans.

One of the important points to note in the preceding discussion is that *quantitative analysis* becomes possible by the application of computers to biomedical signals. The logic of medical or clinical diagnosis via signal analysis could then be *objectively* encoded and *consistently* applied in routine or repetitive tasks. However, it should be emphasized that the end goal of biomedical signal analysis should be seen as computer-*aided* diagnosis and not automated diagnosis. A physician or medical specialist typically uses a significant amount of information in addition to signals and measurements, including the general physical appearance and mental state of the patient, family history, and socioeconomic factors affecting the patient, many of which are not amenable to quantification and logical rule-based processes. Biomedical signals are, at best, indirect indicators of the state of the patient; most cases lack a direct or unique signal–pathology relationship [45]. The results of signal analysis need to be integrated with other clinical signs, symptoms, and information by a physician. Above all, the *intuition* of the specialist plays an important role in arriving at the final diagnosis. For these reasons, and keeping in mind the realms of practice of various licensed and regulated professions, liability, and legal factors, the final diagnostic decision is best left to the physician or medical specialist. It is expected that quantitative and objective analysis facilitated by the application of computers to biomedical signal analysis will lead to an accurate diagnostic decision by the physician.

The techniques used for and applications of CAD in medicine have been given various names, labels, and attributes, some of which are pattern recognition, pattern classification, machine learning (ML), deep learning (DL), and artificial intelligence (AI). Classical pattern recognition and CAD methods use symbolic representation and expert systems based on established rules and logic; in such a system, the process and reasoning behind a decision or diagnosis can be explained; see Chapter 10. DL systems are based on massive artificial neural networks (ANNs) with multiple lay-

ers (hence the label "deep") of computational neurons, weights, and synaptic connections; such a system requires tremendous amounts of data for training and learning (referred to as "big data") as well as enormous computational resources. A typical DL or AI system cannot provide the reasoning behind a certain result and, therefore, is referred to as a "black box" whose internal details are unknown. Whereas the labels CAD and ML accurately depict the nature of the methods of our interest in this discussion, the term "AI" gives a connotation that goes beyond the true nature of the subject matter and the procedures or systems being used. CAD incorporates, encodes, and encapsulates the knowledge, intelligence, and expertise of several professionals from multiple disciplines spanning engineering, science, and medicine. CAD arises from natural human collaborative endeavors: the label "artificial" in AI is demeaning and undermines the contributions of the various professionals involved in the exercise. It is important to use apppropriate terminology to recognize, admire, and respect the contributing professionals and their subject areas. Ultimately, in life-and-death matters such as medical diagnosis and healthcare, it is best to have an appropriately qualified human expert in charge.

Further discussion on practical issues related to CAD, as well as the strengths and limitations of CAD systems, is presented in Section 10.15.

## 1.6 Remarks

We have taken a general look at the nature of biomedical signals in this chapter and have seen a few signals illustrated for the purpose of gaining familiarity with their typical appearance and features. Specific details of the characteristics of the signals and their processing or analysis are provided in the subsequent chapters.

We have also stated the objectives of biomedical instrumentation and signal analysis. Some of the challenges and difficulties that arise in biomedical signal investigation were discussed in order to draw attention to the relevant practical issues. The suitability and desirability of the application of computers for biomedical signal analysis were discussed, with emphasis on objective and quantitative analysis toward the end goal of CAD for improved diagnosis and therapy. The remaining chapters provide descriptions of specific signal processing techniques and applications.

> **On the importance of quantitative analysis:** "When you can measure what you are speaking about, and express it in numbers, you know something about it; but when you cannot measure it, when you cannot express it in numbers, your knowledge is of a meager and unsatisfactory kind: it may be the beginning of knowledge, but you have scarcely, in your thoughts, advanced to the stage of *science*."
>
> — *Lord Kelvin (William Thomson, 1824–1907)* [140]

> **On assumptions made in quantitative analysis:** "Now, things do not, in general, run around with their measures stamped on them like the capacity of a freight-car: it requires a certain amount of investigation to discover what their measures are ... What most experimenters do take for granted before they begin their experiments is infinitely more important and interesting than any results to which their experiments lead."
>
> — *Norbert Wiener (1894–1964)* [141]

## 1.7 Study Questions and Problems

*Note:* Some of the questions may require background preparation with other sources on the ECG (for example, Rushmer [25]), the EMG (for example, Goodgold and Eberstein [22]), and biomedical instrumentation (for example, Webster [13]).

1. Give two reasons to justify the use of electronic instruments and computers in medicine.

2. State any two objectives of using biomedical instrumentation and signal analysis.
3. Distinguish between open-loop and closed-loop monitoring of a patient.
4. List three common types or sources of artifact in a biomedical instrument.
5. A nerve cell has an action potential of duration $10\ ms$ including the refractory period. What is the maximum rate (in pulses per second) at which this cell can transmit electrical activity?
6. Consider a myocardial cell with an action potential of duration $300\ ms$ including its refractory period. What is the maximum rate at which this cell can be activated (fired) into contraction?
7. Distinguish between spatial and temporal recruitment of motor units to obtain increasing levels of muscular activity.
8. Consider three motor units with action potentials (SMUAPs) that are of different biphasic and triphasic shapes. Consider the initial stages of contraction of the related muscle. Draw three plots of the net EMG of the three motor units for increasing levels of contraction with the spatial and temporal recruitment phenomena invoked individually and in combination. Assume low levels of contraction, and that the SMUAPs do not overlap.
9. Draw a typical ECG waveform over one cardiac cycle indicating the important component waves, their typical durations, and the typical intervals between them. Label each wave or interval with the corresponding cardiac event or activity.
10. Draw the waveform corresponding to two cycles of a typical ECG signal and indicate the following waves and periods: (a) the P, QRS, and T waves; (b) the RR interval; (c) atrial contraction; (d) atrial relaxation; (e) ventricular contraction; and (f) ventricular relaxation.
11. Explain why the P and T waves are low-frequency signals, whereas the QRS complex is a high-frequency signal. Include diagrams of action potentials and an ECG waveform in your reasoning.
12. Explain the reasons for widening of the QRS complex in the case of certain cardiac diseases.
13. Give two examples that call for the use of electronic instruments and/or computers in ECG analysis.
14. A heart patient has a regular SA node pulse (firing) pattern and an irregular ectopic focus. Over a period of $10\ s$, the SA node was observed to fire regularly at $t = 0, 1, 2, 3, 4, 5, 6, 7, 8$, and $9\ s$. The ectopic focus was observed to fire at $t = 1.3, 2.8, 6.08$, and $7.25\ s$.

    Draw two impulse sequences corresponding to the firing patterns of the SA node and the ectopic focus. Draw a schematic waveform of the resulting ECG of the patient. Explain the source of each beat (SA node or ectopic focus) and give reasons.
15. A patient has ventricular bigeminy, where every other pulse from the SA node is replaced by a premature ventricular ectopic beat with a full compensatory pause. (See Figure 10.10 for an illustration of bigeminy.) The firing rate of the SA node is regular at $80$ beats a minute, and each ectopic beat precedes the blocked SA node pulse by $100\ ms$. (a) Draw a schematic trace of the ECG for $10$ beats, marking the time scale in detail. (b) Draw a histogram of the RR intervals for the ECG trace. (c) What is the average RR interval computed over the $10$ beats?
16. Draw a typical PCG (heart sound signal) waveform over one cardiac cycle indicating the important component waves, their typical durations, and the typical intervals between them. Label each wave or interval with the corresponding cardiac event or activity.
17. Give two examples that require the application of electronic instruments and/or computers in EEG analysis.
18. Distinguish between ECG rhythms and EEG rhythms. Sketch one example of each.
19. What are the causes and characteristics of ventricular ectopic beats (PVCs)? Draw a sample ECG signal including five normal beats and two PVCs. Label parts of the signal indicating atrial contraction, ventricular contraction, and the premature nature of PVCs.
20. Describe two cardiac abnormalities that cause changes in the shape of the QRS complex. Draw the ECG waveforms for the two cases and compare their features with those of a normal ECG waveform.
21. What is the ENG? Describe an experimental procedure to acquire an ENG. Describe the typical result obtained from ENGs and a potential application.

22. Explain the cardiac events that cause the second heart sound (S2). Identify the valves and their actions associated with S2. Explain how the dicrotic notch in the carotid pulse is related to S2.
23. Draw Einthoven's triangle and indicate the axes representing the six leads of the ECG obtained using the four limb leads. Mark the positions of the four limb leads in your diagram.
24. Draw a schematic representation of an ECG signal over one cardiac cycle. Label intervals related to atrial contraction and ventricular contraction. Overlay the ECG signal with schematic representations of the action potentials of atrial and ventricular myocytes. Explain the relationships between the various parts of the action potentials and the ECG signal.
25. Draw a schematic representation of Einthoven's triangle showing the directions (polarities) of leads I, II, and III of the ECG signal. Rearrange the vectors and derive the relationship between the three leads I, II, and III using vectorial arithmetic.
26. Consider the contraction of a muscle at a low level of effort. Suppose that two motor units are active. Assume that one of the motor units has a biphasic action potential and is firing at the rate of $10\ pps$. Assume that the other motor unit has a triphasic action potential and is firing at the rate of $12\ pps$. For a duration of $0.5\ s$, draw a schematic sketch of the action potential trains for the two motor units individually and separately. Draw a schematic sketch of the overall or combined EMG signal of the muscle. (Assume that the action potentials do not overlap.) Mark the time axis clearly in your drawings.
27. Draw a schematic diagram of a motor unit including labels (names) for each part. Explain the generation of the EMG signal, including the following: (a) single motor unit action potential, (b) innervation ratio, (c) temporal recruitment, and (d) spatial recruitment. Include sketches of at least two sample EMG signals in your discussion.
28. Describe the events in the cardiac system that cause (a) the components of the first heart sound (S1), and (b) the components of the second heart sound (S2). Describe an abnormal condition that could cause (c) a systolic murmur (SM), and (d) a diastolic murmur (DM). Draw a schematic representation of the PCG signal and the corresponding ECG signal over two cardiac cycles and label the PCG signal with the parts related to S1, S2, SM, and DM.
29. (a) Draw a schematic graphical representation of a normal ECG signal over one cardiac cycle. Identify all the waves and their typical durations. Identify the isoelectric parts of the signal. (b) Draw an ECG signal with a wide and jagged QRS complex. (c) Draw an ECG signal with an elevated ST segment. (d) Draw an ECG signal with a depressed ST segment.
30. Draw a schematic sketch of a normal ECG signal as well as the corresponding PCG and carotid pulse signals over one cardiac cycle. Identify the following waves in the signals: P, QRS, T, S1, S2, and the dicrotic notch. Indicate the temporal relationships between the waves mentioned. Label your figure with the relationships between the waves listed above and the following events in the cardiac cycle: atrial contraction, ventricular contraction, ventricular relaxation, and closure of the aortic valve. Label the intervals where systolic and diastolic murmurs could appear.

## 1.8 Laboratory Exercises and Projects

*Note: In exercises involving visits to a medical facility or biomedical data acquisition, attention should be paid to the following items of advice.*

- *Obtain the necessary ethical and other administrative permissions.*
- *Respect the privacy, sensitivities, priorities, and confidentiality of patients, medical professionals, and experimental subjects.*
- *Request a medical practitioner or technologist to explain the related procedures and processes.*
- *Observe the precautions related to the safety and well-being of the patients, subjects, and observers.*
- *Get assistance from a qualified technician in the operation of any equipment used.*
- *Discuss the project with a medical expert and a technologist specialized in the relevant area and obtain information on the differences between normal and abnormal patterns in the experiments conducted and the signals acquired.*

- *Collect a few sample signals for use in signal processing experiments.*
- *Ensure that no patient identification or confidential information is taken out of the laboratory or facility.*

*Attention to the points made above can help in gaining purposeful and worthwhile experience with biomedical signal acquisition and related matters.*

1. Visit an ECG, EMG, or EEG laboratory in a local hospital or health sciences center. View a demonstration of the acquisition of a few biomedical signals. Request a specialist in a related field to explain how he or she would interpret the signals. Volunteer to be the experimental subject and experience first-hand a biomedical signal acquisition procedure!
2. Set up an ECG acquisition system and study the effects of the following conditions or actions on the quality and nature of the signal: loose electrodes; lack of electrode gel; the subject holding his/her breath or breathing freely during the recording procedure; and the subject coughing, talking, or squirming during signal recording. Record noise-free and noisy ECG signals under various conditions for use in exercises on filtering.
3. Using a stethoscope, listen to your own heart sounds and those of your friends. Examine the variability of the sounds with the site of auscultation. Study the effects of heavy breathing and speaking by the subject as you are listening to the heart sound signal.
4. Record speech signals of vowels (/A/, /I/, /U/, /E/, /O/), diphthongs (/EI/, /OU/), fricatives (/S/, /F/), and plosives (/T/, /P/) as well as words with all four types of sounds (for example, safety, explosive, hearty, heightened, and house). You may be able to perform this experiment with the microphone on your computer. Study the waveform and characteristics of each signal. Use the signals in exercises on filtering, segmentation, and spectral analysis.
5. Using surface electrodes placed on the forearm, record EMG signals at various levels of force exerted by clenching the fist using a device with a force transducer. Provide for rest between repetitions of the experiment to avoid the development of fatigue in the muscle. Plot and study variations in the signal's characteristics with the level of force.

## References

[1] Lathi BP. *Linear Systems and Signals*. Oxford University Press, New York, NY, 2nd edition, 2005.

[2] Oppenheim AV, Willsky AS, and Nawab SH. *Signals and Systems*. Prentice-Hall, Englewood Cliffs, NJ, 2nd edition, 1997.

[3] Oppenheim AV and Schafer RW. *Digital Signal Processing*. Prentice-Hall, Englewood Cliffs, NJ, 1975.

[4] Max J. Quantizing for minimum distortion. *IEEE Transactions on Information Theory*, 6:7–12, 1960.

[5] Lloyd SP. Least squares quantization in PCM. *IEEE Transactions on Information Theory*, 28(2):129–137, 1982.

[6] Oppenheim AV and Schafer RW. *Discrete-time Signal Processing*. Pearson, Englewood Cliffs, NJ, third edition, 2010.

[7] Cooper KE, Cranston WI, and Snell ES. Temperature regulation during fever in man. *Clinical Science*, 27(3):345–356, 1964.

[8] Cooper KE. Body temperature and its regulation. In *Encyclopedia of Human Biology*, volume 2, pages 73–83. Academic, New York, NY, 1997.

[9] Rangayyan RM. *Biomedical Image Analysis*. CRC Press, Boca Raton, FL, 2005.

[10] Rangayyan RM, Acha B, and Serrano C. *Color Image Processing with Biomedical Applications*. SPIE, Bellingham, WA, 2011.

[11] Hodgkin AL and Huxley AF. Action potentials recorded from inside a nerve fibre. *Nature*, 144:710–711, 1939.

[12] Hodgkin AL and Huxley AF. Resting and action potentials in single nerve fibres. *Journal of Physiology*, 104:176–195, 1945.

[13] Webster JG, editor. *Medical Instrumentation: Application and Design*. Wiley, New York, NY, 3rd edition, 1998.

[14] Cromwell L, Weibell FJ, and Pfeiffer EA. *Biomedical Instrumentation and Measurements*. Prentice-Hall, Englewood Cliffs, NJ, 2nd edition, 1980.

[15] Plonsey R. Action potential sources and their volume conductor fields. *Proceedings of the IEEE*, 65(5):601–611, 1977.

[16] Clark R. *Action potentials (Personal Communication)*. University of Calgary, Calgary, Alberta, Canada, 1999.

[17] Hille B. Membrane excitability: Action potential propagation in axons. In Patton H, Fuchs A, Hille B, Scher A, and Steiner R, editors, *Textbook of Physiology*, pages 49–79. WB Saunders, Philadelphia, PA, 21st edition, 1989.

[18] Koester J. Action conductances underlying the action potential. In Kandel E and Schwartz J, editors, *Principles of Neural Science*, pages 53–62. Elsevier–North Holland, New York, NY, 1981.

[19] Kimura J. *Electrodiagnosis in Diseases of Nerve and Muscle: Principles and Practice*. Oxford University Press, New York, NY, 4th edition, 2013.

[20] Drake KL, Wise KD, Farraye J, Anderson DJ, and BeMent SL. Performance of planar multisite microprobes in recording extracellular single-unit intracortical activity. *IEEE Transactions on Biomedical Engineering*, 35(9):719–732, 1988.

[21] Frank K and Fuortes MGF. Potentials recorded from the spinal cord with microelectrodes. *Journal of Physiology*, 130:625–654, 1955.

[22] Goodgold J and Eberstein A. *Electrodiagnosis of Neuromuscular Diseases*. Williams and Wilkins, Baltimore, MD, 3rd edition, 1983.

[23] Hodes R, Larrabee MG, and German W. The human electromyogram in response to nerve stimulation and the conduction velocity of motor axons: Studies on normal and on injured peripheral nerves. *Archives of Neurology and Psychiatry*, 60(4):340–365, 1948.

[24] Clark, Jr. JW. The origin of biopotentials. In Webster JG, editor, *Medical Instrumentation: Application and Design*, pages 121–182. Wiley, New York, NY, 3rd edition, 1998.

[25] Rushmer RF. *Cardiovascular Dynamics*. WB Saunders, Philadelphia, PA, 4th edition, 1976.

[26] Buchthal F and Schmalbruch H. Motor unit of mammalian muscle. *Physiological Reviews*, 60(1):90–142, 1980.

[27] Brown GL and Harvey AM. Neuro-muscular transmission in the extrinsic muscles of the eye. *Journal of Physiology*, 99:379–399, 1941.

[28] Brown WF, Strong AM, and Snow R. Methods for estimating numbers of motor units in biceps-brachialis muscles and losses of motor units with aging. *Muscle & Nerve*, 11(5):423–432, 1988.

[29] de Luca CJ. Physiology and mathematics of myoelectric signals. *IEEE Transactions on Biomedical Engineering*, 26:313–325, 1979.

[30] Gath I and Stålberg E. In situ measurement of the innervation ratio of motor units in human muscles. *Experimental Brain Research*, 43:377–382, 1981.

[31] Mambrito B and de Luca CJ. Acquisition and decomposition of the EMG signal. In Desmedt JE, editor, *Progress in Clinical Neurophysiology, Volume 10: Computer-aided Electromyography*, pages 52–72. S. Karger AG, Basel, Switzerland, 1983.

[32] Platt RS, Hajduk EA, Hulliger M, and Easton PA. A modified Bessel filter for amplitude demodulation of respiratory electromyograms. *Journal of Applied Physiology*, 84(1):378–388, 1998.

[33] Nikolic M and Krarup C. EMGTools, an adaptive and versatile tool for detailed EMG analysis. *IEEE Transactions on Biomedical Engineering*, 58(10):2707–2718, 2011.

[34] Amsüss S, Goebel PM, Jiang N, Graimann B, Paredes L, and Farina D. Self-correcting pattern recognition system of surface EMG signals for upper limb prosthesis control. *IEEE Transactions on Biomedical Engineering*, 61(4):1167–1176, 2014.

[35] Chan FHY, Yang YS, Lam FK, Zhang YT, and Parker PA. Fuzzy EMG classification for prosthesis control. *IEEE Transactions on Rehabilitation Engineering*, 8(3):1167–1176, 2000.

[36] Waller AD. A demonstration on man of electromotive changes accompanying the heart's beat. *Journal of Physiology*, 8(5):229–234, 1887.

[37] Einthoven W. The different forms of the human electrocardiogram and their signification. *Lancet*, 1(4622):853–861, 1912.

[38] Tompkins WJ. *Biomedical Digital Signal Processing*. Prentice-Hall, Upper Saddle River, NJ, 1995.

[39] Goldberger E. *Unipolar Lead Electrocardiography and Vectorcardiography*. Lea & Febiger, Philadelphia, PA, 3rd edition, 1954.

[40] Friedman HH. *Diagnostic Electrocardiography and Vectorcardiography*. McGraw-Hill, New York, NY, 2nd edition, 1977.

[41] Malmivuo J and Plonsey R. *Bioelectromagnetism: Principles and Applications of Bioelectric and Biomagnetic Fields*. Oxford University Press, New York, NY, 1995.

[42] Draper HW, Peffer CJ, Stallmann FW, Littmann D, and Pipberger HV. The corrected orthogonal electrocardiogram and vectorcardiogram in 510 normal men (Frank lead system). *Circulation*, 30:853–864, 1964.

[43] Jenkins JM. Computerized electrocardiography. *CRC Critical Reviews in Bioengineering*, 6:307–350, November 1981.

[44] Jenkins JM. Automated electrocardiography and arrythmia monitoring. *Progress in Cardiovascular Disease*, 25(5):367–408, 1983.

[45] Cox Jr. JR, Nolle FM, and Arthur RM. Digital analysis of the electroencephalogram, the blood pressure wave, and the electrocardiogram. *Proceedings of the IEEE*, 60(10):1137–1164, 1972.

[46] Cooper R, Osselton JW, and Shaw JC. *EEG Technology*. Butterworths, London, UK, 3rd edition, 1980.

[47] Kooi KA, Tucker RP, and Marshall RE. *Fundamentals of Electroencephalography*. Harper & Row, Hagerstown, MD, 2nd edition, 1978.

[48] Hughes JR. *EEG in Clinical Practice*. Butterworth, Woburn, MA, 1982.

[49] Agarwal R and Gotman J. Computer-assisted sleep staging. *IEEE Transactions on Biomedical Engineering*, 48(12):1412–1423, 2001.

[50] Johnson L, Lubin A, Naitoh P, Nute C, and Austin M. Spectral analysis of the EEG of dominant and non-dominant alpha subjects during waking and sleeping. *Electroencephalography and Clinical Neurophysiology*, 26(4):361–370, 1969.

[51] Zimmermann-Schlatter A, Schuster C, Puhan MA, Siekierka E, and Steurer J. Efficacy of motor imagery in post-stroke rehabilitation: A systematic review. *Journal of Neuroengineering and Rehabilitation*, 5(1):1–10, 2008.

[52] Yadav R, Swamy MNS, and Agarwal R. Model-based seizure detection for intracranial EEG recordings. *IEEE Transactions on Biomedical Engineering*, 59(5):1419–1428, 2012.

[53] Grewal S and Gotman J. An automatic warning system for epileptic seizures recorded on intracerebral EEGs. *Clinical Neurophysiology*, 116:2460–2472, 2005.

[54] Chisci L, Mavino A, Perferi G, Sciandrone M, Anile C, Colicchio G, and Fuggetta F. Real-time epileptic seizure prediction using AR models and support vector machines. *IEEE Transactions on Biomedical Engineering*, 57(5):1124–1132, 2010.

[55] Whittington MA, Cunningham MO, LeBeau FEN, Racca C, and Traub RD. Multiple origins of the cortical gamma rhythm. *Developmental Neurobiology*, 71(1):92–106, 2011.

[56] Mantini D, Perrucci MG, Del Gratta C, Romani GL, and Corbetta M. Electrophysiological signatures of resting state networks in the human brain. *Proceedings of the National Academy of Sciences*, 104(32):13170–13175, 2007.

[57] Rennie CJ, Wright JJ, and Robinson PA. Mechanisms of cortical electrical activity and emergence of gamma rhythm. *Journal of Theoretical Biology*, 205(1):17–35, 2000.

[58] De Vos M, Vergult A, De Lathauwer L, De Clercq W, Van Huffel S, Dupont P, Palmini A, and Van Paesschen W. Canonical decomposition of ictal scalp EEG reliably detects the seizure onset zone. *NeuroImage*, 37(3):844–854, 2007.

[59] Verhagen MAMT, van Schelven LJ, Samsom M, and Smout AJPM. Pitfalls in the analysis of electrogastrographic recordings. *Gastroenterology*, 117:453–460, 1999.

[60] Mintchev MP and Bowes KL. Capabilities and limitations of electrogastrograms. In Chen JDZ and McCallum RW, editors, *Electrogastrography: Principles and Applications*, pages 155–169. Raven, New York, NY, 1994.

[61] Mintchev MP and Bowes KL. Extracting quantitative information from digital electrogastrograms. *Medical and Biological Engineering and Computing*, 34:244–248, 1996.

[62] Chen JDZ, Stewart Jr. WR, and McCallum RW. Spectral analysis of episodic rhythmic variations in the cutaneous electrogastrogram. *IEEE Transactions on Biomedical Engineering*, 40(2):128–135, 1993.

[63] Mintchev MP, Stickel A, and Bowes KL. Dynamics of the level of randomness in gastric electrical activity. *Digestive Diseases and Sciences*, 43(5):953–956, 1998.

[64] Rangayyan RM and Lehner RJ. Phonocardiogram signal processing: A review. *CRC Critical Reviews in Biomedical Engineering*, 15(3):211–236, 1988.

[65] Tavel ME. *Clinical Phonocardiography and External Pulse Recording*. Year Book Medical, Chicago, IL, 3rd edition, 1978.

[66] Luisada AA and Portaluppi F. *The Heart Sounds — New Facts and Their Clinical Implications*. Praeger, New York, NY, 1982.

[67] Shaver JA, Salerni R, and Reddy PS. Normal and abnormal heart sounds in cardiac diagnosis, Part I: Systolic sounds. *Current Problems in Cardiology*, 10(3):1–68, 1985.

[68] Reddy PS, Salerni R, and Shaver JA. Normal and abnormal heart sounds in cardiac diagnosis, Part II: Diastolic sounds. *Current Problems in Cardiology*, 10(4):1–55, 1985.

[69] Abbas AK and Bassam R. *Phonocardiography Signal Processing*. Morgan & Claypool and Springer, 2009.

[70] Brown CC, Giddbon DB, and Dean ED. Techniques of plethysmography. *Psychophysiology*, 1(3):253–266, 1965.

[71] Criée CP, Sorichter S, Smith HJ, Kardos P, Merget R, Heise D, Berdel D, Köhler D, Magnussen H, Marek W, Mitfessel H, Rasche K, Rolke M, Worth H, and Jörres RA. Body plethysmography–its principles and clinical use. *Respiratory Medicine*, 105(7):959–971, 2011.

[72] Allen J. Photoplethysmography and its application in clinical physiological measurement. *Physiological Measurement*, 28(3):R1, 2007.

[73] Kyriacou PA. Pulse oximetry in the oesophagus. *Physiological Measurement*, 27(1):R1, 2005.

[74] Galli A, Frigo G, Narduzzi C, and Giorgi G. Robust estimation and tracking of heart rate by PPG signal analysis. In *2017 IEEE International Instrumentation and Measurement Technology Conference (I2MTC)*, pages 1–6. IEEE, 2017.

[75] Patterson JAC, McIlwraith DC, and Yang GZ. A flexible, low noise reflective PPG sensor platform for ear-worn heart rate monitoring. In *2009 Sixth International Workshop on Wearable and Implantable Body Sensor Networks*, pages 286–291. IEEE, 2009.

[76] Fortino G and Giampà V. PPG-based methods for non invasive and continuous blood pressure measurement: An overview and development issues in body sensor networks. In *2010 IEEE International Workshop on Medical Measurements and Applications*, pages 10–13. IEEE, 2010.

[77] Alnaeb ME, Alobaid N, Seifalian AM, Mikhailidis DP, and Hamilton G. Optical techniques in the assessment of peripheral arterial disease. *Current Vascular Pharmacology*, 5(1):53–59, 2007.

[78] Madhav KV, Ram MR, Krishna EH, Komalla NR, and Reddy KA. Robust extraction of respiratory activity from PPG signals using modified MSPCA. *IEEE Transactions on Instrumentation and Measurement*, 62(5):1094–1106, 2013.

[79] Childers DG and Bae KS. Detection of laryngeal function using speech and electroglottographic data. *IEEE Transactions on Biomedical Engineering*, 39(1):19–25, 1992.

[80] Tsanas A, Little MA, McSharry PE, Spielman J, and Ramig LO. Novel speech signal processing algorithms for high-accuracy classification of Parkinson's disease. *IEEE Transactions on Biomedical Engineering*, 59(5):1264–1271, 2012.

[81] Rabiner LR and Schafer RW. *Digital Processing of Speech Signals*. Prentice-Hall, Englewood Cliffs, NJ, 1978.

[82] Rueda A, Vásquez-Correa JC, Orozco-Arroyave JR, Nöth E, and Krishnan S. Empirical mode decomposition articulation feature extraction on Parkinson's Diadochokinesia. *Computer Speech and Language*, 24(101322), 2021.

[83] Maciel CD, Pereira JC, and Stewart D. Identifying healthy and pathologically affected voice signals [lecture notes]. *IEEE Signal Processing Magazine*, 27:120–123, January 2010.

[84] Umapathy K, Krishnan S, Parsa V, and Jamieson DG. Discrimination of pathological voices using a time-frequency approach. *IEEE Transactions on Biomedical Engineering*, 52(3):421–430, March 2005.

[85] Umapathy K and Krishnan S. Feature analysis of pathological speech signals using local discriminant bases technique. *Medical and Biological Engineering and Computing*, 43:457–464, 2005.

[86] Ghoraani B, Umapathy K, Sugavaneswaran L, and Krishnan S. Pathological speech signal analysis using time-frequency approaches. *Critical Reviews in Biomedical Engineering*, 40(1):63–95, 2012.

[87] Arias-Londoño JD, Godino-Llorente JI, Sáenz-Lechón N, Osma-Ruiz V, and Castellanos-Domínguez G. Automatic detection of pathological voices using complexity measures, noise parameters, and Mel-Cepstral coefficients. *IEEE Transactions on Biomedical Engineering*, 58(2):370–379, 2011.

[88] Ellison AE. *Athletic Training and Sports Medicine*. American Academy of Orthopaedic Surgeons, Chicago, IL, 1984.

[89] Moore KL. *Clinically Oriented Anatomy*. Williams/Wilkins, Baltimore, MD, 1984.

[90] Tortora GJ. Articulations. In Wilson CM and Helfgott N, editors, *Principles of Human Anatomy*, pages 167–203. Harper and Row, New York, NY, 1986.

[91] Frankel VH and Nordin M, editors. *Basic Biomechanics of the Skeletal System*. Lea and Febiger, Philadelphia, PA, 1980.

[92] Nicholas JA and Hershman EB, editors. *The Lower Extremity and Spine in Sports Medicine*. CV Mosby, Missouri, KS, 1986.

[93] Rangayyan RM, Krishnan S, Bell GD, Frank CB, and Ladly KO. Parametric representation and screening of knee joint vibroarthrographic signals. *IEEE Transactions on Biomedical Engineering*, 44(11):1068–1074, 1997.

[94] Zhang YT, Rangayyan RM, Frank CB, and Bell GD. Adaptive cancellation of muscle contraction interference from knee joint vibration signals. *IEEE Transactions on Biomedical Engineering*, 41(2):181–191, 1994.

[95] Frank CB, Rangayyan RM, and Bell GD. Analysis of knee sound signals for non-invasive diagnosis of cartilage pathology. *IEEE Engineering in Medicine and Biology Magazine*, pages 65–68, March 1990.

[96] Wu YF, Krishnan S, and Rangayyan RM. Computer-aided diagnosis of knee-joint disorders via vibroarthrographic signal analysis: A review. *Critical Reviews in Biomedical Engineering*, 38(2):201–224, 2010.

[97] Tavathia S, Rangayyan RM, Frank CB, Bell GD, Ladly KO, and Zhang YT. Analysis of knee vibration signals using linear prediction. *IEEE Transactions on Biomedical Engineering*, 39(9):959–970, 1992.

[98] Moussavi ZMK, Rangayyan RM, Bell GD, Frank CB, Ladly KO, and Zhang YT. Screening of vibroarthrographic signals via adaptive segmentation and linear prediction modeling. *IEEE Transactions on Biomedical Engineering*, 43(1):15–23, 1996.

[99] Krishnan S, Rangayyan RM, Bell GD, Frank CB, and Ladly KO. Adaptive filtering, modelling, and classification of knee joint vibroarthrographic signals for non-invasive diagnosis of articular cartilage pathology. *Medical and Biological Engineering and Computing*, 35(6):677–684, 1997.

[100] Kernohan WG, Beverland DE, McCoy GF, Hamilton A, Watson P, and Mollan RAB. Vibration arthrometry. *Acta Orthopedica Scandinavia*, 61(1):70–79, 1990.

[101] Chu ML, Gradisar IA, and Mostardi R. A noninvasive electroacoustical evaluation technique of cartilage damage in pathological knee joints. *Medical and Biological Engineering and Computing*, 16:437–442, 1978.

[102] Wu Y. *Knee Joint Vibroarthrographic Signal Processing and Analysis*. Springer, 2015.

[103] Zhang YT, Frank CB, Rangayyan RM, and Bell GD. A comparative study of vibromyography and electromyography obtained simultaneously from active human quadriceps. *IEEE Transactions on Biomedical Engineering*, 39(10):1045–1052, 1992.

[104] Zhang YT, Frank CB, Rangayyan RM, and Bell GD. Relationships of the vibromyogram to the surface electromyogram of the human rectus femoris muscle during voluntary isometric contraction. *Journal of Rehabilitation Research and Development*, 33(4):395–403, 1996.

[105] Probst R, Lonsbury-Martin B, and Martin GK. A review of otoacoustic emissions. *Journal of the Acoustical Society of America*, 89(5):2027–2067, 1991.

[106] Pasterkamp H, Kraman SS, and Wodicka GR. Respiratory sounds: Advances beyond the stethoscope. *American Journal of Respiratory and Critical Care Medicine*, 156:974–987, 1997.

[107] Fenton TR, Pasterkamp H, Tal A, and Chernick V. Automated spectral characterization of wheezing in asthmatic children. *IEEE Transactions on Biomedical Engineering*, 32(1):50–55, 1985.

[108] Kompis M, Pasterkamp H, and Wodicka GR. Acoustic imaging of the human chest. *Chest*, 120(4):1309–1321, 2001.

[109] Gnitecki J and Moussavi Z. The fractality of lung sounds: A comparison of three waveform fractal dimension algorithms. *Chaos, Solitons & Fractals*, 26(4):1065–1072, 2005.

[110] Yadollahi A and Moussavi ZMK. A robust method for estimating respiratory flow using tracheal sounds entropy. *IEEE Transactions on Biomedical Engineering*, 53(4):662–668, 2006.

[111] Alshaer H, Fernie GR, Maki E, and Bradley TD. Validation of an automated algorithm for detecting apneas and hypopneas by acoustic analysis of breath sounds. *Sleep Medicine*, 14(6):562–571, 2013.

[112] Alshaer H, Fernie GR, and Bradley TD. Monitoring of breathing phases using a bioacoustic method in healthy awake subjects. *Journal of Clinical Monitoring and Computing*, 25(5):285–294, 2011.

[113] Hadjileontiadis LJ. *Lung Sounds: An Advanced Signal Processing Perspective*. Morgan & Claypool and Springer, 2009.

[114] Moussavi Z. *Fundamentals of Respiratory Sounds and Analysis*. Morgan & Claypool and Springer, San Rafael, CA, 2006.

[115] Issa FG, Morrison D, Hadjuk E, Iyer A, Feroah T, and Remmers JE. Digital monitoring of sleep-disordered breathing using snoring sound and arterial oxygen saturation. *American Review of Respiratory Disease*, 148:1023–1029, 1993.

[116] Dalmasso F and Prota R. Snoring: Analysis, measurement, clinical implications and applications. *European Respiratory Journal*, 9:146–159, 1996.

[117] Lazareck LL and Moussavi ZMK. Classification of normal and dysphagic swallows by acoustical means. *IEEE Transactions on Biomedical Engineering*, 51(12):2103–2112, 2004.

[118] Tomomasa T, Morikawa A, Sandler RH, Mansy HA, Koneko H, Masahiko T, Hyman PE, and Itoh Z. Gastrointestinal sounds and migrating motor complex in fasted humans. *The American Journal of Gastroenterology*, 94(2):374–381, 1999.

[119] Gay T, Bertolami CN, and Solonche DJ. *Method and Apparatus for the Acoustic Detection and Analysis of Joint Disorders*. US Patent 4,836,218, 1989.

[120] Pavesi L, Subburaj S, and Porter-Shaw K. Application and validation of a computerized cough acquisition system for objective monitoring of acute cough: A meta-analysis. *Chest*, 120(4):1121–1128, 2001.

[121] Várallyay Jr. G. The melody of crying. *International Journal of Pediatric Otorhinolaryngology*, 71(11):1699–1708, 2007.

[122] Kaniusas E, Pfützner H, and Saletu B. Acoustical signal properties for cardiac/respiratory activity and apneas. *IEEE Transactions on Biomedical Engineering*, 52(11):1812–1822, 2005.

[123] Aston R. *Principles of Biomedical Instrumentation and Measurement*. Merrill, Columbus, OH, 1990.

[124] Bronzino JD. *Biomedical Engineering and Instrumentation*. PWS Engineering, Boston, MA, 1986.

[125] Bronzino JD, editor. *The Biomedical Engineering Handbook*. CRC and IEEE, Boca Raton, FL, 1995.

[126] Cohen A. *Biomedical Signal Processing*. CRC Press, Boca Raton, FL, 1986.

[127] *Electrical Geodesics, Inc.* `www.egi.com`, accessed on 2023-06-26.

[128] *g.Nautilus wireless biosignal acquisition*. `www.gtec.at`, accessed on 2023-06-26.

[129] *BTS bioengineering*. `www.btsbioengineering.com`, accessed on 2023-06-26.

[130] *PLUX wireless biosignals S.A.* `www.pluxbiosignals.com`, accessed on 2023-06-26.

[131] Krishnan S. *Biomedical Signal Analysis for Connected Healthcare*. Academic Press, New York, NY, 2021.

[132] Junnila S, Akhbardeh A, and Värri A. An electromechanical film sensor based wireless ballistocardiographic chair: Implementation and performance. *Journal of Signal Processing Systems*, 57:305–320, 2009.

[133] Guerrero G, Kortelainen JM, Palacios E, Bianchi AM, Tachino G, Tenhunen M, Méndez MO, and van Gils M. Detection of sleep-disordered breathing with pressure bed sensor. In *Proceedings of the 35th Annual International Conference of the IEEE Engineering in Medicine and Biology Society*, pages 1342–1345, Osaka, Japan, July 2013.

[134] Peltokangas M, Verho J, and Vehkaoja A. Night-time EKG and HRV monitoring with bed sheet integrated textile electrodes. *IEEE Transactions on Information Technology in Biomedicine*, 16(5):935–942, 2012.

[135] Mikhelson IV, Lee P, Bakhtiari S, Elmer II TW, Katsaggelos AK, and Sahakian AV. Noncontact millimeter-wave real-time detection and tracking of heart rate on an ambulatory subject. *IEEE Transactions on Information Technology in Biomedicine*, 16(5):927–934, 2012.

[136] Widrow B, Glover Jr. JR, McCool JM, Kaunitz J, Williams CS, Hearn RH, Zeidler JR, Dong Jr. E, and Goodlin RC. Adaptive noise cancelling: Principles and applications. *Proceedings of the IEEE*, 63(12):1692–1716, 1975.

[137] Goldberger AL, Amaral LAN, Glass L, Hausdorff JM, Ivanov PC, Mark RG, Mietus JE, Moody GB, Peng CK, and Stanley HE. PhysioBank, PhysioToolkit, and PhysioNet: Components of a new research resource for complex physiologic signals. *Circulation*, 101:e215–e220, 2000.

[138] Penzel T, Moody GB, Mark RG, Goldberger AL, and Peter JH. The Apnea-ECG database. In *Proceedings of IEEE Computers in Cardiology*, pages 255–258, `https://www.physionet.org/content/apnea-ecg/1.0.0/`, 2000.

[139] Moody GB, Mark RG, and Goldberger AL. PhysioNet: A web-based resource for the study of physiologic signals. *IEEE Engineering in Medicine and Biology*, pages 70–75, May/June 2001.

[140] Bartlett J. *Familiar Quotations*. Little, Brown and Co., Boston, MA, 15th edition, 1980.

[141] Wiener N. A new theory of measurement: A study in the logic of mathematics. In *Proceedings of the London Mathematical Society, Series 2, Volume 19*, pages 181–205, 1919.